Characterizing the putative G1/S transcription factor complex composition and function in *Candida albicans*

Vinitha Joice Chidipi

A Thesis
in
The Department
of
Biology

Presented in Partial Fulfillment of the Requirements
For the Degree of Master of Science (Biology) at
Concordia University

April 2015

CONCORDIA UNIVERSITY

School of Graduate Studies

This is to certify that the thesis prepared

By: Vinitha Joice Chidipi

Entitled: Characterizing the putative G1/S transcription factor complex composition and function in *Candida albicans*

and submitted in partial fulfillment of the requirements for the degree of

Master of Science (Biology)

complies with the regulations of the University and meets the accepted standards with respect to originality and quality.

Signed by the final examining committee:

Jin Suk Lee Chair

Malcolm Whiteway Examiner

Alisa Piekny Examiner

Vladimir Titorenko External Examiner

Catherine Bachewich Supervisor

Approved by Selvadurai Dayanandan .
Chair of Department or Graduate Program Director

Andre Roy .
Dean of Faculty

Date April 22, 2015 .

ABSTRACT

Characterizing the putative G1/S transcription factor complex composition and function in *Candida albicans*

Vinitha Joice Chidipi

The G1/S transition is a critical control point for cell proliferation, and involves the essential transcription complexes SBF and MBF in *Saccharomyces cerevisiae,* or MBF in *Schizosaccharomyces pombe.* In *S. cerevisiae,* Swi4p and Mbp1p comprise the DNA binding elements for SBF and MBF, respectively, while Swi6p is a common activating component. In the fungal pathogen *Candida albicans*, G1/S regulation is not yet clear. Orthologues of Swi6p, Swi4p and Mbp1p exist and previous work suggested that Swi4p and Swi6p form a single G1/S transcription factor complex, while the function of Mbp1p remained unclear as its absence did not affect growth. Additionally, unknown factors were suggested to contribute to G1/S regulation in *C. albicans* as cells lacking Swi4p and Swi6p, or Swi4p and Mbp1p were still viable, unlike the situation in *S. cerevisiae.* A previous graduate student from the Bachewich lab demonstrated through tandem-affinity purification of Swi4p, Swi6p and Mbp1p coupled with Orbitrap LC/MS, and co-immunoprecipitation that Swi6p interacted with Swi4p as well as Mbp1p, but an interaction between Swi4p and Mbp1p was not clear, questioning the current model that Swi4p and Swi6p are the major components of a single MBF-like complex in *C. albicans*. Additional putative interacting proteins were identified but not validated. Further, identification of Swi4p targets using genome-wide location analysis revealed cell-cycle related factors but also regulators of filamentous growth, including *EFG1*. In this study, the composition of the putative

G1/S transcription factor complex was further investigated using co-immunoprecipitation experiments that utilized lower amounts of input protein and variations in epitope tags. The results confirm that Swi6p similarly interacts with Swi4p and Mbp1p. However, Swi4p and Mbp1p showed a weak interaction that could only be detected with higher amounts of input protein and only when Swi4p was immune-precipitated. Thus, separate Swi6p/Swi4p and Swi6/Mbp1p complexes may exist in *C. albicans*, but the function of the Swi6p/Mbp1p complex remains unknown. We next carried out co-immunoprecipiation experiments to validate additional proteins identified in the previous Swi6p affinity purification screen, including the mitotic polo-like kinase Cdc5p. When Cdc5p was immune-precipitated from G1-phase arrested cells, Swi6p co-purified, suggesting a novel interaction between these two proteins. Finally, in order to validate the functional significance of Swi4p occupation of the *EFG1* promoter, *EFG1* expression in the presence and absence of Swi4p was investigated by Northern blotting, and the effects of deleting *EFG1* on the Swi4p-depleted phenotype were determined. In the absence of Swi4p, *EFG1* was moderately induced. Furthermore, absence of *EFG1* reduced the extent to which *swi4Δ/swi4Δ* cells became enlarged and formed long filaments. Thus, Swi4p may contribute to the regulation of *EFG1* and possibly filamentous morphogenesis, as well as the G1/S transition, suggesting that it may lie at the interface between cell cycle regulation and development in *C. albicans.*

Acknowledgements

I would like to thank Dr. Catherine Bachewich for her extreme support, help, guidance, co-operation and encouragement during my research studies from start till the end at Concordia University. It would have been very difficult to obtain data that I currently have, if you were not my supervisor. I truly thank you for giving me an amazing opportunity to learn about *C.albicans* and bringing to my attention the importance of understanding its biological processes.

I am grateful for my committee members, Dr.Alisa Piekny and Dr.Malcolm Whiteway for their help and support during my studies. I appreciate your helpful comments and suggestions, which allowed me to look at my research from a different perspective and encouraged me to improve my results.

Without the abundant help and encouragement given by my colleague Amandeep Glory, I would have been lost in the lab. Thank you for helping me whenever I came to you with questions and for questioning me back in return to help me better understand the concepts and experimental techniques. You were not only my colleague in lab, but my sister who was always there for me to cheer me up. So, thank you very much! Samantha Spararani, I would have been a loner without you in lab! Thank you for your company and for your help whenever I needed it. I truly appreciate your tremendous encouragement during stressful times, which kept me going forward. I would also like to thank former lab member, Yaolin Chen and other colleagues Jim, Sara, Jeremy and Gayathri for your help.

I appreciate all the help provided by Dr. Martine Raymond, Dr. Sandra Weber and Dr. Eric Bonneil from University of Montreal with ChIP-chip experiment and proteomics.

Table of Contents

List of Figures

List of Tables

List of Acronyms

Bp	base pair(s)
cAMP	Cyclic adenosine monophosphate
Cdk	Cyclin-dependent kinase
Co-IP	Co-immunoprecipitation
ChIP	Chromain immunoprecipitation
DNA	Deoxyribonucleic acid
DEPC	Diethylpyrocarbonate
dNTP	Deoxyribonucleotide triphosphate
DTT	Dithiothreitol
ECL	Enhanced chemiluminescence
EDTA	Ethylenediaminetetraacetic acid
EGTA	Ethylene glycol tetraacetic acid
G	Gram(s)
gDNA	Genomic DNA
h	Hour(s)
HA	Hemagglutinin
Kac	Potassium acetate
Kb	Kilo base pair(s)
L	Litre(s)
M	Molar
MAPK	Mitogen-activated protein kinase
MBF	*MluI* binding factor
-MC	SC medium lacking methionine and cysteine
+MC	SC medium supplemented with 2.5mM methionine and 0.5mM cysteine
$MgCl_2$	Magnesium chloride
Min	Minute(s)
Ml	Milliliter(s)
mM	Milli molar
$(NH_4)_2SO_4$	Ammonium sulfate
µg	Microgram(s)
µl	Microliter(s)
Mg	Milligram(s)
NaCl	Sodium chloride
Ng	nanogram(s)
NP40	Nonyl phenoxypolyethoxylethanol
OD	Optical Density
PCR	Polymerase chain reaction
PEG	Polyethylene glycol
PMSF	Phenyl methane sulfonyl fluoride
PKA	Protein kinase A
pRb	Retinoblastoma protein

PVDF	Polyvinyl difluoride
RNA	Ribonucleic acid
RNase	Ribonuclease
rpm	Rotations per minute
SBF	Swi4-Swi6 cell cycle box binding factor
SC	0.67% yeast nitrogen base, 2% glucose, amino acids with or without methionine and cysteine
SDS	Sodium Dodecyl Sulfate
Sec	second(s)
ssDNA	Salmon sperm DNA
TAME	Tosyl-L-Arginine Methyl Ester
TE	Tris-EDTA
TPCK	Tosyl phenylalanyl chloromethyl ketone
YPD	1% yeast extract, 2% peptone, 2% dextrose

1. Introduction

1.1 Eukaryotic Cell Cycle

1.1.1 General Overview

The cell cycle is a series of events that lead to duplication of DNA and creation of two new daughter cells. In many organisms, it consists of G1, S, G2, M phases and cytokinesis. Cell growth and DNA replication occur in G1 and S phase, respectively. The cell continues to grow in G2. In M phase, the duplicated DNA aligns on a spindle and then is segregated to two daughter cells. The cells divide during cytokinesis [1].

Progression through the cell cycle is controlled at many levels, and several checkpoints, to ensure that processes in each phase are successfully completed before proceeding into the next phase. The cyclin-dependent kinases (Cdks) associated with specific cyclins are major regulators of cell cycle transitions. For example, in the model yeast *Saccharomyces cerevisiae*, the G1 cyclins Cln1 – Cln3 bind to Cdk Cdc28p to regulate the G1/S transition. However, Cdc28p associates with B-type cyclins to regulate the transition from G2 phase into mitosis [2].

Proper cell cycle progression is crucial for cell viability and proliferation. Defects in genes encoding regulatory proteins that control cell cycle events can lead to uncontrolled cell division, eventually giving rise to many diseases such as cancer. For example, in humans, mutations that lead to overexpression of *CDK1* and *CDK2* can be a cause for certain types of colon adenomas as well as for focal carcinomas in adenomatous tissue [3]. Increased amplification of cyclin D gene can lead to breast, esophageal, bladder, lung, and squamous cell carcinomas [4].

1.1.2 G1/S transition

G1 is a crucial stage of cell cycle as it determines whether cells commit to mitosis and proliferate or exit the cell cycle for differentiation [5, 6]. The G1/S transition is known as the Restriction point in higher organisms such as mammals, or Start in lower organisms such as fungi. The circuitry controlling this cell cycle stage shows some conservation from yeast to humans. An upstream Cdk associated with cyclins is required to activate a downstream G1/S transcription factor complex (Fig. 1A). This complex, in turn, regulates a battery of genes required for cell cycle entry, including DNA replication [7]. In mammals, Cdk4 associates with cyclin D, and this complex activates a family of G1/S transcription factors E2F1-E2F3 [8], by phosphorylating and inactivating their inhibitor, Retinoblastoma protein (pRb). Targets of E2F include cyclins E and A, for example, which then associate with Cdk2 to further phosphorylate pRb forming a positive feedback loop [9]. Activated E2F initiates transcription of additional genes involved in DNA synthesis, chromosome replication as well as genes related to cell cycle regulation [8], DNA damage repair, apoptosis, differentiation and development [10]. In late S phase, cyclin A/Cdk2 complex phosphorylates E2F1 to inhibit its DNA binding capacity, thereby leading to its inactivation [11].

In fungi, the G1/S transition has only been well characterized in the model yeasts *Saccharomyces cerevisiae* and *Schizosaccharomyces pombe.* In *S. cerevisiae,* Start requires that cells have obtained a critical cell size and protein synthesis rate [12]. In *S. cerevisiae*, the Cdk Cdc28p associates with the G1 cyclin Cln3p. This complex phosphorylates and inhibits Whi5p, an inhibitor of one G1/S transcription complex, which is called SBF [13, 14]. A second G1/S transcription complex, called MBF, is activated by inhibition of the co-repressor Nrm1p [15]. SBF is composed of a transcriptional activator Swi6p and a DNA binding factor Swi4p, which

binds to SCB (CGCGAAA) elements [16] on target promoters of genes. It activates transcription of G1 cyclin genes, *CLN1* and *CLN2,* for example*,* which in turn stimulate the activity of Cdc28p. This allows for a positive feedback loop, as well as transcription of B-type cyclin genes, *CLB5* and *CLB6,* by inactivating their inhibitor, Sic1p via phosphorylation. The B-type cyclins with their associated Cdk activate S-phase targets to initiate DNA synthesis as well as spindle maturation and chromosome segregation [13]. MBF consists of Swi6p and a DNA binding factor Mbp1p that binds to MCB (CGCGT) elements [16] in genes linked to DNA synthesis and metabolism. Unlike SBF, MBF is involved in repressing transcription of genes outside of G1. It is later inactivated by Nrm1p, which accumulates in S phase and binds to MBF [16]. On the other hand, SBF activity is inhibited by Clb1/2p-Cdk1p complex, which accumulates during the G1-S transition to phosphorylate SBF, thereby causing its dissociation from promoter regions of target genes [16] (Fig. 1B).

In the fission yeast model *S. pombe,* the cyclin Pas1p associates with the Cdk Pef1p to activate a single MBF complex that regulates the G1/S transition. This complex consists of the activating factor Cdc10p, a homologue of Swi6p, and two DNA binding elements, Res1p and Res2p, homologues of Mbp1p, that recognize MCB elements in genes involved in DNA synthesis, DNA repair and cell cycle control [17]. Res1p and Res2p bind to DNA through their N termini and to Cdc10p through their C termini. In contrast to *S. cerevisiae*, Res1p and Res2p together are not equally important in G1/S transition specifically. Although Res1p/Cdc10p complex is crucial in G1 to S progression, Res2p is additionally involved in meiosis where it forms a complex with Cdc10p only without the presence of Res1p. Hence, Res2p plays an important role in both mitotic as well as meiotic stages of cell cycle [18]. MBF activity is inactivated outside of G1 by transcriptional repressors Nrm1p and Yox1p, which accumulate in S

phase and bind to MBF. On the other hand, it is kept activated through a stress-induced mechanism, in which protein kinase Cds1p phosphorylates Nrm1p, Yox1p, Cdc10p, as well as Ste9p, which inhibits Res2p degradation by ubiquitin ligase until later stages of cell cycle [17].

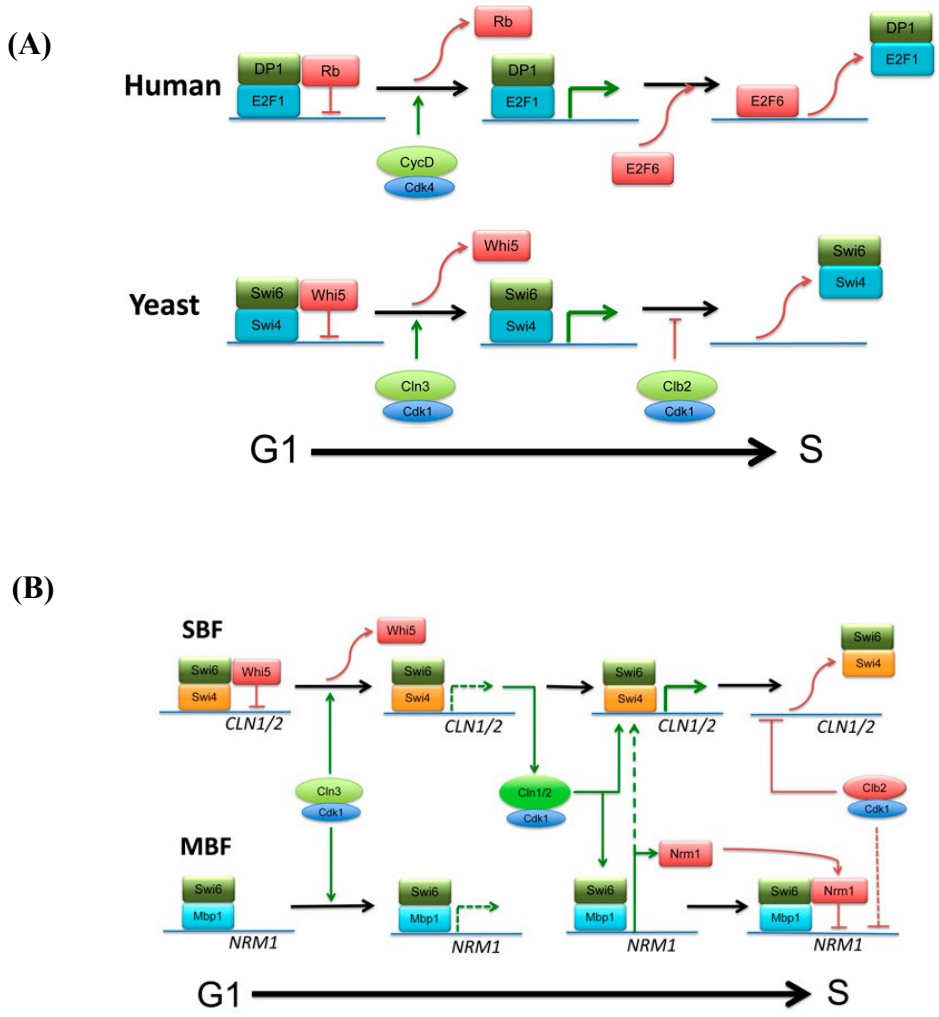

Figure 1. G1/S phase of cell cycle.
(A) Activation of G1/S transition in human and yeast. (B) The components of G1/S transcription factor complex in G1/S transition pathway of *S .cerevisiae* [19].

1.2 *Candida albicans*

1.2.1 Opportunistic fungal pathogen in humans

Candida albicans is a commensal fungus that resides in the gastrointestinal tract and mucosal membranes of humans [20, 21]. Although harmless under most circumstances, *C. albicans* is an opportunistic pathogen. It can cause mucosal infections or more life-threatening systemic infections in immunocompromised individuals [21]. For example, patients with AIDS are susceptible to oral and oesophageal candidiasis. Moreover, 75% of women are affected by vulvovaginal candidiasis, one of the frequently occurring infections [22]. Candidaemia, a bloodstream infection caused by *C. albicans*, is capable of spreading to internal organs such as brain, heart, and kidney [23]. Common drugs to address candidiasis include fungistatic drugs, such as fluconazole and other azoles, which inhibit the biosynthesis of fungal cell membrane components such as ergosterol. Other drugs are fungicidal, including the echinocandins, which cause cell death through the inhibition of β-1,3-glucan synthase, an enzyme required for cell wall biosynthesis. However, due to severe side effects and increased resistance to these drugs [24], new drug targets and strategies for treating infection are required. To this end, a comprehensive understanding of the biology of *C. albicans* and its virulence traits is crucial.

1.2.2 Virulence-associated traits: Differentiation

One aspect of the biology of *C. albicans* that is essential for virulence is its ability to differentiate into multiple cell types, including yeast, pseudohyphae, hyphae, and chlamydospores [21]. Yeast cells are oval and separate after cytokinesis. Pseudohyphae are elongated yeast due to an extended period of polarized growth, but remain attached after cell division and thus have constrictions at the sites of septation. Hyphae consist of elongated cells

that maintain growth in a polarized manner, and do not contain constrictions at septation sites. Chlamydospores have thicker cell walls and are larger compared to yeast cells [20]. Plasticity in form allows the fungus to survive and adapt to the different environments of the host. For example, yeast cells are more adept to dissemination in the blood stream, while the filamentous cells are optimized for penetrating host tissues during infection [25]. Hyphae generate physical forces and secrete lytic enzymes such as aspartic proteases, that aide in disintegration of cell surface components and contribute to entry into host cells [26]. Mutants locked in one cell form, including yeast or hyphae, are significantly less virulent in mouse models of infection, underscoring the importance of differentiation in virulence potential. An understanding of the factors that regulate differentiation may thus identify effective targets for anti-fungal therapies.

Differentiation is triggered by various environmental cues. The regulation of differentiation is one of the best understood with respect to the yeast-to-hyphae switch. The yeast to hyphal transition is induced by several stimuli such as serum, high pH, nutrient limitation, and high CO_2 concentrations under the condition of high temperature, or under embedded conditions [21]. Several signaling pathways are activated by stimuli, including a mitogen-activated protein kinase (MAPK) pathway involving the Cph1p transcription factor as well as a cyclic AMP-dependent pathway involving the Efg1p transcription factor [21] (Fig. 2), for example. Efg1p is acted upon by additional pathways and is required for hyphal development under most hyphal-inducing conditions [27]. Efg1p in turn acts on expression of various Hyphal Specific Genes (HSGs), including *HWP1*, a cell wall protein involved in adhesion to host tissue [28] for example. In addition to Efg1p, Ume6p is another important transcription factor that regulates hyphal growth. *UME6* is activated in part by Efg1p [29]. A target of Ume6p is *HGC1,* a hyphal-specific gene crucial for development of hyphae [30, 31]. Hgc1p forms a complex with Cdc28p

to contribute to hyphal growth through various mechanisms [32]. For example, the Cdc28p/Hgc1p complex phosphorylates Rga2p, which is a GTPase-activating protein (GAP) of the polarity regulator Cdc42p [33], which in turn maintains active Cdc42p at the hyphal tip [33, 34]. Importantly, Cdc28p/Hgc1p also phosphorylates Efg1p, which causes it to associate with and repress genes involved in cell separation [35].

Furthermore, Efg1p functions with five other important transcriptional regulators including Bcr1p, Tec1p, Ndt80p, Rob1p and Brg1p to regulate biofilm formation, which is crucial for virulence [36]. Other additional functions controlled by Efg1p include white cell-specific transcriptional profile [37, 38], regulation of oxidative/fermentative metabolism [39], and heat stress resistance [40].

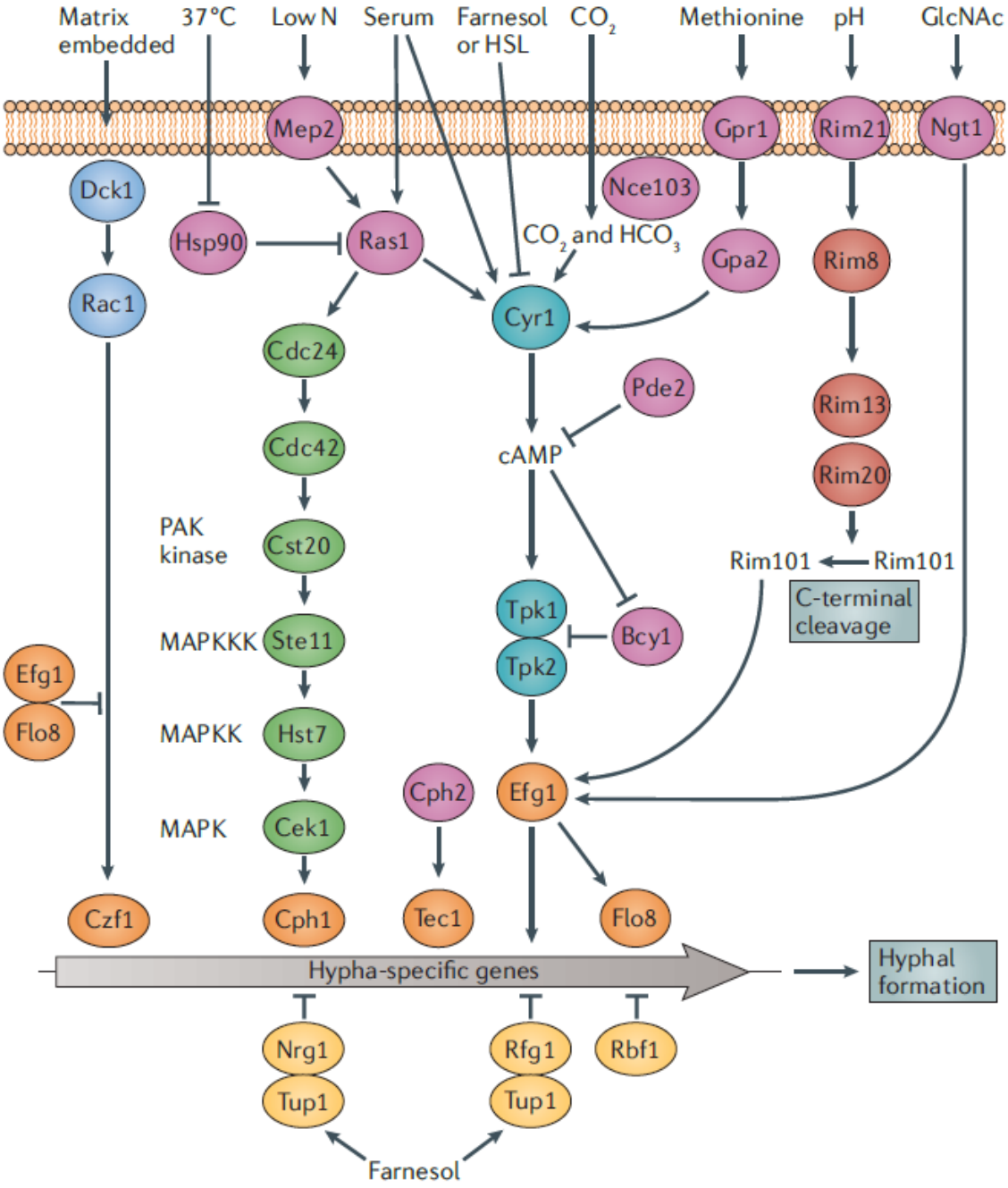

Figure 2. Different signal transduction pathways involved in yeast to hyphal transition [21].

1.2.3 Virulence associated traits: Cell proliferation

Another aspect of the biology of *C. albicans* that is important for virulence and survival in host organisms is cell proliferation, which is regulated by the cell cycle. In contrast to *S. cerevisiae* and *S. pombe,* the circuitry controlling the cell cycle in *C. albicans* is not well defined, due in part to the diploid nature of the fungus [41], difficulty in synchronizing cells [42], and an emerging theme of differences in function of the few sequence homologues that have been characterized in *C. albicans* [43]. However, one study demonstrated the ability to synchronize the opaque yeast form of *C. albicans* [42], and through this identified genes that are modulated at the transcriptional level during G1/S, S/G2, G2/M, and M/G1 transitions. This work revealed some similarity to *S. cerevisiae*, but also identified many novel genes whose expression was modulated at G1/S and other cell cycle transitions. However, few have been functionally characterized. Of the G1/S modulated genes, there was a significant enrichment of MCB motifs in promoter regions, but not SCB, unlike that found with G1/S-modulated genes in *S. cerevisiae* [42]. Hence, a model was proposed whereby a single MBF complex that binds MCB elements might control genes at the G1/S transition in *C. albicans*, more similar to the situation in *S. pombe.*

Sequence comparisons and limited genetic studies demonstrated that *C. albicans* shares some similarity in the putative G1/S regulatory circuit with *S. cerevisiae*. For example, *C. albicans* contains orthologues of Cdc28p, the G1 cyclin, Cln3p and the G1/S transcription complex factors Swi6p, Swi4p and Mbp1p. Repression of Cdc28p caused cell elongation as well as changes in expression of hyphal-associated genes and transcription factors related to morphogenesis [44]. Depletion of the G1 cyclin Cln3p in yeast cells resulted in large, unbudded cells with a single nucleus, implying a role in G1 phase [45, 46]. However, in contrast to Cln3p-

depleted *S. cerevisiae* cells, which eventually resume budding due to the presence of Bck2p [47], which *C. albicans* lacks, Cln3p-depleted *C. albicans* cells switched to hyphal and pseudohyphal growth, in the absence of environmental cues [45, 46]. This suggested a link between G1 phase and hyphal development. *C. albicans* also contains orthologues of *SWI4, SWI6* and *MBP1*. Deletion of *SWI4* or *SWI6*, but not *MBP1*, resulted in yeast cell enlargement, suggesting a G1 phase delay, and production of filaments [48]. However, in contrast to the situation in *S. cerevisiae*, absence of both *SWI6* and *SWI4* or *SWI4* and *MBP1*, resulted in viable cells. This suggests that additional factors contribute to the regulation of the G1/S transition. Furthermore, cells lacking Swi6p/Swi4p also showed changes in expression in G1/S-associated genes including G1 cyclins *CCN1* and *PCL2*, linking their function to G1/S control. Together, these results support the model that Swi4p and Swi6p might be key players in a single G1/S transcription factor complex, and thus may be the functional equivalent of MBF. A novel gene proposed to be the Nrm1p functional homologue was identified, but it does not appear to be identical [49]. Other factors required for the G1/S transition in *S. cerevisiae,* including Whi5p and Bck2p, are missing in *C. albicans*. In summary, *C. albicans* appears to have a similar framework for the G1/S transition network as seen in *S. cerevisiae* (Fig. 3), but a number of differences exist, including the role of Mbp1p and identity of additional contributing factors. Further, biochemical data supporting complex composition and a direct demonstration of functional targets of the putative G1/S transcription factor complex was lacking.

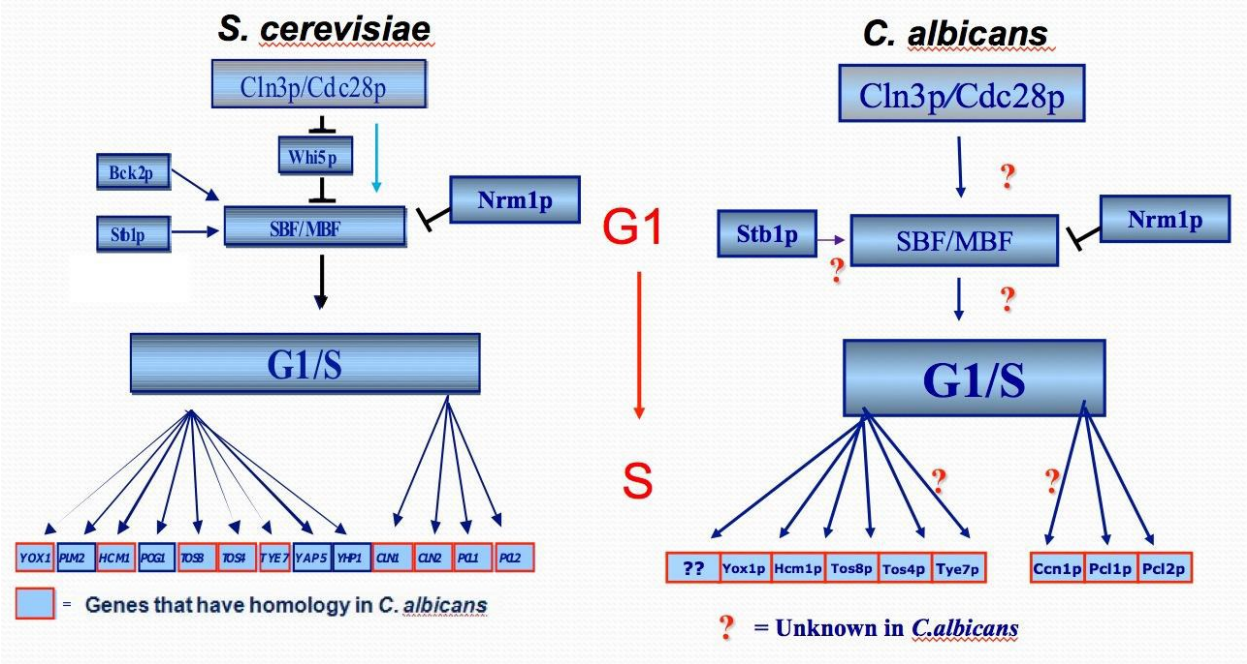

Figure 3. The putative components of G1/S transition pathway in *C.albicans* compared to *S.cerevisiae* (B.Hussein, MSc thesis, 2011).

In order to further address these questions, a previous graduate student in the Bachewich lab carried out a systematic affinity purification of Swi4p, Swi6p and Mbp1p (Yaolin Chen, MSc thesis). Results indicated that Swi6p was the predominant binding factor of Swi4p but also for Mbp1p. Interestingly, affinity purification of Swi4p did not reveal enriched peptides corresponding to Mbp1p, nor did Swi4p co-purify with affinity-purified Mbp1p. This suggested that there may be two separate complexes in *C. albicans*, which contrasts the current model that suggests *C. albicans* contains a single complex composed of Swi4p and Swi6p. However, subsequent co-immunoprecipitation (Co-IP) experiments with strains carrying Mbp1p-TAP and Swi4p-HA, or Swi4p-5MYC and Mbp1p-HA revealed an interaction in the former but not the latter. Thus, the ability of Swi4p and Mbp1p to interact, and the composition and number of the of G1/S transcription complex(es) in *C. albicans* remain unclear.

Further, data from the affinity purification assays revealed additional factors that bind Swi4p and Swi6p that were not previously identified in other systems. For example, a novel interacting factor of Swi6p was determined to be Cdc5p, a polo-kinase involved in mitotic spindle formation and morphogenesis [50]. Furthermore, additional Swi4p interacting factors included a group of regulatory subunits associated with 26S proteasome such as Rpn1p, Rpt6p, and Pr26p. These proteins do not show a physical interaction with Swi4p in *S. cerevisiae*. The findings have important implications for the potential regulation of Swi4p in *C. albicans.*

In order to determine the binding sequence of Swi4p and identity specific targets, Y. Chen also performed a genome-wide location analysis with a tiling array (ChIP-chip). Results showed enriched Swi4p binding at promoter regions of G1 cyclins such as *CCN1* and *PCL2* as well as G1, S phase cell cycle regulatory factors like *YOX1, HSL1* and *RAD53*. Intriguingly, genes associated with filamentous growth were also identified, including important regulators of hyphal growth, such as Efg1p. Given that arresting cells in G1 phase can induce hyphal growth, and cells depleted of Swi4p or Swi6p form filaments, this promoter occupation may reflect a mechanism by which the G1/S machinery could be linked to the hyphal development program. In contrast to the enrichment for MCB elements within G1/S-associated genes indicated by the transcriptional analysis of cell cycle-associated genes in *C. albicans* [42], the Swi4p targets were not enriched for the MCB motif. Rather, a motif related to SBF and similar to the binding site for the transcription factor Ndt80p was identified. However, the analysis was based on a single tiling array.

1.3 Summary

A proper understanding of the G1/S transition in *C. albicans* is important in order to gain more insight about how cell proliferation is regulated and to further identify the specific

mechanisms that link this particular transition stage to hyphal development. Cell proliferation, and differentiation are crucial for virulence of *C.albicans*. Ultimately, potential drug targets could be identified in order to control the development of life-threatening infections in humans. However, the organization of G1/S transcription factor complex is not entirely clear. Additional components that may contribute to the regulation and/or function of this complex remain unknown. Furthermore, validation of direct Swi4p targets and the specific binding sites of Swi4p is required.

1.4 Objectives

The objectives of this study include: 1) characterizing the composition of G1/S transcription factor complex by determining whether Swi4p and Mbp1p interact and validating additional interactors of Swi4p and Swi6p identified in the previous affinity purification system study; and 2) validating an important target of Swi4p identified by ChIP-chip, including Efg1p in order to understand the specific role of Swi4p and its link to the hyphal development pathway.

2. Materials and Methods

2.1 Strains, oligonucleotides and plasmids

Strains, oligonucleotides and plasmids used in this study are shown in Tables 1, 2, and 3 respectively.

Table 1. *Candida albicans* strains used in this study

Strain	Genotype	Parent/Source
AH110	*SWI4-3HA-HIS1/SWI4, Δswi6::URA3/SWI6-TAP-ARG4*	C.Bachewich
AM201.5	*Δswi6::URA3/SWI6-TAP-ARG4*	C.Bachewich
BH114	*Δswi4::hisG/SWI4*	[48]
YC396	*MBP1-TAP-ARG4/MBP1, Δswi6::HIS1/SWI6-3HA-URA3*	YC216
YC367	*Δmbp1::HIS1/MBP1-TAP-URA3*	RM100
YC216	*Δswi6::HIS1/ SWI6-HA-URA3*	BH101
YC221	*SWI6-TAP-URA3/SWI6, Δcln3::hisG/MET::CLN3-ARG4*	BH253
VC132	*MBP1-3HA-HIS1/MBP1, SWI6-TAP-URA3/SWI6, Δcln3::hisG/MET::CLN3-ARG4*	YC221
YC351	*MBP1-HA-URA3/mbp1::HIS1*	BH137
YC101	*SWI4-HA-HIS1/SWI4*	BWP17
VC108	*Δswi4::hisG/SWI4-13MYC-HIS1*	BH114
BH440	BWP17 (pBS-Ca*HIS1,* pBS-Ca*URA3*)	BWP17
VC150	*Δswi4::hisG/SWI4-13MYC-HIS1, MBP1-3HA-ARG4/MBP1*	VC108
VC300	*Δswi4::hisG/SWI4-3HA-URA3*	BH114
VC304	*MBP1-13MYC-HIS1/MBP1*	BWP17
VC324	*MBP1-13MYC-HIS1/MBP1, Δswi4::hisG/SWI4-3HA-URA3*	VC300
VC181	*CDC5-3HA-HIS1/CDC5, SWI6-TAP-URA3/SWI6, Δcln3::hisG/MET::CLN3-ARG4*	YC221
AG625	*CDC5-13MYC-HIS1/CDC5*	C. Bachewich
VC348	*SWI6-3HA-URA3/SWI6, CDC5-13MYC-HIS1/CDC5*	AG625
BH339	*Δswi4::hisG/Δswi4::URA3*	BWP17
VC166	*Δefg1::ARG4/EFG1, Δswi4::hisG/Δswi4::URA3*	BH339
VC171	*Δefg1::ARG4/EFG1*	BWP17
VC199	*Δefg1::ARG4/ Δefg1::HIS1, Δswi4::hisG/Δswi4::URA3*	VC163
VC200	*Δefg1::ARG4/ Δefg1::HIS1*	VC171
VC380	*CDC5/CDC5-3HA-HIS1, Δcln3::hisG/MET::CLN3-ARG4*	BH253
VC426	*SWI6/SWI6-3HA-URA3, Δcdc5::hisG/MET::CDC5-ARG4*	AG500
YC161	(Δ*swi4::URA3/*Δ*swi4::HIS1*, pBS-*ARG4-SWI4)*	BH185

YC171	Δ*swi4::URA3*/Δ*swi4::HIS1*, pBS-*ARG4*	BH185
YC201	Δ*swi6::HIS1*/Δ*swi6::URA3*, pBS-*ARG4-SWI6*	BH120
YC233	Δ*swi6::HIS1*/Δ*swi6::URA3*, pBS-*ARG4*	BH120
YC323	Δ*mbp1::HIS1*/Δ*mbp1::URA3*, pBS-*ARG4-MBP1*	BH261
YC381	Δ*mbp1::HIS1*/Δ*mbp1::URA3*, pBS-*ARG4*	BH261
BH420	BWP17, pRM100-Ca*URA3,* Ca*HIS1*, pBS-Ca*ARG4*	BWP17
BH150	Δ*swi4::hisG/MET3::SWI4-ARG4*	BWP17

Table 2. Oligonucleotides used in this study

Oligo	**Sequence 5'-3'**
AG1F	TTTGAAGCAAGGAAACTTTCAGCATGAAAATGTTCCGGACTGTATG GAGAAGATAATGGTCATCAAAGAAGCTATCAAGAAAAAAGCATTTA AAGAAGCTGGTCGACGGATCCCCGGGTT
AG1R	TATTATATCTCTTGTTTTATAATGAATATGGGCTACAGTTCAATTTGC AGTAGTACTACTAAATAAAAGGATGTTTATTAGCAACGTGAAAGTG GCATATTCGATGAATTCGAGCTCGTT
AG2R	ATAGTTACGATTAGTGGTGG
AG4F	GGTCGACGGATCCCCGGGTTATACCCATACGATGTTCCTGAC
AG4R	TCG ATG AAT TCG AGC TCG TT
AG4F-MBP1-HA	GGTCGACGGATCCCCGGGGAATACCCATACGATGTTCCT
AG4R-MBP1-HA	AGG CGC AGC GGT CGG GCT GA
AG29F	GCTATATAAATATTGCAAATTAATTTCGTTAAGCTGTGGAATTCCAA TGGATGAAATTGAAACTTCGATTGATGCTATGGAAGAATCATTGGTC AAAAAAGGTCGACGGATCCCCGGGGA
AG29R	GAATTGGAAAGTTTGATTAAATTAGCAAAAGAAGCTTATGTGTAGA CATTTATGTATATTTAGTACATAATATTATAATAATAATACAATTGTT CATCATAGGCGCAGCGGTCGGGCTGA
AG30R	GTTATTACTGAAGGCGGTGG
BH14R	AATATTTGTGTTGGCCACATTTGAGTCTGA
CaHIS1F	CCTGCAGCTGATATCCCAGT
CaHIS1R	ACTGGGATATCAGCTGCAGG
CaURA3F	GGTAATACCGTGAAGAAACA
CaARG4F	ACTATGGATATGTTGGCTAC
CaARG4R	ACTATGGATATGTTGGCTAC
EFG1F1	GTGGTGCCCCCATACCTTCC
EFG1R1	GGAACCTGCACCAGAAGCAC
SWI4F1	TAAATATAGAAAATTGCTTAGTTTGAGTTGTGGTGTTAAAGTTGAAG AAATTGACAGTTTAATTGATGGAATTGCCGAATCATTAACTGAAGGT ATGACGGGTCGACGGATCCCCGGGTT
SWI4R1	GACCCAAAGCACAATAAGAAAATGAGCATAAGAGAATTCATTAAGTAGCA GTTATACATTGCCAGTACGATAATTCAAACATAATATTACAATTATTCTAAT CGATGAATTCGAGCTCGTT

SWI4SF1	CTTGAACGTAATCGATTGGTCAATA
SWI4SR1	CCGATGGTGGAATTACCGGAAGATC
SWI6F1	TTCTAAGTTTAAGAAAGTTGTCAGCATATGTACAAATGTTGGTGTAA ACGAAGTTGATGAATTTTTAGACGGGTTGTTGGAAGCAGTGGAAGG ACAACAGGGTCGACGGATCCCCGGGTT
SWI6R1	ATTCAGGAATAGCTGCGGCGCTAAACTCCTATCTGGGTTTGGTATAG AGAGCCATATAAAACAATACACGGGGAATTAGAAGTATACATGTGT TCGATTATCGATGAATTCGAGCTCGTT
SWI6SR1	GATCTTCCGGTAATTCCACCATCGG
VC1F	CAACCAATTGCCCTACCCATCTACTCGCGT
VC1R	CGTGACCTGAGCAACTAATGTGGGAGGCAA
VC2F	GGTTCAGTTCACCCTTCACCCCAACAACAT
VC2R	TACTGCTTGCTGCTTGCTGCTTGCTCGTGC
VC3F	TTGCCTCCCACATTAGTTGCTCAGGTCACGTATAGGGCGAATTGGAG CTC
VC3R	ATGTTGTTGGGGTGAAGGGTGAACTGAACCGACGGTATCGATAAGC TTGA
VC4F	GCTCAAAAGTCTGGAAAGAA
VC4RR	TCTAGTGACGTCTGTGAGTG
VC5F	GTCAGATCAGCANCAAGCTTCTACACCAAGTGGTGGTGCAGAAACT AGATCTGTGCACCAATCACCCCAAGTTCAGTCATGGTCGACGGATCC CCG GGTT
VC5R	TATTACTTTTCTTCTTTGGCAACAGTGCTAGCTGATTGATTAGCTTGA TGTTGTTGGGGTGAAGGGTGAACTGAACCTTGTCGATGAATTCGAGC TCGTT
VC6F	AAGCTGTGGAATTCCAATGGATGAAATTGAAACTTCGATTGATGCTA TGGAAGAATCATTGGTCAAAAAAGGTGGTGGTCGGATCCCCGG GTT AAT TAA
VC6R	TAGTGAATTGGAAAGTTTGATTAAATTAGCAAAAGAAGCTTATGTGT AGACATTTATGTATATTTAGTACGAATTCCGGAATATTTATGA GAAAC
VC8F	ATGAATGGATAAGTTTGAGTAGTTCATTAGAAGGGGTTGTTATTTTG AAAAAGAATCCAGAATATATGGAAATTGATAGTGGTCGACGGATCC CCGGGTT
VC8R	AACTTTAGTAAATAGTTTTGTCTTACCCTTATAAACAATTAATCAAC TAACTAACAAACTAACAAACTAACAAACTAAACTCGATGAATTCGA GCTCGTT
VC9F	AGTTGGTCAAGCAGTTGATG
VC9R	ACCTATTCTGGTGGTCGTAG
YC15R	GGTGGTACATGTACTATTGCTCATAGACTTAG
YC21F	ACGAAAGAGAAGTATCTGGAGATGAATCAA
YC25F	TGGTGTTAAAGTTGAAGAAATTGACAGTTTAATTGATGGAATTGCCG AATCATTAACTGAAGGTATG ACG
YC25R	GAGAATTCATTAAGTAGCAGTTATACATTGTTAGTACGATAATTCAA ACATAATATTACAATTATTCTAA

Table 3. Plasmids used in this study

Plasmid	Description	Parent/Source
pBS-Ca*HIS1*	pBluescript Ca*HIS1*	C.Bachewich
pBS-Ca*ARG4*	pBluescript Ca*ARG4*	H.Huang
pFA-HA-Ca*HIS1*		[51]
pFA-HA-Ca*URA3*		[51]
pMG2093		[52, 53]

2.2 Medium and Growth Conditions

Most strains were grown at 30ºC in YPD medium containing 1% yeast extract, 2% peptone and 2% glucose. Conditional strains were grown at 30ºC in synthetic complete (SC) medium containing 0.67% yeast nitrogen base, 2% glucose and amino acids supplemented with or without 2.5 mM methionine and 0.5 mM cysteine for repression or induction of the *MET3* promoter, respectively [54]. All media were supplemented with 100 mg/L of uridine, histidine or arginine to allow optimal growth of *URA3*+, *HIS1*+ or *ARG4*+ auxotrophs [55], except under conditions of selection. For assays involving protein extraction, strains were incubated overnight in YPD medium at 30°C, diluted into fresh medium to an $O.D._{600nm}$ of 0.1 to 0.2, and incubated until the $O.D._{600nm}$ reached 0.8-1.0. In the case of the *MET3p-CLN3* conditional strain, cells were incubated overnight at 30°C in SC medium lacking methionine, then diluted into fresh SC medium containing 2.5mM methionine and 0.5mM cysteine and incubated for 4 h to block cells in G1 phase.

2.3 Construction of strains

2.3.1 *SWI4*

2.3.1.1 *SWI4-13MYC*

In order to tag the 3' end of *SWI4* with 13 copies of the MYC epitope, oligonucleotides YC25F and YC25R containing 70 bp homologous to regions immediately upstream and downstream of the *SWI4* stop codon, respectively, as well as 20 bp homology to plasmid pMG2093 [52, 53] were used to amplify 3.9 kb fragment containing the 13*MYC-HIS1* cassette. The PCR reaction mix was composed of 0.6 µM oligonucleotides, 0.4 mM dNTPs, 50 ng of pMG2093 as template, 3.75U of Expand Long Template Polymerase (Roche), and 10X Buffer 3. The reaction conditions were the following: 94℃ for 4 min, followed by 25 cycles of 94℃ for 1 min, 44℃ for 1 min, 68℃ for 3 min, 45 sec, followed by a 7 min extension at 68℃ and storage at 4℃. The product was purified using a PCR purification kit (OMEGA) and 10 µg were transformed into strain BH114 (*Δswi4::hisG/SWI4*), resulting in strain VC108 (*Δswi4::hisG/SWI4-13MYC-HIS1*).

2.3.1.2 *SWI4-3HA*

In order to tag *SWI4* with 3 copies of the hemagglutinin (HA) epitope at the C-terminal, oligonucleotides AG4F and AG4R were used to amplify a 1.7 kb *HA-URA3* fragment from plasmid pFA-HA-Ca*URA3* [56]. The PCR reaction mix included 0.6 µM oligonucleotides, 0.4 mM dNTPs, 100 ng of template, 3.75U of Expand Long Template Polymerase, and 10X Buffer 3. The PCR reaction conditions were: 94℃ for 4 min, followed by 25 cycles of 94℃ for 1 min, 40℃ for 1 min, 68℃ for 1 min, 44 sec, followed by a 7 min extension at 68℃ and storage at 4℃. Next, oligonucleotides SWI4F1 and SWI4R1 were used to amplify a final 1.9 kb fragment from the product of the previous PCR reaction, consisting of *HA-URA3* surrounded by 100 bp sequences homologous to regions flanking either side of the stop codon of *SWI4*. Reaction conditions used were: 94℃ for 4 min, followed by 25 cycles of 94℃ for 1 min, 40℃ for 1 min, 68℃ for 1 min, 56 sec, followed by a 7 min extension at 68℃ and storage at 4℃. The resulting

final product was purified and 7 μg were transformed into strain BH114 (*Δswi4::hisG/SWI4*), resulting in strain VC300 (*Δswi4::hisG/SWI4-3HA-URA3*).

2.3.2 *MBP1*

2.3.2.1 *MBP1-3HA*

Oligonucleotides AG4F-MBP1-HA and AG4R-MBP1-HA were used to amplify a 1.4 kb *HA-HIS1* fragment from plasmid pFA-HA-Ca*HIS1* [56]. The PCR reaction mix included 0.6 μM oligonucleotides, 0.4 mM dNTPs, 100 ng of template, 3.75U of Expand Long Template Polymerase, and 10X Buffer 3. The reaction conditions included 94℃ for 4 min, followed by 25 cycles of 94℃ for 1 min, 52℃ for 1 min, 68℃ for 2 min, 45 sec, followed by a 7 min extension at 68℃ and storage at 4℃. The resulting fragment was used as a template, with oligonucleotides AG29F and AG29R, in order to produce a final 2.6 kb fragment consisting of an *HA-HIS1* cassette and 100 bp sequences homologous to regions flanking either side of the stop codon of *MBP1*. The PCR reaction mix included 0.6 μM oligonucleotides, 0.4 mM dNTPs, 100 ng of template, 3.75U of Expand Long Template Polymerase, and 10X Buffer 3. The reaction conditions included 94℃ for 4 min, followed by 25 cycles of 94℃ for 1 min, 55℃ for 1 min, 68℃ for 2 min, 45 sec, followed by a 7 min extension at 68℃ and storage at 4℃. The final product was purified, and 6.2 μg were transformed into strain YC221 (*SWI6-TAP-URA3/SWI6, Δcln3::hisG/MET::CLN3-ARG4*), resulting in strain VC132 (*MBP1-3HA-HIS1/MBP1*, *SWI6-TAP-URA3/SWI6, Δcln3::hisG/MET::CLN3-ARG4*).

MBP1 was similarly tagged with 3 copies of *HA* epitope at the C-terminus in strain VC108 (*Δswi4::hisG/SWI4-13MYC-HIS1*), with the difference of using plasmid pFA-HA-Ca*ARG4* in the first step PCR reaction with the following conditions: 94℃ for 4 min, followed

by 25 cycles of 94℃ for 1 min, 52℃ for 1 min, 68℃ for 3 min, followed by a 7 min extension at 68℃ and storage at 4℃. The product was used as template in a second PCR reaction as described above, with the following conditions: 94℃ for 4 min, followed by 25 cycles of 94℃ for 1 min, 52℃ for 1 min, 68℃ for 3 min, 15 sec, followed by a 7 min extension at 68℃ and storage at 4℃. The product was purified and 5 µg were transformed into strain VC108 (*Δswi4::hisG/SWI4-13MYC-HIS1*), resulting in strain VC150 (*Δswi4::hisG/SWI4-13MYC-HIS1, MBP1-3HA-ARG4/MBP1*).

2.3.2.2 *MBP1-13MYC*

In order to tag the C-terminus of *MBP1* with 13 copies of the MYC epitope, oligonucleotides VC6F and VC6R containing 70 bp homologous to region*s* upstream and downstream of the *MBP1* stop codon, respectively, as well as 20 bp homology to plasmid pMG2093 [52, 53] were used to amplify 3.8 kb fragment containing 13*MYC-HIS1*. The PCR reaction mix was composed of 0.6 µM oligonucleotides, 0.4 mM dNTPs, 50 ng of pMG2093 as template, 3.75U of Expand Long Template Polymerase, and 10X Buffer 3. The reaction conditions were the following: 94℃ for 4 min, followed by 25 cycles of 94℃ for 1 min, 41℃ for 1 min, 68℃ for 3 min, 50 sec, followed by a 7 min extension at 68℃ and storage at 4℃. The product was purified and 6.2 µg were transformed into strains VC300 (*Δswi4::hisG/SWI4-3HA-URA3*) and BWP17, resulting in strains VC324 (*MBP1-13MYC-HIS1/MBP1, Δswi4::hisG/SWI4-3HA-URA3*) and VC304 (*MBP1-13MYC-HIS1/MBP1*), respectively.

2.3.3 *SWI6*

2.3.3.1 *SWI6-3HA*

In order to tag *SWI6* at the C-terminus with 3 copies of the HA epitope, a similar two-step PCR strategy described for tagging *SWI4* with HA was utilized, with the exception of using oligonucleotides SWI6F1 and SWI6R1 to amplify a final 1.9 kb fragment from the first PCR, consisting of *HA-URA3* and 100 bp sequences homologous to regions flanking the stop codon of *SWI6*. Reaction conditions for this second PCR reaction included: 94℃ for 4 min, followed by 25 cycles of 94℃ for 1 min, 40℃ for 1 min, 68℃ for 1 min, 56 sec, followed by a 7 min extension at 68℃ and storage at 4℃. The resulting final product was purified and 6.7 μg were transformed into strain AG625 (*CDC5-13MYC-HIS1/CDC5*), resulting in strain VC348 (*SWI6-3HA-URA3/SWI6, CDC5-13MYC-HIS1/CDC5*).

2.3.4 *CDC5*

2.3.4.1 *CDC5-3HA*

In order to tag *CDC5* at the C-terminus with 3 copies of the HA epitope, a similar two-step PCR strategy described for tagging *SWI4* with HA was utilized, with the exception of using plasmid pFA-HA-Ca*HIS1* [56] and oligonucleotides AG4F and AG4R for the first PCR amplification. Reaction conditions used were: 94℃ for 4 min, followed by 25 cycles of 94℃ for 1 min, 40℃ for 1 min, 68℃ for 1 min, 10 sec, followed by a 7 min extension at 68℃ and storage at 4℃. The resulting fragment was purified and used as the template with oligonucleotides AG1F and AG1R to amplify a final 2.0 kb fragment consisting of an *HA-HIS1* cassette and 100 bp sequences homologous to regions flanking the stop codon of *CDC5*. The following reaction conditions were used: 94℃ for 4 min, followed by 25 cycles of 94℃ for 1 min, 40℃ for 1 min, 68℃ for 2 min, followed by a 7 min extension at 68℃ and storage at 4℃. The final product was purified and 7.1 μg were transformed into strains YC221 (*SWI6-TAP-URA3/SWI6,*

Δcln3::hisG/MET::CLN3-ARG4) and BH253 (*Δcln3::hisG/MET::CLN3-ARG4*) to obtain strains VC181 (*CDC5-3HA-HIS1/CDC5, SWI6-TAP-URA3/SWI6, Δcln3::hisG/MET::CLN3-ARG4*) and VC380 (*CDC5-3HA-HIS1*, *Δcln3::hisG/MET::CLN3-ARG4*), respectively.

2.3.5 *RPN1*

2.3.5.1 *RPN1-3HA*

In order to tag the C-terminus of *RPN1* with 3 copies of HA in strains VC108 and BWP17, the two step PCR strategy described above for tagging strains with HA was utilized. Exceptions include use of oligonucleotides VC8F and VC8R to amplify the final 1.9 kb PCR product with the following reaction conditions: 94℃ for 4 min, followed by 25 cycles of 94℃ for 1 min, 40℃ for 1 min, 68℃ for 1 min, 54 sec, followed by a 7 min extension at 68℃ and storage at 4℃. The resulting final product was purified and 6.0 μg were transformed into strains VC108 (*Δswi4::hisG/SWI4-13MYC-HIS1*) and BWP17, resulting in strains VC389 (*RPN1-3HA-URA3/RPN1*, *Δswi4::hisG/SWI4-13MYC-HIS1)* and VC394 (*RPN1-3HA-URA3/RPN1*).

2.3.6 *EFG1*

2.3.6.1 Δ*efg1*/Δ*efg1*

In order to create a *SWI4*-conditional strain that lacked *EFG1,* both alleles were replaced with the *ARG4* and *HIS1* markers, using 2-step PCR fusion constructs. First, a 709 bp fragment corresponding to the 5' flank of *EFG1*, located 127 bp upstream of the start codon, was amplified from gDNA with oligonucleotides VC1F and VC1R. The components of the PCR reaction mix include 0.6 μM oligonucleotides, 0.4 mM dNTPs, 100 ng of template, 3.75U of Expand Long Template Polymerase (Roche), and 10X Buffer 3. The following reaction

conditions were used: 94°C for 3 min, followed by 25 cycles of 94°C for 30 sec, 54°C for 30 sec, 68°C for 41 sec, followed by a 7 min extension at 68℃ and storage at 4℃. Second, a 616 bp fragment corresponding to the 3' flank of *EFG1,* located 5 bp after the stop codon, was similarly amplified using oligonucleotides VC2F and VC2R. The following reaction conditions were used: 94°C for 3 min, followed by 25 cycles of 94°C for 30 sec, 53°C for 30 sec, 68°C for 35 sec, followed by a 7 min extension at 68℃ and storage at 4℃. To amplify the 2193 bp *ARG4* fragment from plasmid pBS-Ca*ARG4* (H. Huang), oligonucleotides VC3F and VC3R containing homology to the plasmid plus additional 30 bp sequences that were the reverse complement of oligonucleotides VC1R and VC2F, respectively, were utilized. The components of the PCR reaction mix include 0.6 μM oligonucleotides, 0.4 mM dNTPs, 100 ng of pBS-Ca*ARG4* as template, 3.75U of Expand Long Template Polymerase, and 10X Buffer 3. The following reaction conditions were used: 94°C for 3 min, followed by 25 cycles of 94°C for 30 sec, 61°C for 30 sec, 68°C for 2 min, 12 sec, followed by a 7 min extension at 68℃ and storage at 4℃. The final construct was created by amplifying a 1:2:1 (50ng:100ng:50ng) amount of the three PCR fragments with oligonucleotides VC1F and VC2R. The reaction mix included 0.6 μM oligonucleotides, 0.4 mM of dNTPs, 3.75U of Expand Long Template Polymerase, and 1X Buffer 3. The following reaction conditions were used: 94°C for 3 min, followed by 10 cycles of 94°C for 10 sec, 61°C for 30 sec, and 68°C for 3 min 28 sec, followed by 15 cycles of 95°C for 10 sec, 61°C for 30 sec, 68°C for 3 min 28 sec with a 20 sec auto-segment extension, followed by a 7 min extension at 68℃ and storage at 4℃. The final 3400 bp PCR product was purified and 7.5 μg or 5.6 μg were transformed into strain BH339 (*Δswi4::hisG/Δswi4::URA3*) or BWP17, resulting in strains VC166 (*Δefg1::ARG4/EFG1, Δswi4::hisG/Δswi4::URA3*) and VC171 (*Δefg1::ARG4/EFG1*), respectively.

To delete the second copy of *EFG1,* a similar strategy was utilized with the exception of amplifying a 1404 bp *HIS1* cassette fragment from plasmid pBS-Ca*HIS1*, with oligonucleotides VC3F and VC3R. The following reaction conditions were used: 94°C for 3 min, followed by 25 cycles of 94°C for 30 sec, 61°C for 30 sec, 68°C for 1 min 24 sec, followed by a 7 min extension at 68℃ and storage at 4℃. The final fusion construct was created by amplifying 1:2:1 (50ng:100ng:50ng) amount of the three PCR fragments with oligonucleotides VC1F and VC2R in a reaction with the following conditions: 94°C for 3 min, followed by 10 cycles of 94°C for 10 sec, 61°C for 30 sec, and 68°C for 2 min 37 sec, followed by 15 cycles of 95°C for 10 sec, 61°C for 30 sec, 68°C for 2 min 37 sec with a 20 sec auto-segment extension, followed by a 7 min extension at 68℃ and storage at 4℃. The final 2611 bp product was purified and 6.25 μg or 6.35 μg were transformed into strains VC166 (*Δefg1::ARG4/EFG1, Δswi4::hisG/Δswi4::URA3*) and VC171 (*Δefg1::ARG4/EFG1*), resulting in strains VC199 (*Δefg1::ARG4/Δefg1::HIS1, Δswi4::hisG/Δswi4::URA3*) and VC200 (*Δefg1::ARG4/ Δefg1::HIS1*), respectively.

2.4 Transformation

C. albicans was transformed according to [57], with a few modifications. Briefly, the One-Step-Buffer (OSB) consisted of 25 μl of 10 mg/ml salmon sperm DNA (ssDNA) (Invitrogen), 0.0154g of dithiothreital (DTT), 800 μl of 50% PEG 4000 (Sigma) and 200 μl of 1 M lithium acetate. A pellet obtained from centrifuging 300 μl of an overnight cell culture at 13,000 rpm for 3 min was washed with sterile water and re-suspended in 100 μl of OSB solution. A maximum volume of 10 μl of approximately 5-7 μg of DNA was added. The mixture was vortexed for 1 min, incubated overnight at 30°C, heat-shocked at 43℃ for 1 h and plated on

selective solid medium. Transformants were subsequently streaked to single colony three times before screening. For strains containing *CLN3* under control of the *MET3* promoter, cells were grown overnight in an inducing medium lacking methionine and cysteine (-MC), then transferred into rich YPD medium for 2 h prior to collection, to increase the transformation efficiency.

2.5 Genomic DNA extraction

For gDNA extraction, the method of [58] was utilized. Briefly, cells were inoculated into 5 ml of YPD medium or -MC medium that lacked methionine and cysteine, and incubated overnight at 30°C. Cell cultures were then centrifuged for 5 min at 3000 rpm, the pellet was washed with 700 µl sterile distilled water, and re-suspended in 1 ml of sorbitol buffer (1M sorbitol, 0.1M EDTA) followed by the addition of 10 µl of lyticase ((10U/µl); Sigma) and 2 µl of 4.0 M DTT. The mixture was incubated at 37°C for 1.5 h, centrifuged for 2 min at 13500 rpm, and the supernatant was removed. The pellet was re-suspended in 200 µl Tris-EDTA solution (50 mM Tris, 20 mM EDTA), and SDS was added to 1%. Cells were incubated at 65°C for 30 min, followed by the addition of 100 µl of 5.0 M potassium acetate (KAc). This mixture was incubated on ice for 60 min, and centrifuged for 10 min at 13500 rpm. An equal amount of 100% isopropanol was added to the supernatant. The samples were mixed for 1 min, centrifuged at 13500 rpm for 1 min, and the resulting DNA pellet was washed with 70% ethanol. After air-drying, the pellet was re-suspended into 100 µl of TE buffer (1 mM EDTA, 10 mM Tris-HCl pH 8.0) with 2 µl of RNaseA (10 mg/ml), and incubated at 37°C for 30 min. The concentration of the extracted genomic DNA was determined using a fluorometer (Hoefer DQ300) and Hoechst Dye (Invitrogen).

2.6 Screening transformants

Transformants were screened for correct integration of DNA constructs using PCR. The PCR reaction mix consisted of 0.6 µM of oligonucleotides, 0.4 mM of dNTPs, 100 ng of gDNA as template, 3 mM of $MgCl_2$, 1X Taq Buffer with $(NH_4)_2SO_4$ and 5 U Taq DNA Polymerase (Fermentas). Confirmation of strain VC108 (*Δswi4::hisG/SWI4-13MYC-HIS1*) was done using oligonucleotides YC21F located 743 bp upstream and BH14R which locates 766 bp downstream of stop codon to amplify a 5000 bp product. For this screening, 3.75U of Expand Long Template Polymerase (Roche) and 10X buffer were used due to the large PCR product size. The following reaction conditions were used: 94℃ for 3min, 30 cycles of 94℃ for 30 sec, 48℃ for 30 sec, 68℃ for 5 min, followed by a 7 min extension at 68℃ and storage at 4℃. To confirm strain VC132, oligonucleotides CaHIS1F (located inside the plasmid pFA-HA-Ca*HIS1*), and AG30R (located 427 bp downstream of stop codon of *MBP1*) were used to amplify a 1923 bp product. The reaction conditions used were as follows: 95℃ for 3min, 30 cycles of 95℃ for 30 sec, 42℃ for 30 sec, 72℃ for 2 min 32 sec, followed by a 7 min extension at 72℃ and storage at 4℃. Strain VC150 was confirmed with oligonucleotides CaARG4F, located inside the plasmid pFA-HA-Ca*ARG4* and YC15R, located 224 bp downstream of stop codon of *MBP1*, to amplify a 1264 bp product. The following reaction conditions were used: 95℃ for 3 min, 30 cycles of 95℃ for 30 sec, 36℃ for 30 sec, 72℃ for 1 min 16 sec, followed by a 7 min extension at 72℃ and storage at 4℃. Confirmation of strain VC300 was done by using oligonucleotides SWI4SF1, which locates 145 bp upstream of stop codon of *SWI4*, and SWI4SR1, which locates 252 bp downstream of stop codon of *SWI4*, to amplify a 2046 bp product. The reaction conditions used were as follows: 94℃ for 3 min, 30 cycles of 94℃ for 30 sec, 44℃ for 30 sec, 68℃ for 2 min 3 sec, followed by a 7 min extension at 68℃ and storage at 4℃. The strain VC324 was confirmed by using

oligonucleotides CaHIS1F, located inside the plasmid pMG2093 and YC15R, located 224 bp downstream of stop codon of *MBP1*, to amplify a 970 bp product. The following reaction conditions were used: 95℃ for 3 min, 30 cycles of 95℃ for 30 sec, 36℃ for 30 sec, 72℃ for 58 sec, followed by a 7 min extension at 72℃ and storage at 4℃. Confirmation of strain VC181 was done by using oligonucleotides CaHIS1F (located inside the plasmid pFA-HA-Ca*HIS1*) and AG2R, which locates 258 bp downstream of stop codon of *CDC5,* to amplify a 1773 bp product. The following reaction conditions were used: 95℃ for 3 min, 30 cycles of 95℃ for 30 sec, 38℃ for 30 sec, 72℃ for 1 min 46 sec, followed by a 7 min extension at 72℃ and storage at 4℃. The strain VC348 was confirmed by using oligonucleotides CaURA3F (located inside the plasmid pFA-HA-Ca*URA3*) and SWI6SR1, located 307 bp downstream of stop codon of *SWI6*, to amplify an 898 bp product. Confirmation of VC163 and VC171 was done by using oligonucleotides VC4F, located 920 bp upstream of start codon of *EFG1* and CaARG4R, located inside the plasmid pFA-HA-Ca*ARG4*, to amplify a 1200 bp product. The reaction conditions used were as follows: 95℃ for 3 min, 30 cycles of 95℃ for 30 sec, 38℃ for 30 sec, 72℃ for 2 min 10 sec, followed by a 7 min extension at 72℃ and storage at 4℃. The strains VC199 and VC200 were confirmed using oligonucleotides VC4F, located 920 bp upstream of start codon of *EFG1* and CaHIS1R, located inside the plasmid pFA-HA-Ca*HIS1*, to amplify a 1348 bp product. The following reaction conditions were used: 95℃ for 3 min, 30 cycles of 95℃ for 30 sec, 38℃ for 30 sec, 72℃ for 1 min 21 sec, followed by a 7 min extension at 72℃ and storage at 4℃. Confirmation of VC389 and VC394 was done using oligonucleotides CaURA3F, located inside the plasmid pFA-HA-Ca*URA3* and VC9R, located 225 bp downstream of stop codon of *RPN1*, to amplify an 892 bp product. Reaction conditions used were as follows: 95℃ for 3 min, 30

cycles of 95℃ for 30 sec, 36℃ for 30 sec, 72℃ for 54 sec, followed by a 7 min extension at 72℃ and storage at 4℃.

2.7 Protein extraction and Western blotting

Protein was extracted according to the method outlined in [59]. Briefly, cells were inoculated into 2 ml of YPD or -MC minimal medium, incubated overnight at 30°C, diluted to an OD_{600nm} of 0.1 into a final volume of 50 ml, and incubated at 30°C until an OD_{600nm} of 0.8-1.0 was reached. Cell pellets were obtained by centrifugation for 5 min at 3000 rpm. The pellets were washed with sterile water, lyophilized for 24 h in a freeze dryer (ThermoSavant, Modulyo D), and ground to a fine powder using a sterile toothpick. Subsequently, 1 ml of cold HK buffer (25 mM TRIS pH7.5, 0.5% NP40, 300 mM NaCl, 5 mM EDTA pH8.0, 15 mM EGTA pH8.0, 60 mM Beta Gly.PO_4, 500 μM Na Vanadate, 10 mM Na Fluoride, 1 μg/ml Pepsatin A, 10 μg/ml Leupeptin, 10 μg/ml Trypsin ChymoT inhibitor, 10 μg/ml Aprotinin, 10 μg/ml TPCK, 2 mM TAME, 5 mM Benzamidine, 250 μg/ml PMSF, 1 mM DTT) per 0.8 g dry weight was added. The samples were vortexed 4X 10 sec with a 3 min break on ice in between rounds, and centrifuged at 13,500 rpm for 10 min at 4°C to remove cell debris. The supernatant was then centrifuged at 13,500 rpm for 30 min (for Western confirmation, but 1 h for Co-IPs) at 4°C and stored at -80°C. Protein concentration was determined using the Bradford assay.

For Western blotting, 30 μg of protein was separated on 7.5% SDS PAGE gels, and transferred to a polyvinyl difluoride (PVDF) membrane (BIO-RAD) overnight at 30V and 4°C. The membrane was air-dried completely, incubated in blocking solution (5% milk in 1X TBST with 0.05% Tween-20) for 90 min, washed 3 x with 1X TBST (50 mM Tris, 0.15 M NaCl, 0.05% Tween-20, pH 7.6) for 10 min each, followed by incubation with primary antibody diluted

in 1X TBST for 2 h. Primary antibodies included mouse monoclonal antibody clone 9E10 IgG (Roche Diagnostics, 1:1000 dilution) and mouse monoclonal antibody clone 12CA5 (Roche Diagnostics, 1:500 dilution). The membrane was washed 3 x with 1X TBST for 10 min each, and then incubated with secondary antibody (Goat anti-rabbit IgG-HRP, Santa Cruz Biotechnology, 1:10000 dilution) for 1 h. After washing 3 x with 1X TBST for 10 min each, signal was detected with chemiluminescence using ECL (GE Healthcare). Membranes were stripped in 15 ml of stripping solution (0.4% SDS, 1.2 mM Tris pH 6.8, 0.25g DTT) for 30 min at 50°C.

2.8 Co-Immunoprecipitation (Co-IP)

Cultures were obtained and protein extracted as described above with the exception that 1 L culture volumes were utilized. For Co-IP, Mono HA 11 Affinity beads (Covance), mouse monoclonal anti-Myc on Sepharose beads (Covance) or IgG Sepharose 6 Fast Flow beads (GE Healthcare) were utilized. Briefly, volumes of bead slurry were centrifuged at 1500 x g for 2 min at 4°C to remove the buffer, and washed 3 x in 500 µl of HK buffer. The beads were then suspended in fresh HK buffer and combined with protein. For 40, 20 or 2 mg of protein, 60, 40 or 10 µl of bead slurry were utilized, respectively. The samples were incubated overnight at 4°C with rocking, centrifuged at 1500 x g for 2 min at 4°C, and washed 5 x with 1 ml HK buffer. Protein was then eluted from beads by boiling in same amount as bead volume plus an additional 10 µl of 1X SDS sample buffer (50 mM Tris pH 6.8, 2% SDS, 0.01% Bromophenol blue, 10% Glycerol, 100mM DTT) for 10 min. The samples were centrifuged for 2 min at 13500 rpm at room temperature. The bead pellets were boiled again in same amount of 1X SDS sample buffer as bead volume (1:1) for 10 min. Samples were subsequently loaded onto SDS PAGE gels for Western blotting as described.

2.9 RNA extraction and Northern blotting

For RNA extraction, 50 ml of culture at an OD_{600nm} of 0.8-1.0 were collected through centrifugation for 5 min at 5000 rpm. The pellet was washed with sterile water and lyophilized in a freeze dryer. Freeze-dried cell pellet was ground to fine powder using a sterile toothpick and RNA extracted according to [60]. Briefly, 1 ml of TRI reagent (Molecular Research Center, Inc.) was added to 100 µl of dried pellet. The samples were vortexed 10 x, 10 sec followed by incubation for 5 min at room temperature. After addition of 0.2 ml of chloroform, samples were shaken vigorously for 15 sec, incubated at room temperature for 5 min, and then centrifuged at 12000 x g for 15 min at 4°C. The supernatant was transferred to new Eppendorf tubes, to which 0.5 ml of cold isopropanol was added. The tubes were inverted 3 x, incubated on ice for 5 min, then centrifuged at 12000 x g for 8 min at 4°C. The resulting RNA pellet was washed twice with 1 ml of ice-cold 70% DEPC-treated ethanol, and tubes were left on ice for 5 min for complete evaporation. The RNA pellet was re-suspended in 60 µl of ice-cold DEPC-treated water by incubation at 60°C for 10 min. To re-precipitate the RNA, one-tenth volume of 3M sodium acetate and 3X the volume of 100% ethanol were added and samples were stored at -20°C overnight. Samples were subsequently centrifuged at 13000 rpm for 10 min at 4°C to remove ethanol followed by washing 2 x with 70% DEPC-treated ethanol. The pellet was then air-dried and dissolved with 50 µl DEPC water. The concentration of samples was next measured using a spectrophotometer.

Northern blotting was performed according to [61]. DNA probes were amplified by PCR. The reaction mix consisted of 0.6 µM oligonucleotides, 0.4 mM dNTPs, 100 ng of gDNA, 3.75U of Expand Long Template Polymerase (Roche), and 10X Buffer 3. The *EFG1* probe utilized oligonucleotides EFG1F1 and EFG1R1 with the following reaction conditions: 94℃ for

4 min, followed by 25 cycles of 94℃ for 1 min, 40℃ for 1 min, 68℃ for 1 min, 10 sec, followed by a 7 min extension at 68℃ and storage at 4℃.

3. Results

3.1 Organization of the G1/S transcription factor complex

3.1.1 Co-immunoprecipitation utilizing low amounts of input protein confirms that Swi6p physically interacts with Swi4p and Mbp1p.

Previous work from the Bachewich lab (Y. Chen, MSc thesis) showed that Swi6p was the major interacting factor of Swi4p and Mbp1p via affinity purification and mass spectrometry analyses. These physical interactions were subsequently confirmed via Co-IP. However, 40 mg of protein was used for these experiments. In order to determine whether the physical interactions could be detected with lower amounts of protein, I repeated the Co-IPs with 2 mg of protein. For testing an interaction between Swi4p and Swi6p, strains AH110 (*SWI4-3HA-HIS1/ SWI4,* Δ*swi6::URA3/SWI6-TAP-ARG4*), AM201.5 (Δ*swi6::URA3/SWI6-TAP-ARG4*), and YC113 (Δ*swi4::hisG/SWI4-3HA-HIS1*) were incubated at 30 °C until they reached an O.D. $_{600nm}$ of 0.8, collected and protein was extracted. A total of 2 mg was incubated with anti-HA or IgG-sepharose beads for Co-IP reactions. When Swi4p-3HA was precipitated with anti-HA beads, Swi6p-TAP co-purified (Fig. 4A). Furthermore, Swi4p-3HA was present in the pull down when Swi6p-TAP was precipitated with IgG sepharose (Fig. 4B). The detection of either protein in reciprocal Co-IPs using lower amounts of input protein supports a physical interaction.

In order to determine whether an interaction between Swi6p and Mbp1p could also be detected with lower input levels of protein, strains YC396 (*MBP1-TAP-ARG4/MBP1, Δswi6::HIS1/SWI6-3HA-URA3*), YC367 (*Δmbp1::HIS1/MBP1-TAP-URA3*), and YC216 (Δ*swi6::HIS1/SWI6-3HA-URA3*) were utilized in Co-IP experiments as described above. When Swi6p-3HA was precipitated from 2 mg of protein with anti-HA beads, Mbp1p-TAP co-purified (Fig. 5A). In addition, when Mbp1p-TAP was precipitated with IgG sepharose, Swi6p-3HA was detected (Fig. 5B). Thus, Swi6p also strongly interacts with Mbp1p.

Previous work showed that Mbp1p was not among the enriched peptides that co-purified with Swi6p when affinity purified from cells blocked in G1 phase (Y. Chen, MSc thesis). In order to confirm whether Swi6p and Mbp1p interact during G1 phase, a Co-IP was performed. For this, a strain carrying a conditional allele of the G1 cyclin *CLN3* and one allele of *SWI6* tagged with TAP (YC221; *SWI6-TAP-URA3/SWI6,* Δ*cln3::hisG/MET::CLN3-ARG4*), was transformed with a DNA construct that would tag a single copy of *MBP1* at the C-terminus with three copies of HA, resulting in strain VC132 (*MBP1-3HA-HIS1/MBP1, SWI6-TAP-URA3/SWI6,* Δ*cln3::hisG/MET::CLN3-ARG4*) (Fig. 6). Strains VC132 and control strain YC221 were incubated in inducing (-MC) media overnight, then diluted into repressing (+MC) media and incubated at 30°C for 4 h. When Mbp1p-3HA was pulled out using anti-HA beads, Swi6p-TAP co-purified (Fig. 7), suggesting that the proteins do interact in G1-phase-blocked cells. A reverse Co-IP using IgG beads was not done due to strong non-specific cross-reaction problems associated with the TAP tag. Thus, Swi6p interacts with Mbp1p in G1 phase cells.

3.1.2 Swi4p and Mbp1p do not physically interact in the manner that Swi6p binds Swi4p or Mbp1p.

Since Swi6p binds both Swi4p and Mbp1p, this suggests that *C. albicans* may either contain two separate complexes, as seen in *S. cerevisiae* or one complex that includes Mbp1p. In the case of the latter, it is predicted that Swi4p and Mbp1p should physically interact. However, previous attempts to test for this interaction were inconclusive. Although Swi4p-HA co-purified with Mbp1p-TAP that was pulled out from 40 mg of protein (Y. Chen thesis), the proteins were similar in size, and the reverse Co-IP showed non-specific binding to beads. Further, when a strain carrying Swi4p-5MYC and Mbp1p-3HA was utilized, Swi4p-5MYC did not co-purify with affinity-purified Mbp1p-3HA. In order to further address this question, a new strain was constructed whereby a single copy of *SWI4* in strain BH114 (Δ*swi4::hisG/SWI4*) was tagged with 13 copies of MYC at the C-terminus in order to enhance the MYC detection, resulting in strain VC108 (Δ*swi4::hisG/SWI4-13MYC-HIS1*). Western blotting confirmed that the protein was expressed (Fig. 8). Next, *MBP1* was tagged with 3 copies of HA in strain VC108, resulting in strain VC150 (Δ*swi4::hisG/SWI4-13MYC-HIS1, MBP1-3HA-ARG4/MBP1)* (Fig. 9). Strains VC150, VC108 and YC351 (Δ*mbp1::HIS1/MBP1-3HA-URA3)* were subsequently used for Co-IP experiments. When Mbp1p-3HA was precipitated from 40 mg of protein with anti-HA beads, Swi4p-13MYC was not present in the pull down, suggesting that these two proteins do not interact (Fig. 10A). In contrast, a reverse Co-IP using anti-MYC beads to precipitate Swi4p-13MYC was inconclusive, since there was strong non-specific cross-reaction in the control strain (Fig. 10B). In order to determine whether the anti-MYC beads would bind other proteins non-specifically, immunoprecipitation with anti-MYC beads was performed with strain YC101 (*SWI4-3HA-HIS1/SWI4*) and a second strain containing *MBP1-3HA*, YC352

(Δ*mbp1::HIS1/MBP1-3HA-URA3*). When immune extracts were incubated with anti-HA antibody, Swi4p-3HA was not detected, in contrast to Mbp1p-3HA (Fig. 11). This suggests that the anti-MYC beads were unexpectedly interacting with Mbp1p-3HA.

In order to determine whether the issues of non-specific interaction between the anti-MYC beads and Mbp1p-3HA were specific to the strain used, a new strain was constructed whereby *SWI4* was tagged with 3 copies of HA at the C-terminus in strain BH114 (*Δswi4::hisG/SWI4*), resulting in strain VC300 (Δ*swi4::hisG/SWI4-3HA-URA3*) (Fig. 12). Next, the C-terminus of *MBP1* was tagged with 13 copies of MYC in strains BWP17 and VC300, resulting in strains VC304 (*MBP1-13MYC-HIS1/MBP1*) and VC324 (*MBP1-13MYC-HIS1/MBP1,* Δ*swi4::hisG/SWI4-3HA-URA3*) (Fig. 13 and Fig. 14). When Swi4p-3HA was precipitated with anti-HA beads from 40 mg of protein, Mbp1p-13MYC was present in the pull down, suggesting that these two proteins interact (Fig. 15A). In contrast, the reverse Co-IP showed that when Mbp1p-13MYC was precipitated with anti-MYC beads, Swi4p-3HA did not co-purify (Fig. 15B). Furthermore, there was no non-specific cross-reaction observed between anti-MYC beads and Swi4p-3HA control strain.

In order to determine whether the interaction between Swi4p and Mbp1p could be detected with lower amounts of input protein, similar to that observed with Swi6p and Swi4p or with Mbp1p, the Co-IP was repeated with 2 mg of protein. When Swi4p-3HA was precipitated with anti-HA beads, Mbp1p-13MYC did not co-purify (Fig. 16A). The reverse Co-IP using anti-MYC beads also showed absence of Swi4p-3HA in the Mbp1p-13MYC precipitate (Fig. 16B). However, a strong band was observed in the control lane, indicating that the anti-MYC beads in my hands bound non-specifically to Swi4p-3HA in this trial, and that the non-specific cross-

reaction was not specific to Mbp1p-HA as seen in Figure 6. Thus, only the Co-IPs using anti-HA beads were conclusive.

Collectively, the data show that Swi4p and Mbp1p can interact but only with high amounts of input protein and only when Swi4p is pulled out. The lack of interaction between Swi4p and Mbp1p with lower amounts of input proteins indicates that that the interaction is not the same as that seen between Swi6p and Swi4p or Swi6p and Mbp1p, raising the possibility of there being two separate Swi6p-containing complexes in *C. albicans.*

3.1.3 Validation of other proteins that interact with Swi6p: Cdc5p

Previous work involving affinity purification of Swi6p followed by mass spectrometry identified additional proteins that may interact with Swi6p (Y. Chen, MSc thesis), including the mitotic polo-like kinase Cdc5p [43, 46]. The putative interaction was identified in cells arrested in G1 phase, but not in exponential-phase cells. Since this interaction has not been previously reported, we attempted to confirm the result via Co-IP. For this, *CDC5* was tagged with three copies of HA at the C-terminus in strain YC221 (*SWI6-TAP-URA3/SWI6,* Δ*cln3::hisG/MET::CLN3-ARG4*), to obtain strain VC181 (*CDC5-3HA-HIS1/CDC5, SWI6-TAP-URA3/SWI6, Δcln3::hisG/MET::CLN3-ARG4*) (Fig. 17). Next, a control strain VC380 (*CDC5-3HA-HIS1/CDC5, Δcln3::hisG/MET::CLN3-ARG4*) was constructed by tagging *CDC5* with an HA tag in strain BH253 (*Δcln3::hisG/MET::CLN3-ARG4*) (Fig. 18). Strains VC181 and VC380 were incubated in inducing (-MC) media overnight, diluted into repressing (+MC) media and incubated at 30°C for 4 h. When Cdc5p-3HA was precipitated using anti-HA beads, Swi6p-TAP co-purified, indicating that these two proteins interact in G1 phase-arrested cells (Fig. 19A). However, a reverse Co-IP that pulled out Swi6p-TAP was inconclusive as strong non-specific

cross-reaction was noted in the control sample (Fig. 19B). In order to determine whether these Swi6p and Cdc5p interact in exponential phase cells, Co-IP was repeated under these growth conditions, using the same strains. When Cdc5p-3HA was precipitated with anti-HA beads, a band that cross-reacted with the anti-TAP antibody was present, but also in the control strain (Fig. 20). Thus, the result is inconclusive due to non-specific binding of beads.

In an attempt to eliminate non-specific cross-reaction and further investigate whether Swi6p and Cdc5p interact in exponential-phase cells, new strains with different tags were created and the Co-IP was repeated. For this, *SWI6* was tagged with three copies of HA at the C-terminus in a strain that contained *CDC5* tagged with 13 copies of MYC (AG629; *CDC5-13MYC-HIS1/CDC5*) to obtain strain VC348 (*SWI6-3HA-URA3/SWI6, CDC5-13MYC-HIS1/CDC5*). VC348 was confirmed by PCR and Western blot analysis (Fig. 21). When Swi6p-3HA was pulled out with anti-HA beads, a very faint band corresponding to Cdc5p-13MYC was detected (Fig. 22A). Reverse Co-IP using anti-MYC beads to pull out Cdc5p-13MYC revealed non-specific cross-reaction in the control strain and was thus inconclusive (Fig. 22B).

Since an interaction between Swi6p and Cdc5p was detected in cells blocked in G1 phase via affinity purification followed by mass spectrometry, and in one Co-IP experiment, we further explored the interaction by asking whether Swi6p was post-translationally modified by Cdc5p. In order to test this hypothesis, *SWI6* was tagged with three copies of HA tag in a strain containing one copy of *CDC5* under the control of *MET3* promoter (AG500; *Δcdc5::hisG/MET3::CDC5-ARG4*), resulting in strain VC426 (*SWI6-3HA-URA/SWI6, Δcdc5::hisG/MET3::CDC5-ARG4*). VC426 was confirmed via PCR and Western analysis (Fig. 23). Next, strains VC426 and control strain YC216 (*Δswi6::HIS1/SWI6-3HA-URA3*) were diluted to an $O.D._{600nm}$ of 0.0001 and incubated overnight at 30^{o} in inducing (-MC) media. The next day, when cells reached

exponential phase (O.D. of 0.8), they were diluted to an $O.D._{600nm}$ of 0.3 in fresh inducing (-MC) or repressing (+MC) media, and collected at 0, 3, or 6 h. Swi6p was then analyzed via Western blotting (Fig. 24). However, Swi6p did not show significant changes in migration in the presence vs. absence of Cdc5p. The levels of Swi6p appeared to decrease as Cdc5p was depleted, but quantification was not done and we cannot rule out differences in loading. Overall, the results suggest that Swi6p may physically interact with Cdc5p, but the functional significance of this relationship remains unclear.

Other additional Swi6p-interacting factors identified in previous studies include an unknown orf, orf19.5722, which contains a domain with DNA binding activity and has a role in regulation of transcription (Table 4). A physical interaction between these two proteins still requires confirmation via Co-IP.

3.1.4 Confirmation of additional interacting factors of Swi4p: components of the proteasome

Although Swi6p was previously identified to be the dominant interacting factor of Swi4p (Y. Chen MSc thesis), several other putative interacting proteins with functions related to the proteasome were identified, including Pr26p, a sub-unit of the 26S proteasome, and Rpn1p, Rpn3p, Rpt6p, which are components of the 19S regulatory subunit (Table 5). The 19S proteasome is responsible for removing ubiquitin chains and subsequently transferring target proteins into the inner core of 26S proteasome [62]. A physical interaction between Swi4p and the proteasome has not been previously reported. These results may have important implications for divergent Swi4p regulation in *C. albicans*. In order to first confirm the interactions, *RPN1* was tagged with a three copies of HA at the C-terminus in a 13-MYC tagged *SWI4* strain (VC108), resulting in strain VC389 (*RPN1-3HA-URA3/RPN1, Δswi4::hisG/SWI4-13MYC-*

HIS1), which was confirmed via PCR and Western blot (Fig. 25). The control strain VC394 (*RPN1-3HA-URA3/RPN1*) was also constructed and confirmed via PCR and Western (Fig. 26) to use as a control. The strains in hand will now allow for a Co-IP experiment and further investigation of a putative role for the proteasome in Swi4p regulation.

3.2 Validation of putative Swi4p targets: *EFG1*

3.2.1 Expression of *EFG1* is moderately induced as Swi4p is depleted over time

In order to determine the mechanisms of action of Swi4p, a previous study (Y. Chen, MSc thesis) completed a genome-wide location analysis of Swi4p using a single tiling array. Results showed significant enrichment of Swi4p binding at promoter regions of genes associated with budding pattern, cell wall biogenesis, and cell cycle transitions. Intriguingly, most of the genes were linked to biological processes associated with filamentous growth, and included important regulators of hyphal development. One target was *EFG1*, a transcription factor that is required for hyphal growth under most hyphal-inducing conditions [37, 63]. Together with the fact that yeast cells depleted of Swi4p grow predominantly in a filamentous fashion, the data suggests that Swi4p and the G1/S cell cycle machinery may directly impinge on the hyphal development program. In order to gain additional evidence supporting this hypothesis, we investigated the functional significance of Swi4p occupation of the *EFG1* promoter. First, we asked whether *EFG1* expression was modulated in the absence of Swi4p. For this, strains YC161 (Δ*swi4::URA3/*Δ*swi4::HIS1*, pBS-*ARG4-SWI4*), YC171 (Δ*swi4::URA3/*Δ*swi4::HIS1*, pBS-*ARG4*), YC201 (Δ*swi6::HIS1/*Δ*swi6::URA3*, pBS-*ARG4-SWI6*), YC233 (Δ*swi6::HIS1/*Δ*swi6::URA3*, pBS-*ARG4*), YC323 (Δ*mbp1::HIS1/*Δ*mbp1::URA3*, pBS-*ARG4-MBP1*), YC381 (Δ*mbp1::HIS1/*Δ*mbp1::URA3*, pBS-*ARG4*), and BH420 (BWP17, pRM100-Ca*URA3,* Ca*HIS1*, pBS-Ca*ARG4*) were incubated in minimal complete media until they reached

an OD_{600nm} of 0.8. Cells were collected, RNA was extracted and *EFG1* expression was determined using Northern blotting. The levels of *EFG1* did not significantly vary between strains (Fig. 27A).

In order to further investigate *EFG1* expression, we next determined whether it was modulated within a window of Swi4p depletion, since *EFG1* in *C. albicans* decreases rapidly in response to serum but resumes expression at later stages [64]. For this, strain BH150 (Δ*swi4::hisG/MET3::SWI4-ARG4*) and the control strain BH420 (*SWI4/SWI4*) were incubated in inducing (-MC) medium at 30°C overnight, diluted into repressing (+MC) or inducing medium and incubated for set times. Cells were collected, RNA was extracted and a Northern blot was completed. Under these conditions, *EFG1* was moderately induced as Swi4p was depleted overtime (Fig. 27B). Time "0" time points had little RNA, as observed for both *EFG1* and the *ACT1* loading control, which reflects the difficulty in extracting RNA from stationary phase culture cells. Thus, *EFG1* is moderately induced in cells depleted of Swi4p.

3.2.2 Absence of *EFG1* partially suppresses the phenotype of *swi4Δ/swi4Δ* cells

We further tested the functional significance of Swi4p occupation of the *EFG1* promoter by asking if Efg1p was required for the filamentous phenotype of Swi4p-depleted cells. For this, two alleles of *EFG1* were replaced with *ARG4* and *HIS1* markers in strain BH339 (*Δswi4::hisG/Δswi4::URA3*), resulting in strain VC247. Strains were confirmed by PCR, which show two distinct bands corresponding to two *EFG1* alleles replaced by markers (Fig. 28A and B). Importantly, the wild-type *EFG1* allele was not present (Fig. 28C). Next, strains VC247 and VC166 (*Δefg1::ARG4/EFG1, Δswi4::hisG/Δswi4::URA3*) were investigated for phenotype. Heterozygous strain VC166 showed long filaments and enlarged, oval-shaped cells (Fig. 29**)**, as shown previously for Swi4p-depleted cells [48]. However, cells of strain VC247 were short,

spindle-like, and not enlarged, suggesting partial suppression of the Swi4p-depleted filamentous phenotype (Fig. 29**)**. Together, the results demonstrate that *EFG1* expression is influenced by Swi4p, and the Swi4p-depleted phenotype is dependent in part on Efg1p. This supports the idea that *EFG1* is a target of Swi4p.

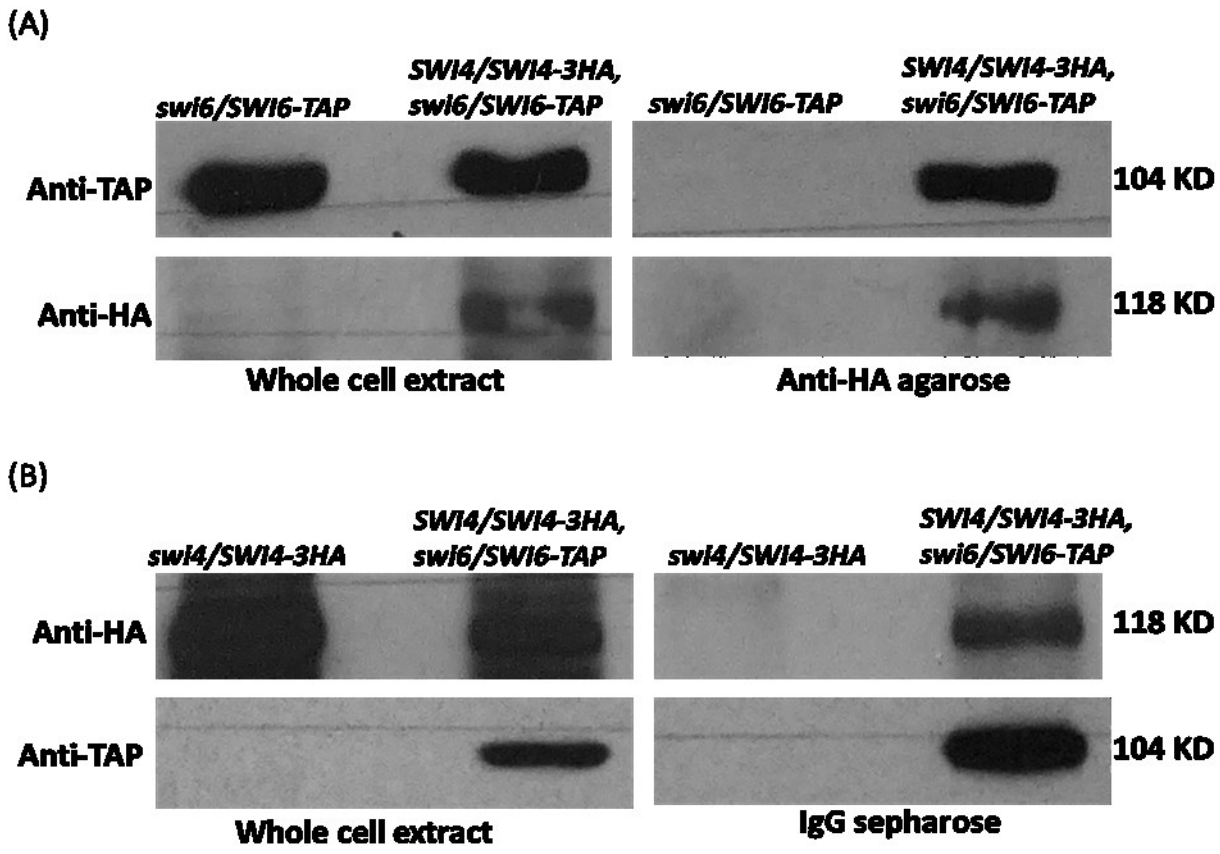

Figure 4. Co-immunoprecipitation demonstrates a positive interaction between Swi6p and Swi4p.
Western blot of whole cell extract and immune-precipitates from strains AM201.5 (Δ*swi6::URA3/SWI6-TAP-ARG4*), AH110 (*SWI4-3HA-HIS1/SWI4, Δswi6::URA3/SWI6-TAP-ARG4*) and YC113 (Δ*swi4:hisG/SWI4-3HA-HIS1*) using anti-HA agarose (A) or IgG sepharose (B). 20 µl of beads were incubated with 2 mg of protein overnight, washed, and boiled in SDS sample buffer to elute interacting proteins.

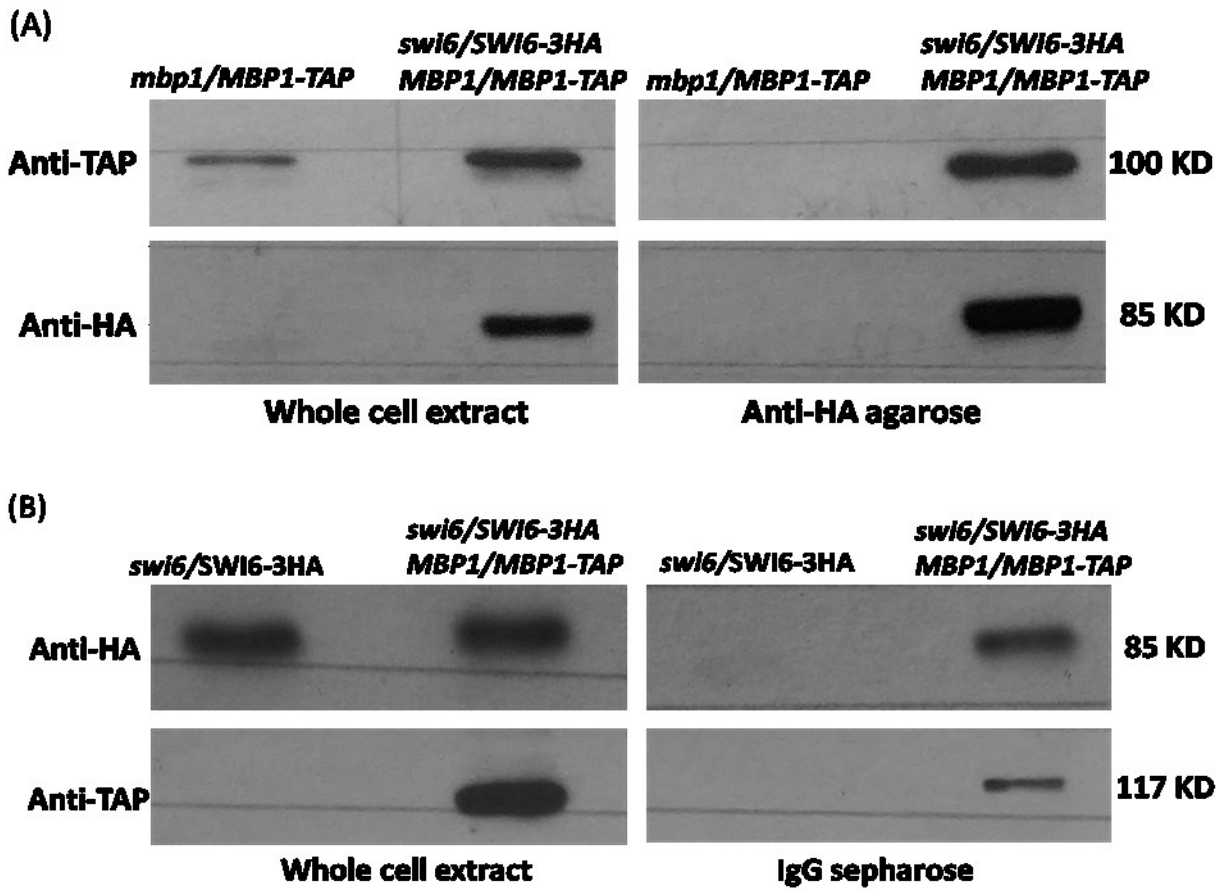

Figure 5. Co-immunoprecipitation demonstrates a positive interaction between Swi6p and Mbp1p.

Western blot of whole cell extract and immune-precipitates from strains YC367 (Δ*mbp1::HIS1/MBP1-TAP-URA3*), YC396 *(*Δ*swi6::HIS1/SWI6-3HA-URA3, MBP1/MBP1-TAP-URA3*) and YC216 (Δ*swi6::HIS1/SWI6-3HA-URA3*) using anti-HA agarose (A) or IgG sepharose (B). 20 µl of beads were incubated with 2 mg of protein overnight, washed, and boiled in SDS sample buffer to elute interacting proteins.

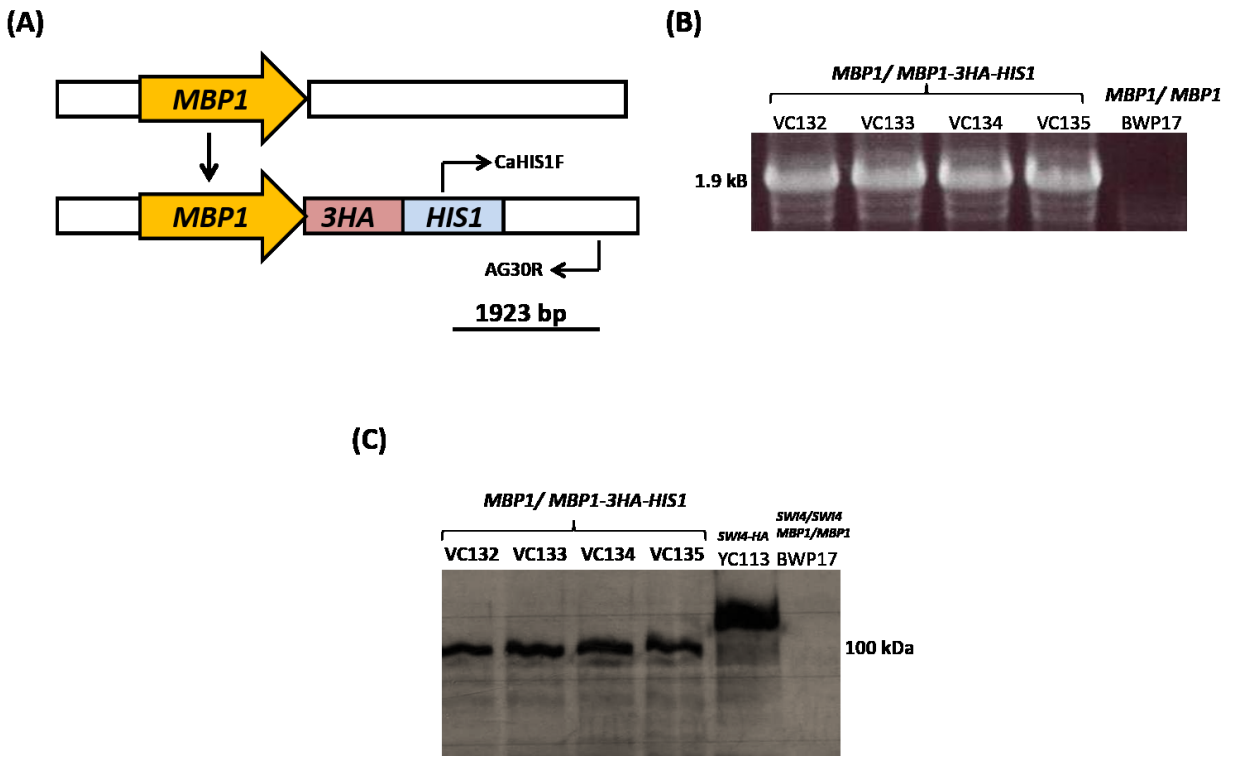

Figure 6. Construction of a strain carrying *MBP1-3HA* in a *SWI6-TAP-URA3/SWI6, Δcln3::hisG/MET::CLN3-ARG4* background.

*(***A, B)** Map and DNA gel of a PCR screen to confirm intergration of a *3HA-HIS1*-containing construct at the C-terminus of MBP1. Oligonucleotides CaHIS1F and AG30R produced a 1923 bp band for *MBP1-3HA*. Positive strains VC132, VC133, VC134, and VC135 (*MBP1/MBP1-3HA-HIS1, SWI6-TAP-URA3/SWI6, Δcln3::hisG/MET::CLN3-ARG4*) and negative control strain BWP17 are shown in (B). **(C)** Western blot containing 30 µg of protein from strains VC132, VC133, VC134, VC135, YC113 (*MBP1-3HA-HIS1/MBP1, SWI6-TAP-URA3/SWI6, Δcln3::hisG/MET::CLN3-ARG4*), and BWP17 incubated with anti-HA antibody. Mbp1-3HA is 100 kDa.

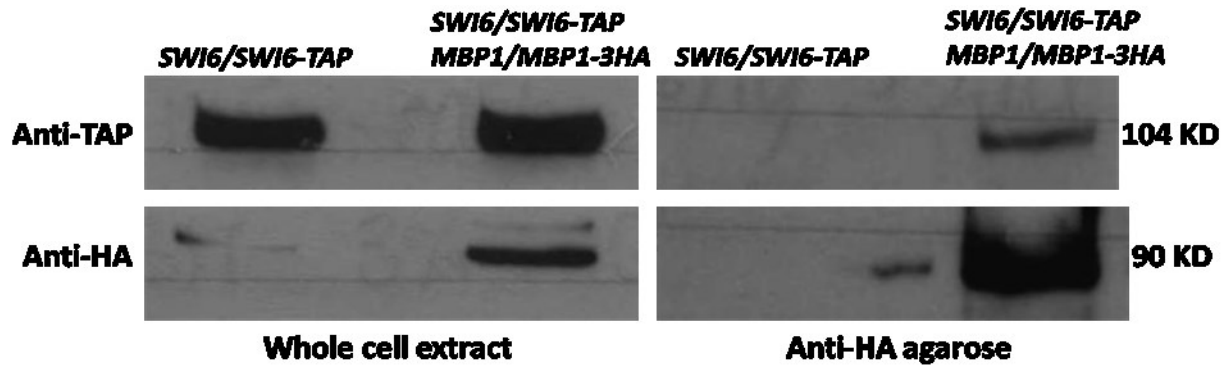

Figure 7. Co-immunoprecipitation confirming an interaction between Mbp1p and Swi6p in G1 phase-blocked cells.

Western blots of whole cell extracts and immune-precipitates from strains YC221 (*SWI6-TAP-URA3/SWI6, Δcln3::hisG/MET::CLN3-ARG4*) and VC132 (*MBP1-3HA-HIS1/MBP1, SWI6-TAP-URA3/SWI6, Δcln3::hisG/MET::CLN3-ARG4*) grown in repressing medium (+MC) for 4 h to induce a G1-phase block, using anti-HA agarose. 40 mg of protein was incubated with 40 µl of beads overnight, washed, and boiled in SDS sample buffer for the elution of interacting proteins.

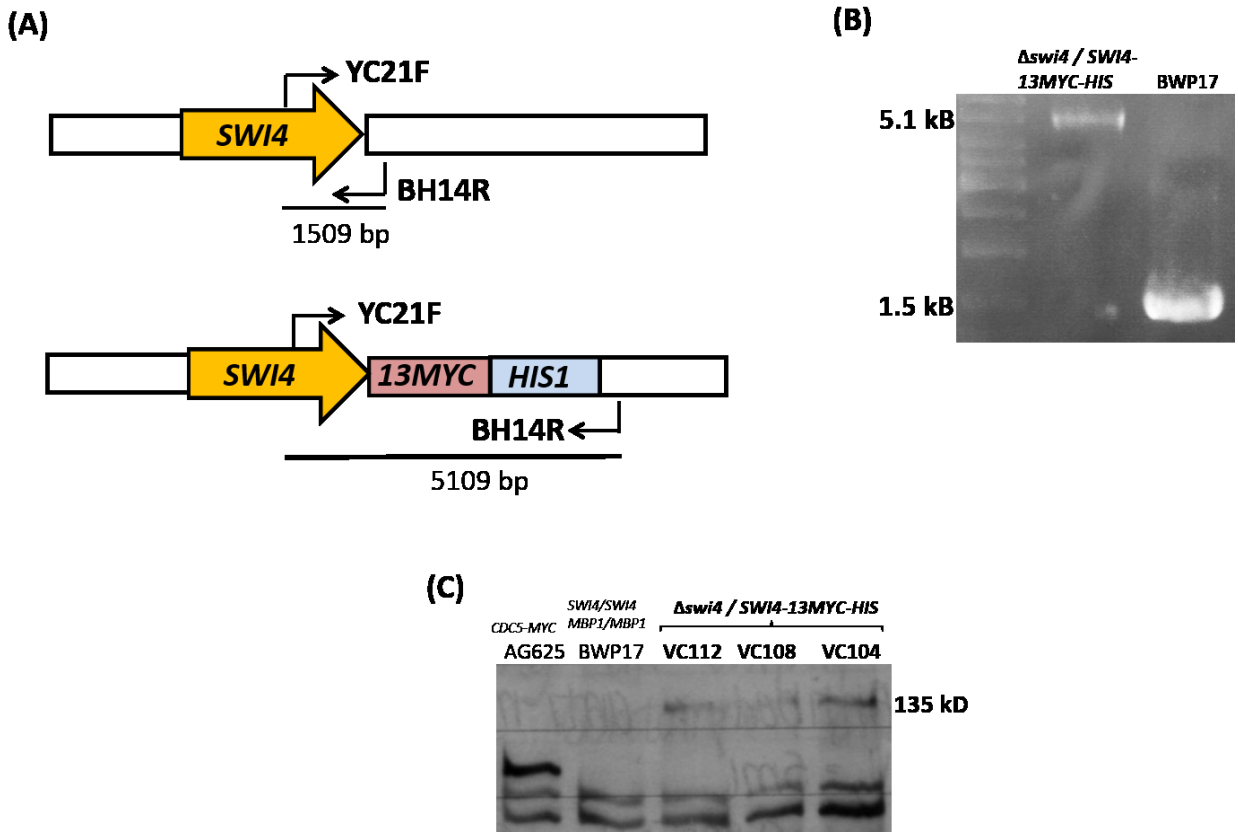

Figure 8. Confirmation of a *Δswi4::hisG/SWI4-13MYC-HIS1* strain.
(A, B) Map and gel of a PCR screen to confirm intergration of a *13MYC-HIS1*-containing construct at the C-terminus of *SWI4*. Oligonucleotides YC21F and BH14R amplify a 5 kB band for *SWI4-13MYC* and a 1.4 kB band for *SWI4/SWI4* (A). Positive strain VC108 (*Δswi4::hisG/SWI4-13MYC-HIS1*) and negative control strain BWP17 are shown in (B). **(C)** Western blot containing 30 µg of whole cell protein extracts from strains VC104, VC108, VC112 (*Δswi4::hisG/SWI4-13MYC-HIS1*), AG625 (*CDC5-13MYC-HIS1/CDC5*), and BWP17 incubated with anti-MYC antibody.

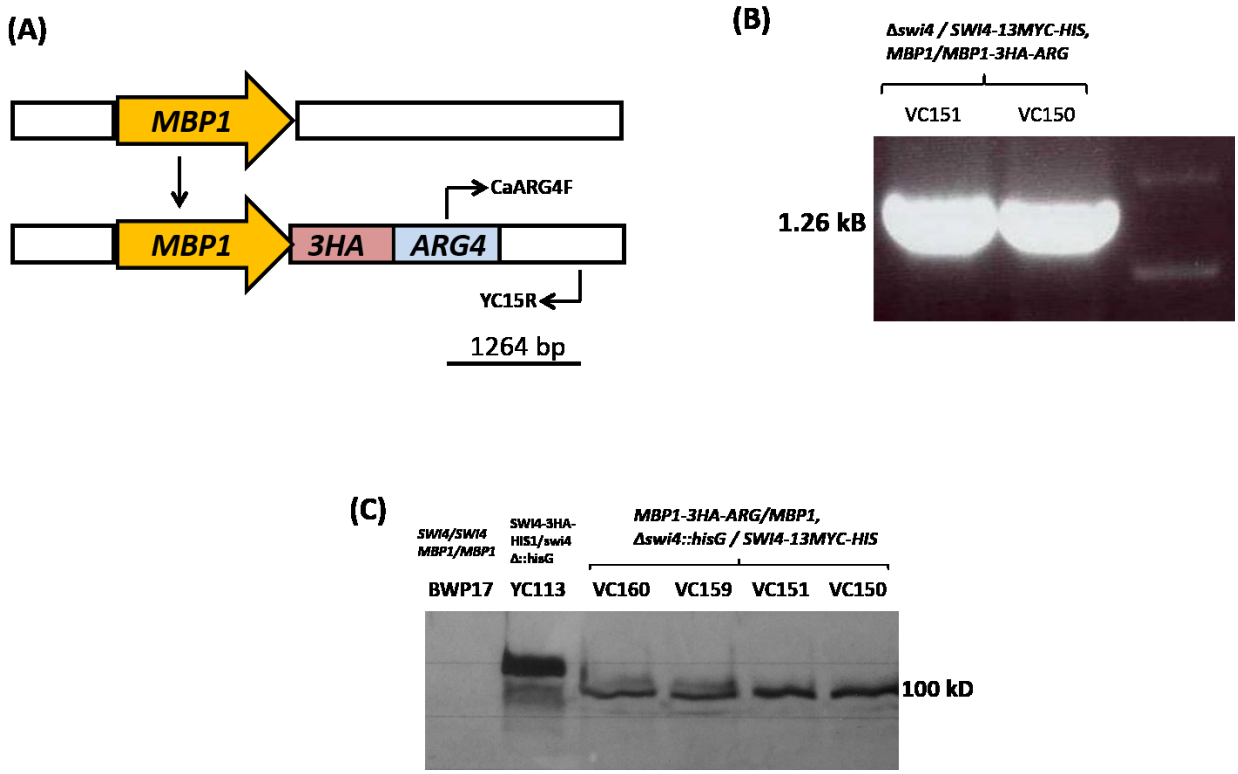

Figure 9. Construction of a strain carrying *MBP1-3HA-ARG4* and *SWI4-13MYC-HIS1*.
(A, B) Map and gel of a PCR screen to confirm intergration of a *3HA-ARG4*-containing construct at the C-terminus of *MBP1*. Oligonucleotides CaARG4F and YC15R amplify a 1264 bp band for *MBP1-3HA* (A). Positive strains VC150 and VC151 (*Δswi4::hisG/SWI4-13MYC-HIS1, MBP1/MBP1-3HA-ARG4*) are shown in (B). **(C)** Western blot containing 30 µg of whole cell protein extracts from strains VC150, VC151, VC159 and VC160 (*Δswi4::hisG/SWI4-13MYC-HIS1, MBP1/MBP1-3HA-ARG4*), YC113 (*Δswi4::hisG/SWI4-3HA-HIS1*), and BWP17 incubated with anti-HA antibody.

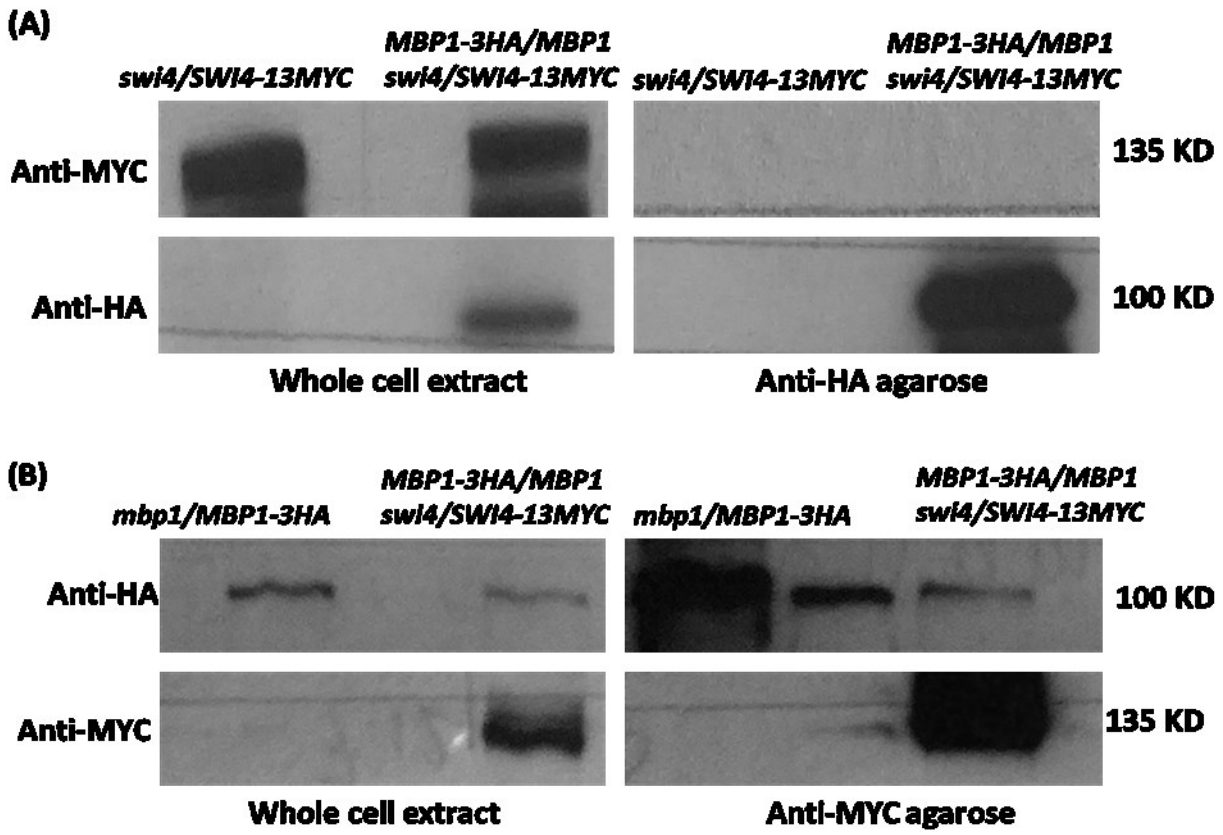

Figure 10. Co-immunoprecipitation demonstrates a negative interaction between Mbp1p and Swi4p when Mbp1p is immune-precipitated.
Western blot of whole cell extract and immune-precipitates from strains VC108 (*Δswi4::hisG/SWI4-13MYC-HIS*1), VC150 (*Δswi4::hisG/SWI4-MYC-HIS1, MBP1/MBP1-HA-ARG*4) and YC351 (*Δmbp1::HIS1/MBP1-3HA-URA3*) using anti-HA agorose (A) or anti-MYC agarose (B). 40 µl of beads were incubated with 40 mg of protein overnight, washed, and boiled in SDS sample buffer to elute interacting proteins.

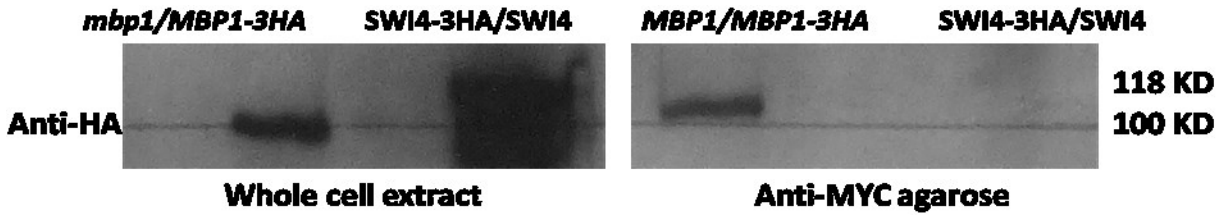

Figure 11. Co-immunoprecipitation shows that non-specific cross reaction of anti-MYC beads is specific to Mbp1p tagged with an HA tag.
Western blot of whole cell extract and immune-precipitates from strains YC352 (*Δmbp1::HIS1/MBP1-3HA-URA3*) and YC101 (*SWI4-3HA-HIS1/SWI4*) using anti-MYC agarose. 40 µl of beads were incubated with 40 mg of protein overnight, washed, and boiled in SDS sample buffer to elute interacting proteins.

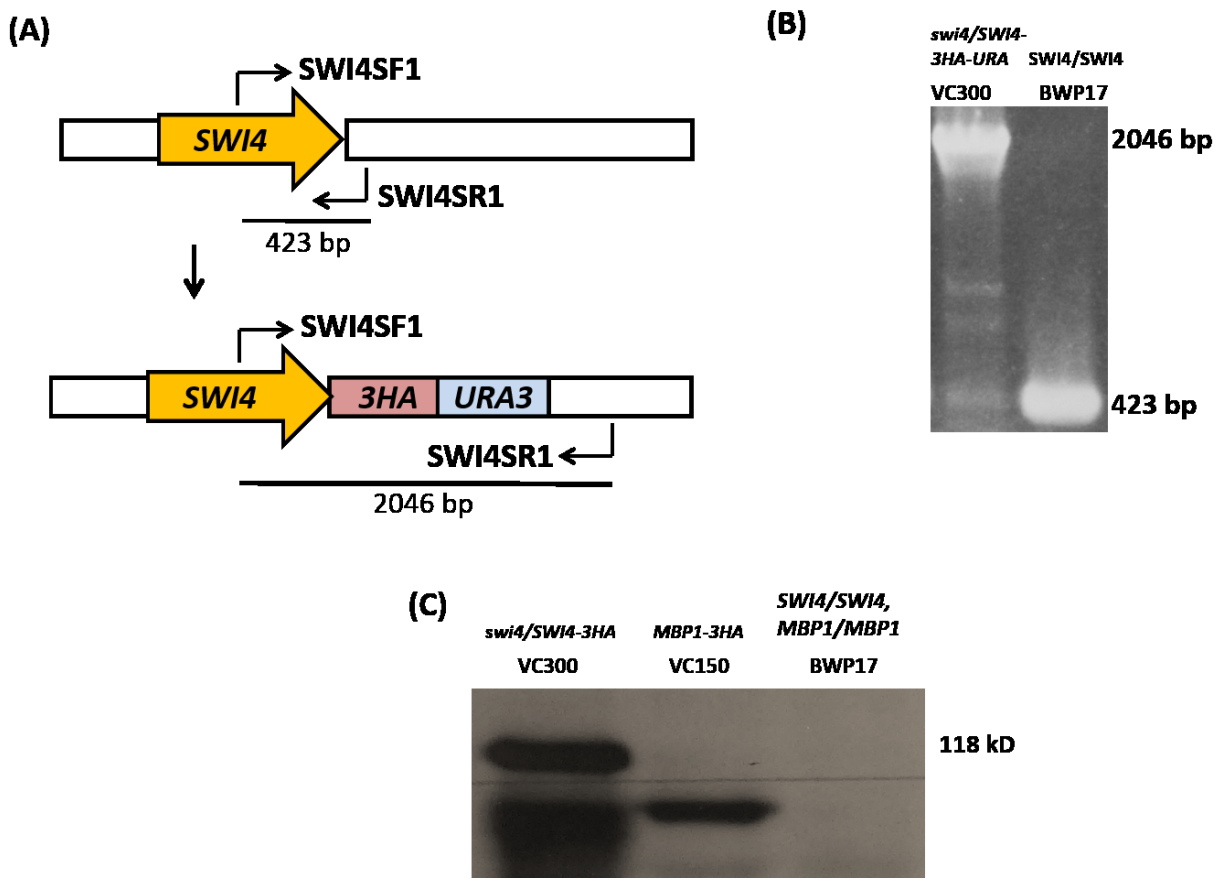

Figure 12. Confirmation of a *Δswi4::hisG/SWI4-3HA-URA3* strain.
(A, B) Map and gel of a PCR screen to confirm intergration of a *3HA-URA3*-containing construct at the C-terminus of *SWI4*. Oligonucleotides SWI4SF1 and SWI4SR1 amplify a 1264 bp band for *SWI4-3HA* (A). Positive strain VC300 (*Δswi4::hisG/SWI4-3HA-URA3*) and negative control strain BWP17 shown in (B). **(C)** Western blot containing 30 µg of whole cell protein extracts from strains VC300, (*Δswi4::hisG/SWI4-3HA-URA3*), VC150 (*Δswi4::hisG/SWI4-13MYC-HIS1, MBP1/MBP1-3HA-ARG4*), and BWP17 incubated with anti-HA antibody.

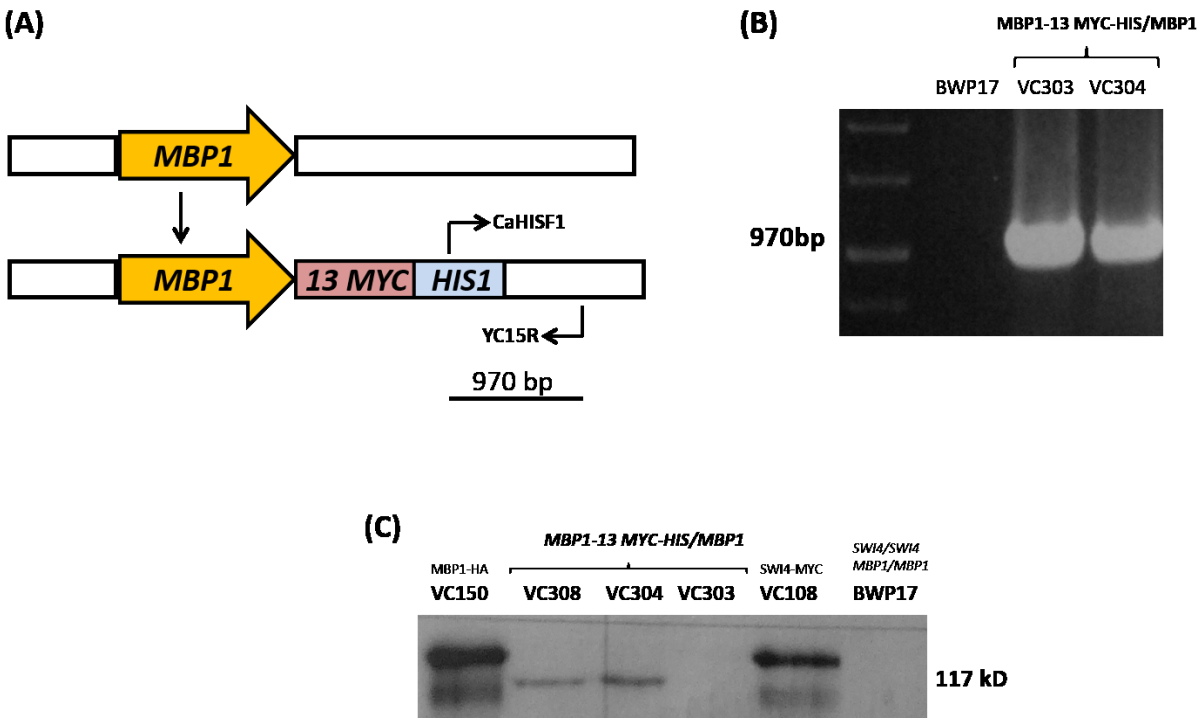

Figure 13. Confirmation of a *MBP1-13MYC-HIS1/MBP1* strain.
(A, B) Map and gel of a PCR screen to confirm intergration of a *13MYC-HIS1*-containing construct at the C-terminus of *MBP1*. Oligonucleotides CaHIS1F and YC15R amplify a 970 bp band for *MBP1-13MYC* (A). Positive strains VC303, VC304 (*MBP1-13MYC-HI1S/MBP1*) and negative control strain BWP17 shown in (B). **(C)** Western blot containing 30 µg of whole cell protein extracts from strains VC303, VC304, VC308 (*MBP1-13MYC-HIS1/MBP1*), VC150 *(Δswi4::hisG/SWI4-13MYC-HIS1, MBP1/MBP1-3HA-ARG4*), VC108 (*Δswi4::hisG/SWI4-13MYC-HIS1*) and BWP17 incubated with anti-MYC antibody.

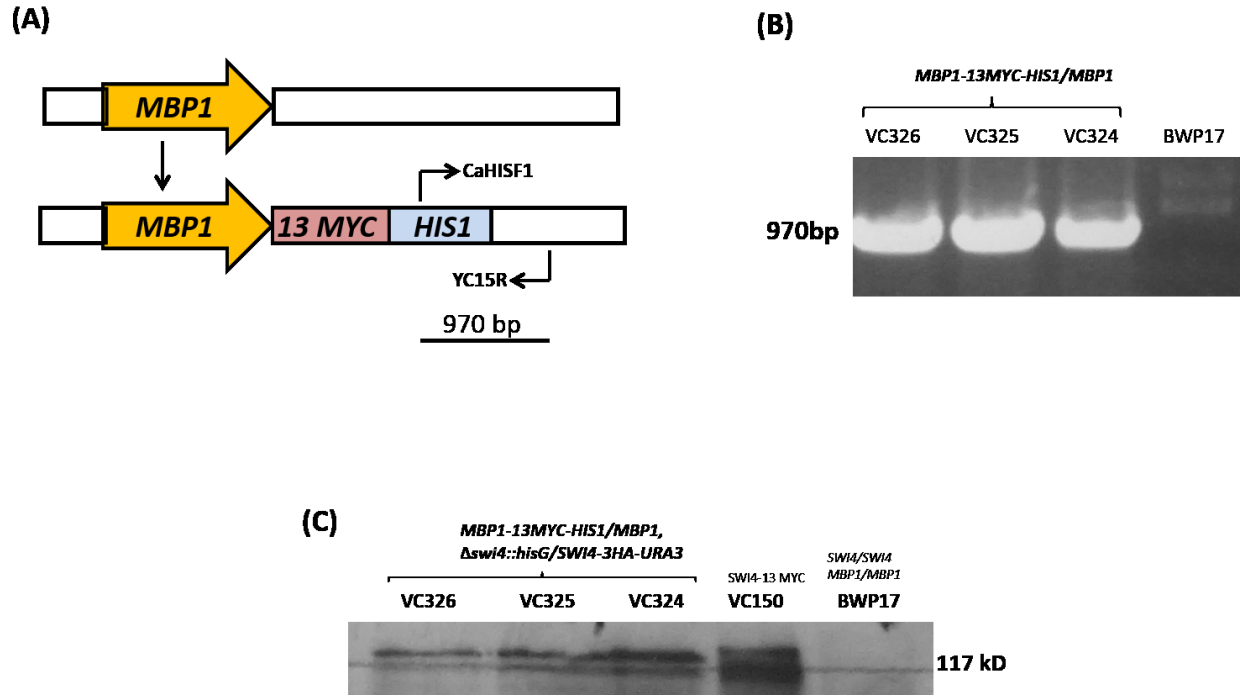

Figure 14. Confirmation of a *MBP1-13MYC-HIS1/MBP1, Δswi4::hisG/SWI4-3HA-URA3* strain.

(A, B) Map and gel of a PCR screen to confirm intergration of a *13MYC-HIS1*-containing construct at the C-terminus of *MBP1*. Oligonucleotides CaHIS1F and YC15R amplify a 970 bp band for *MBP1-13MYC* (A). Positive strains VC324, VC325, VC326 *(MBP1-13MYC-HIS1/MBP1, Δswi4::hisG/SWI4-3HA-URA3*) and negative control strain BWP17 shown in (B). **(C)** Western blot containing 30 µg of whole cell protein extracts from strains VC324, VC325, VC326 (*MBP1-13MYC-HIS1/MBP1, Δswi4::hisG/SWI4-3HA-URA3*), VC150 (*Δswi4::hisG/SWI4-13MYC-HIS1, MBP1/MBP1-3HA-ARG4*), and BWP17 incubated with anti-MYC antibody.

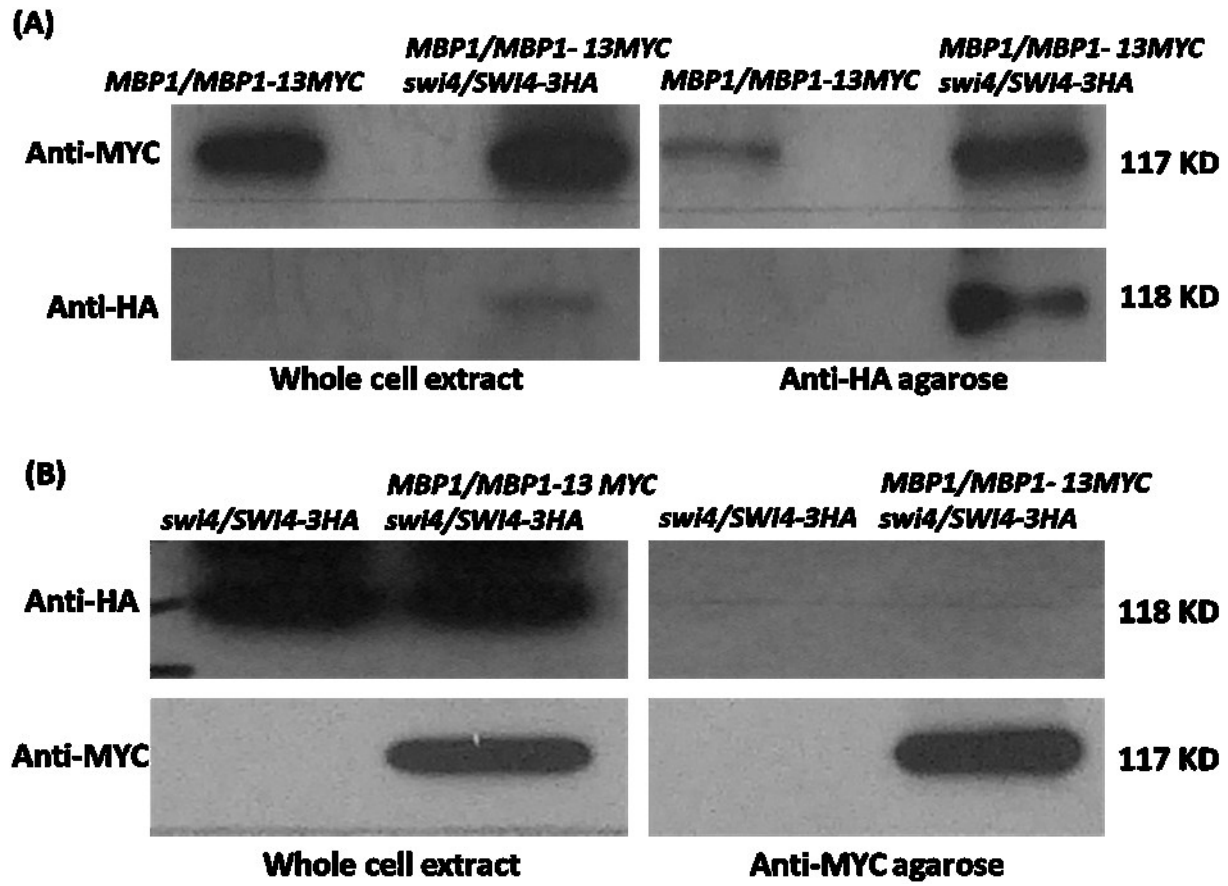

Figure 15. Co-immunoprecipitation demonstrates a possible interaction between Swi4p and Mbp1p when Swi4p is immune-precipitated, but not when Mbp1p is pulled down.
Western blot of whole cell extract and immune-precipitates from strains VC304 (*MBP1-13MYC-HIS1/MBP1*), VC324 (*MBP1-13MYC-HIS1/MBP1, Δswi4::hisG/SWI4-3HA-URA3*), and VC300 (*Δswi4::hisG/SWI4-3HA-URA3*) using anti-HA agaorose (A) or anti-MYC agarose (B). A signal is observed in the control strain (A) but is less intense than that observed in the experimental strain. 40 µl of beads were incubated with 40 mg of protein overnight, washed, and boiled in SDS sample buffer to elute interacting proteins.

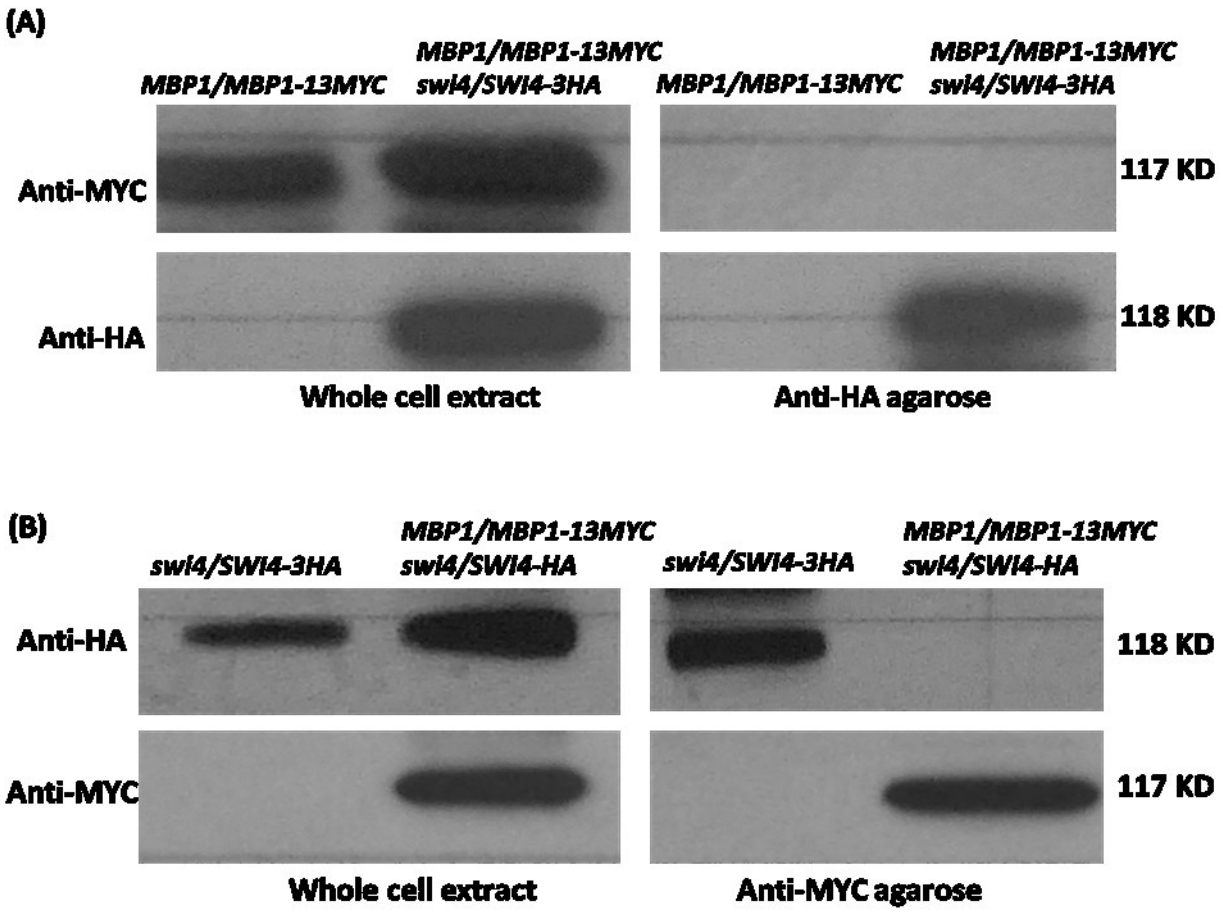

Figure 16. Co-immunoprecipitation demonstrates that Swi4p and Mbp1p do not interact when the amount of input protein is reduced.
Western blot of whole cell extract and immune-precipitates from strains VC304 (*MBP1-13MYC-HIS1/MBP1*), VC324 *(MBP1-13MYC-HIS1/MBP1, Δswi4::hisG/SWI4-3HA-URA3*), and VC300 (*Δswi4::hisG/SWI4-3HA-URA3*) using anti-HA agarose (A) or anti-MYC agarose (B). 20 µl of beads were incubated with 2 mg of protein overnight, washed, and boiled in SDS sample buffer to elute interacting proteins.

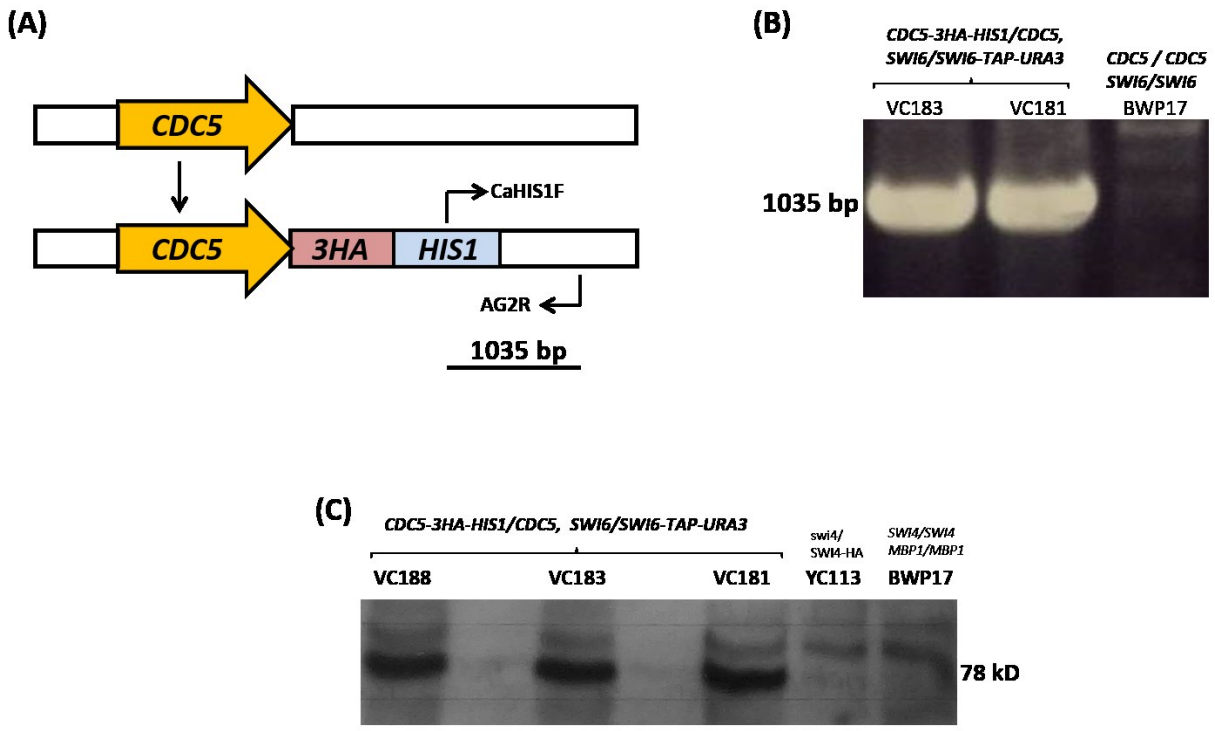

Figure 17. Construction of a strain carrying *CDC5-3HA* in a *SWI6-TAP-URA3/SWI6, Δcln3::hisG/MET::CLN3-ARG4* background.
(A, B) Map and DNA gel of a PCR screen to confirm intergration of a *3HA-HIS1*-containing construct at the C-terminus of *CDC5*. Oligonucleotides CaHIS1F and AG2R produced a 1035 bp band for *CDC5-3HA*. Positive strains VC181, VC183 (*CDC5-3HA-HIS1/CDC5, SWI6-TAP-URA3/SWI6, Δcln3::hisG/MET::CLN3-ARG4*) and negative control strain BWP17 shown in (B). **(C)** Western blot containing 30 µg of whole cell protein extracts from strains VC181, VC183, VC188, (*CDC5-3HA-HIS1/CDC5, SWI6-TAP-URA3/SWI6, Δcln3::hisG/MET::CLN3-ARG4*), YC113 (*Δswi4::hisG/SWI4-3HA-HIS1*), and BWP17 incubated with anti-HA antibody.

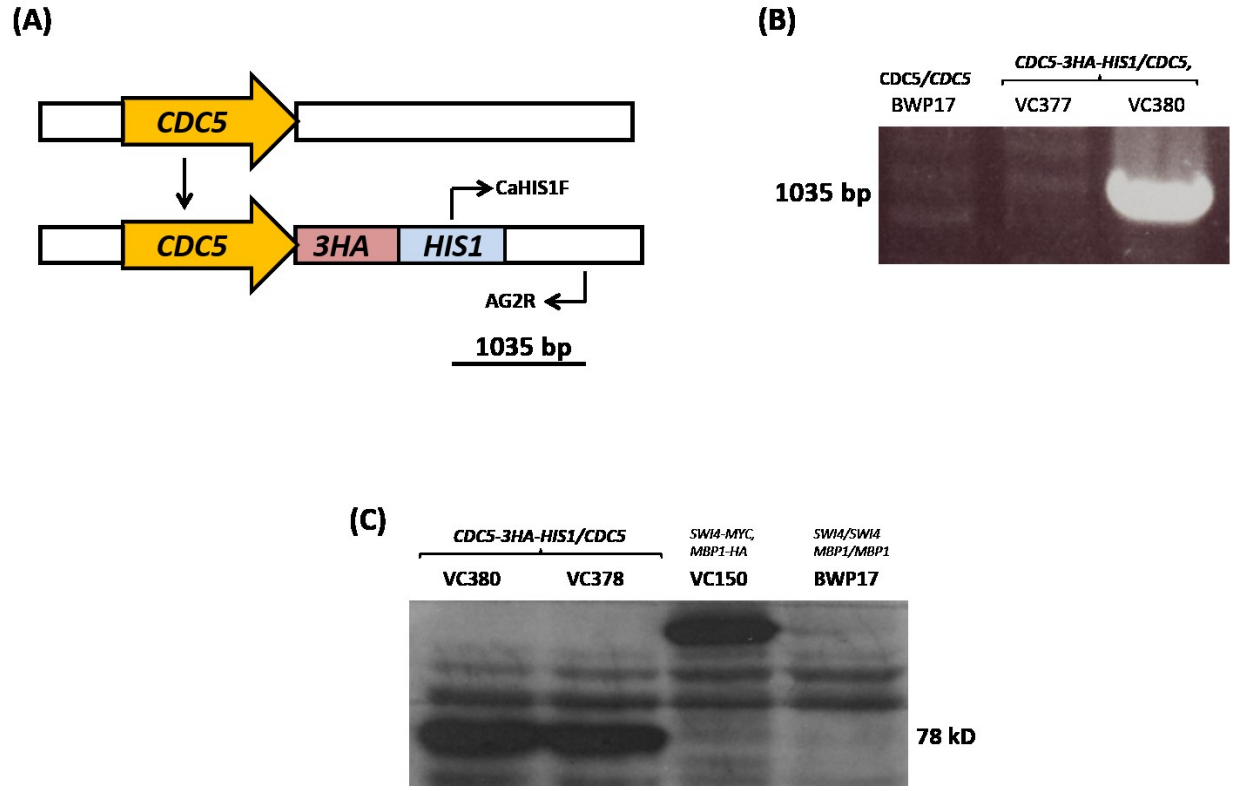

Figure 18. Confirmation of tagging *CDC5* with HA in BH253 (*Δcln3::hisG/MET::CLN3-ARG4*).

(A, B) Map and DNA gel of a PCR screen to confirm intergration of a *3HA-HIS1*-containing construct at the C-terminus of *CDC5*. Oligonucleotides CaHIS1F and AG2R produced a 1035 bp band for *CDC5-3HA*. Positive strains VC380 (*CDC5-3HA-HIS1/CDC5, Δcln3::hisG/MET::CLN3-ARG4*) and negative control strain BWP17 shown in (B). **(C)** Western blot containing 30 µg of whole cell protein extracts from strains VC378, VC380 (*CDC5-3HA-HIS1/CDC5, Δcln3::hisG/MET::CLN3-ARG4*), VC150 (*Δswi4::hisG/SWI4-13MYC-HIS1, MBP1-3HA-ARG4/MBP1*), and BWP17 incubated with anti-HA antibody.

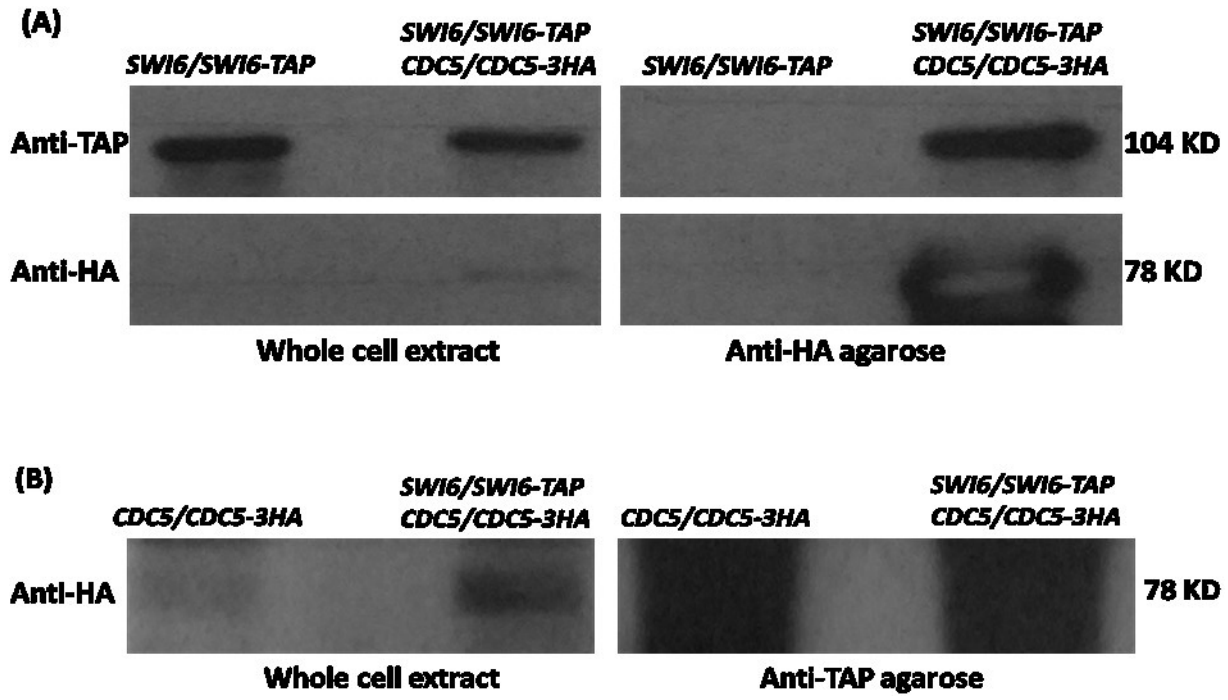

Figure 19. Co-immunoprecipitation demonstrating an interaction between Cdc5p and Swi6p in G1 phase-blocked cells when Cdc5p-HA is immune-precipitated.
Western blot of whole cell extract and immune-precipitates from strains YC221 (*SWI6-TAP-URA3/SWI6, Δcln3::hisG/MET::CLN3-ARG4*), VC181 (*CDC5-3HA-HIS1/CDC5, SWI6-TAP-URA3/SWI6, Δcln3::hisG/MET::CLN3-ARG4*), and VC380 (*CDC5-3HA-HIS1/CDC5, Δcln3::hisG/MET::CLN3-ARG4*) grown in repressing medium (+MC) for 4 h to induce a G1-phase block, using anti-HA agaorose (A) or anti-TAP agarose (B). Proteins were not incubated with anti-TAP antibody in part B due to non-specific cross reaction already seen in control lane when pulled out with IgG beads. 40 µl of beads were incubated with 40 mg of protein for 4 hours, washed, and boiled in SDS sample buffer to elute interacting proteins.

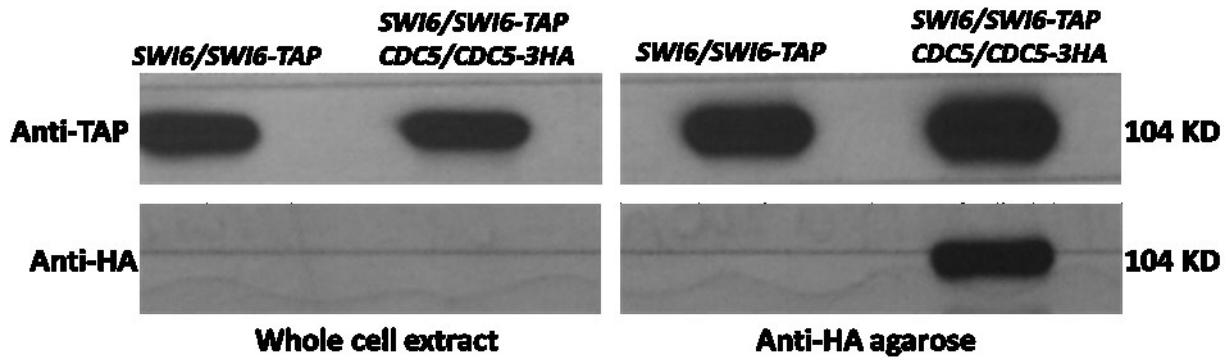

Figure 20. Co-immunoprecipitation does not support an interaction between Cdc5p and Swi6p in exponential growing cells as opposed to G1 phase blocked cells, due to strong non-specific cross reaction.

Western blot of whole cell extract and immune-precipitates from strains YC221 (*SWI6-TAP-URA3/SWI6, Δcln3::hisG/MET::CLN3-ARG4*) and VC181 (*CDC5-3HA-HIS1/CDC5, SWI6-TAP-URA3/SWI6, Δcln3::hisG/MET::CLN3-ARG4*) using anti-HA agaorose. 40 µl of beads were incubated with 40 mg of protein overnight, washed, and boiled in SDS sample buffer to elute interacting proteins.

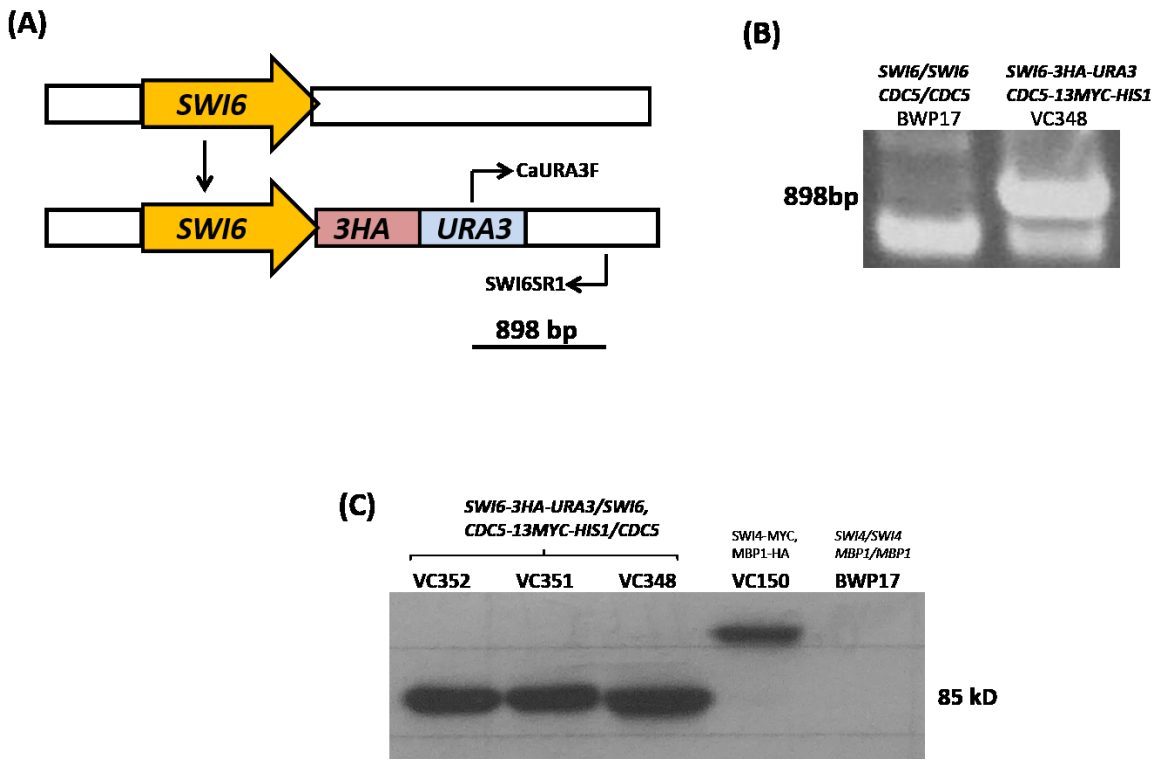

Figure 21. Confirmation of a *SWI6-3HA-URA3/SWI6, CDC5-13MYC-HIS1/CDC5* strain. **(A, B)** Map and DNA gel of a PCR screen to confirm intergration of a *3HA-URA3*-containing construct at the C-terminus of *SWI6*. Oligonucleotides CaURA3F and SWI6SR1 produced an 898 bp band for *SWI6-3HA*. Positive strain VC348 (*SWI6-3HA-URA3/SWI6, CDC5-13MYC-HIS1/CDC5*) and negative control strain BWP17 shown in (B). **(C)** Western blot containing 30 µg of whole cell protein extracts from strains VC348, VC351, VC352 (*SWI6-3HA-URA3/SWI6, CDC5-13MYC-HIS1/CDC5*), VC150 (*Δswi4::hisG/SWI4-13MYC-HIS1, MBP1-3HA-ARG4/MBP1*), and BWP17 incubated with anti-HA antibody.

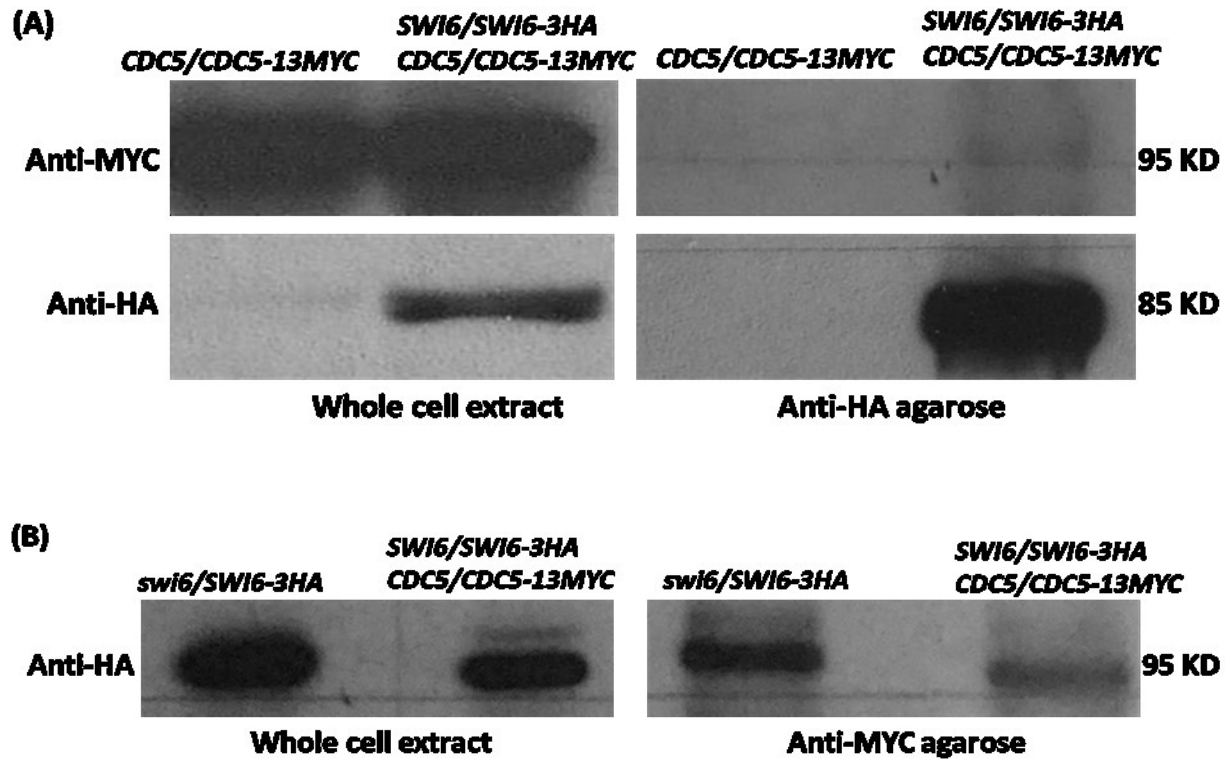

Figure 22. Co-immunoprecipitation demonstrates a possible interaction between Cdc5p and Swi6p when Swi6p-HA is immune-precipitated from exponential-growing cells, but not when Cdc5p-MYC is pulled down.

Western blots of whole cell extracts and immune-precipitates from strains AG625 (*CDC5-13MYC-HIS1/CDC5*), VC348 (*SWI6-3HA-URA3/SWI6, CDC5-13MYC-HIS1/CDC5*), and YC211 (*Δswi6::HIS1/SWI6-3HA-URA3*), using anti-HA agarose (A) or anti-MYC beads (B). Proteins were not incubated with anti-TAP antibody in part B due to non-specific cross reaction already seen in control lane when pulled out with IgG beads. 40 mg of protein was incubated with 40 µl of beads overnight, washed, and were boiled in SDS sample buffer for the elution of interacting proteins.

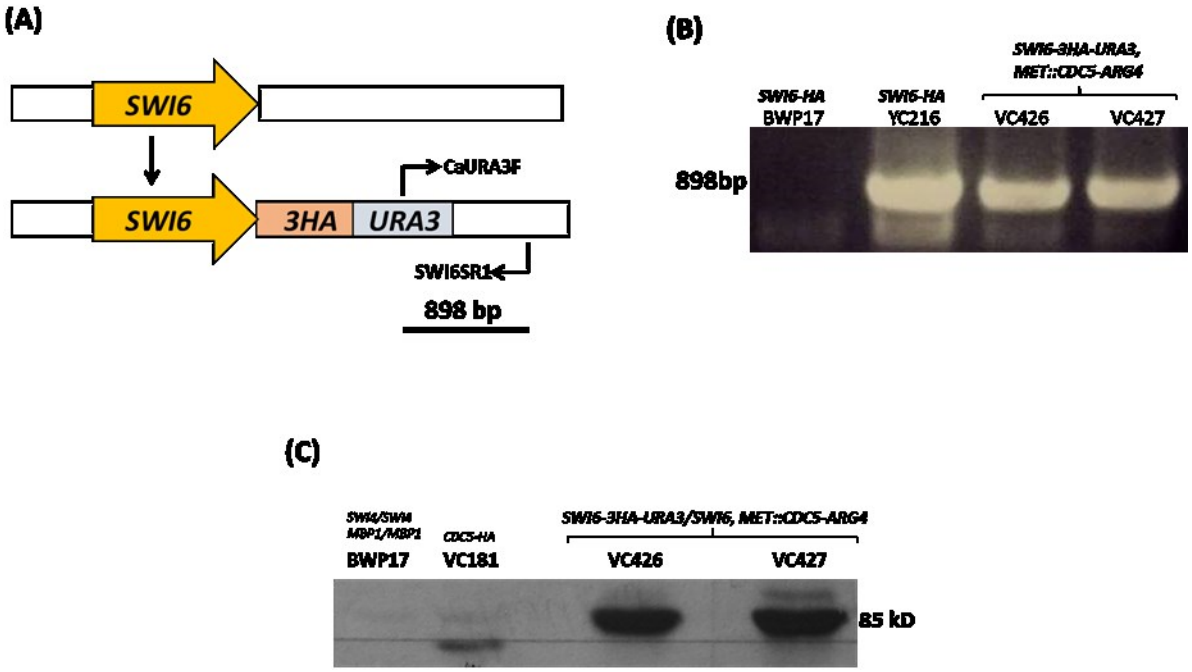

Figure 23. Confirmation of a *SWI6-3HA-URA/SWI6, Δcdc5::hisG/MET3::CDC5-ARG4* strain.

(A, B) Map and DNA gel of a PCR screen to confirm intergration of a *3HA-URA3*-containing construct at the C-terminus of *SWI6*. Oligonucleotides CaURA3F and SWI6SR1 produced an 898 bp band for *SWI6-3HA*. Positive strains VC426, VC427 (*SWI6-3HA-URA3/SWI6, Δcdc5::hisG/MET::CDC5-ARG4*), YC216 (*Δswi6::hisG/SWI6-3HA-URA3*) and negative control strain BWP17 shown in (B). **(C)** Western blot containing 30 µg of whole cell protein extracts from strains VC426, VC427 (*SWI6-3HA-URA3/SWI6, Δcdc5::hisG/MET::CDC5-ARG4*), VC181 (*CDC5-3HA-HIS1/CDC5, SWI6-TAP-URA3/SWI6, Δcln3::hisG/MET::CLN3-ARG4*), and BWP17 incubated with anti-HA antibody.

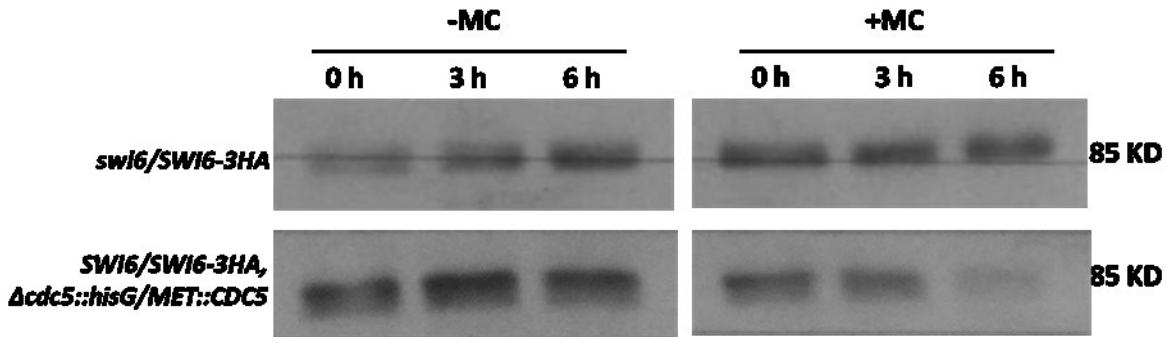

Figure 24. Swi6p is not modulated over time upon depletion of Cdc5p.
Western blot of strains VC426 (*SWI6-3HA-URA3/SWI6, Δcdc5::hisG/MET::CDC5-ARG4*) and YC216 (*Δswi6::HIS1/SWI6-3HA-URA3*) that were incubated in +MC repressing or –MC inducing medium for the indicated times. Blots were incubated with anti-HA antibody to visualize Swi6p-HA.

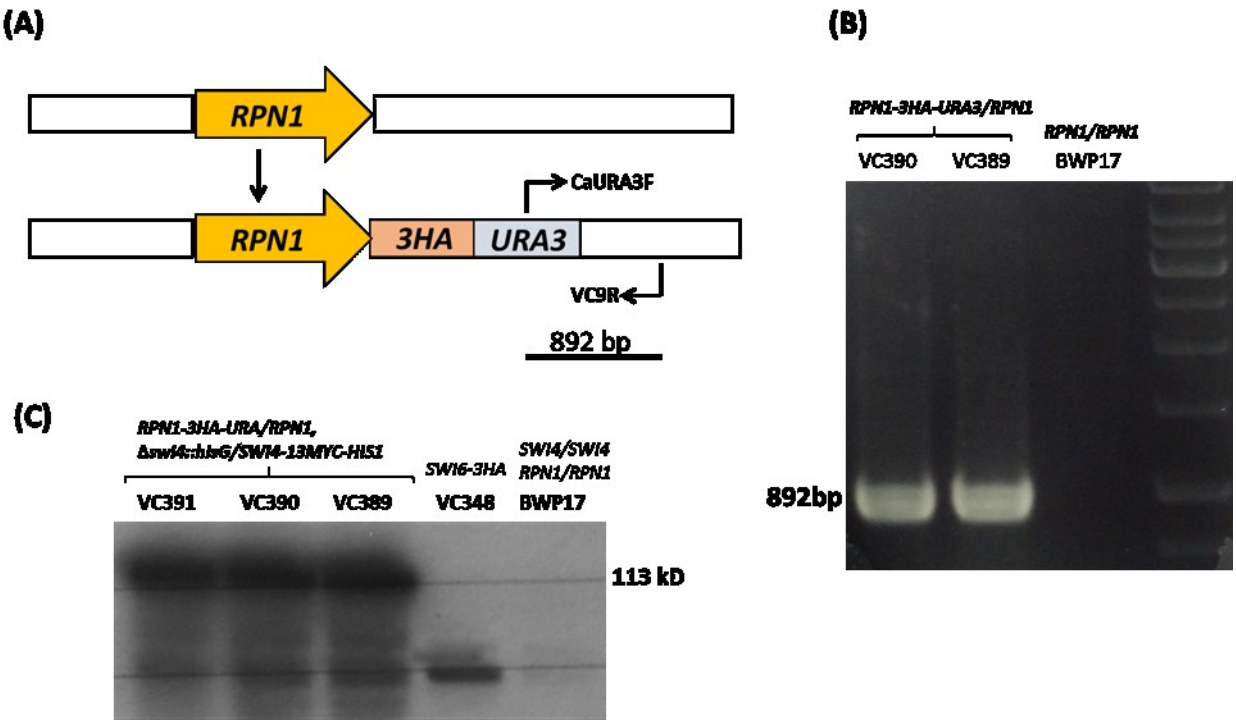

Figure 25. Confirmation of a *RPN1-3HA-URA3/RPN1, Δswi4::hisG/SWI4-13MYC-HIS1* strain.

(A, B) Map and DNA gel of a PCR screen to confirm intergration of a *3HA-URA3*-containing construct at the C-terminus of *RPN1*. Oligonucleotides CaURA3F and VC9R produced an 892 bp band for *RPN1-3HA*. Positive strains VC389, VC390 (*RPN1-3HA-URA3/RPN1, Δswi4::hisG/SWI4-13MYC-HIS*1), and negative control strain BWP17 shown in (B). **(C)** Western blot containing 30 µg of whole cell protein extracts from strains VC389, VC390, VC391 (*RPN1-3HA-URA3/RPN1, Δswi4::hisG/SWI4-13MYC-HIS1*), VC348 (*SWI6-3HA-URA3/SWI6, CDC5-13MYC-HIS1/CDC5*), and BWP17 incubated with anti-HA antibody.

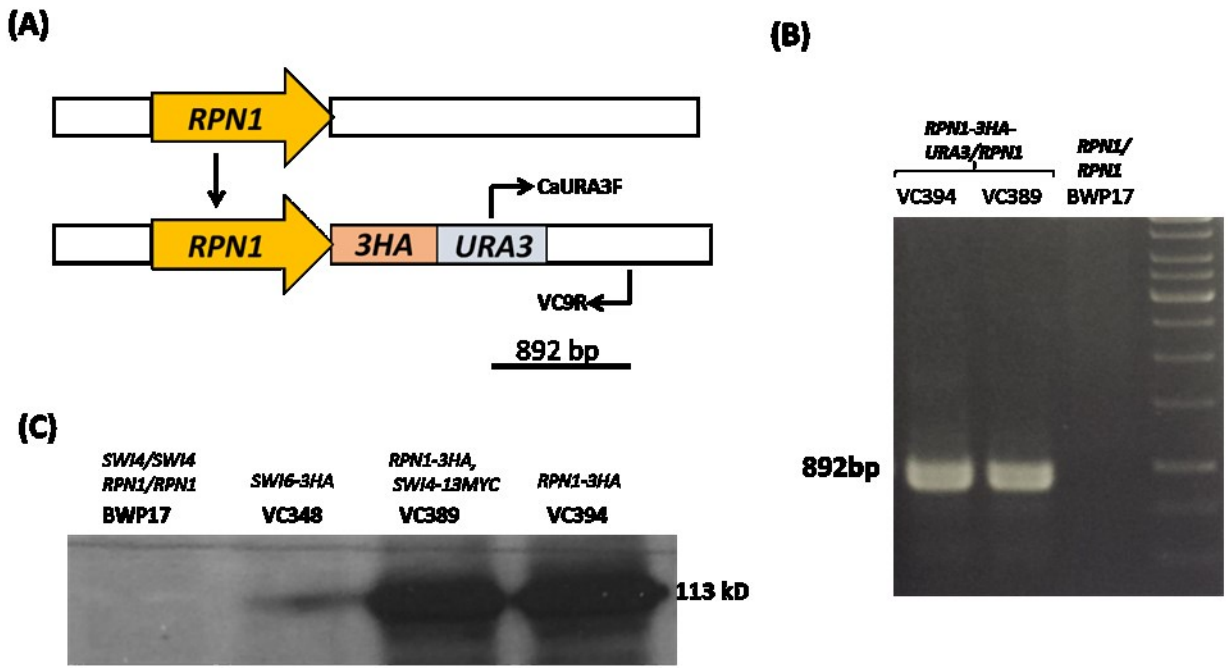

Figure 26. Confirmation of a *RPN1-3HA-URA3/RPN1* strain.
(A, B) Map and DNA gel of a PCR screen to confirm intergration of a *3HA-URA3*-containing construct at the C-terminus of *RPN1*. Oligonucleotides CaURA3F and VC9R produced an 892 bp band for *RPN1-3HA*. Positive strain VC394 (*RPN1-3HA-URA3/RPN1*), and negative control strain BWP17 shown in (B). **(C)** Western blot containing 30 µg of whole cell protein extracts from strains VC394 (*RPN1-3HA-URA3/RPN1*), VC389 (*RPN1-3HA-URA3/RPN1, Δswi4::hisG/SWI4-13MYC-HIS1*), VC348 (*SWI6-3HA-URA3/SWI6, CDC5-13MYC-HIS1/CDC5*), and BWP17 incubated with anti-HA antibody.

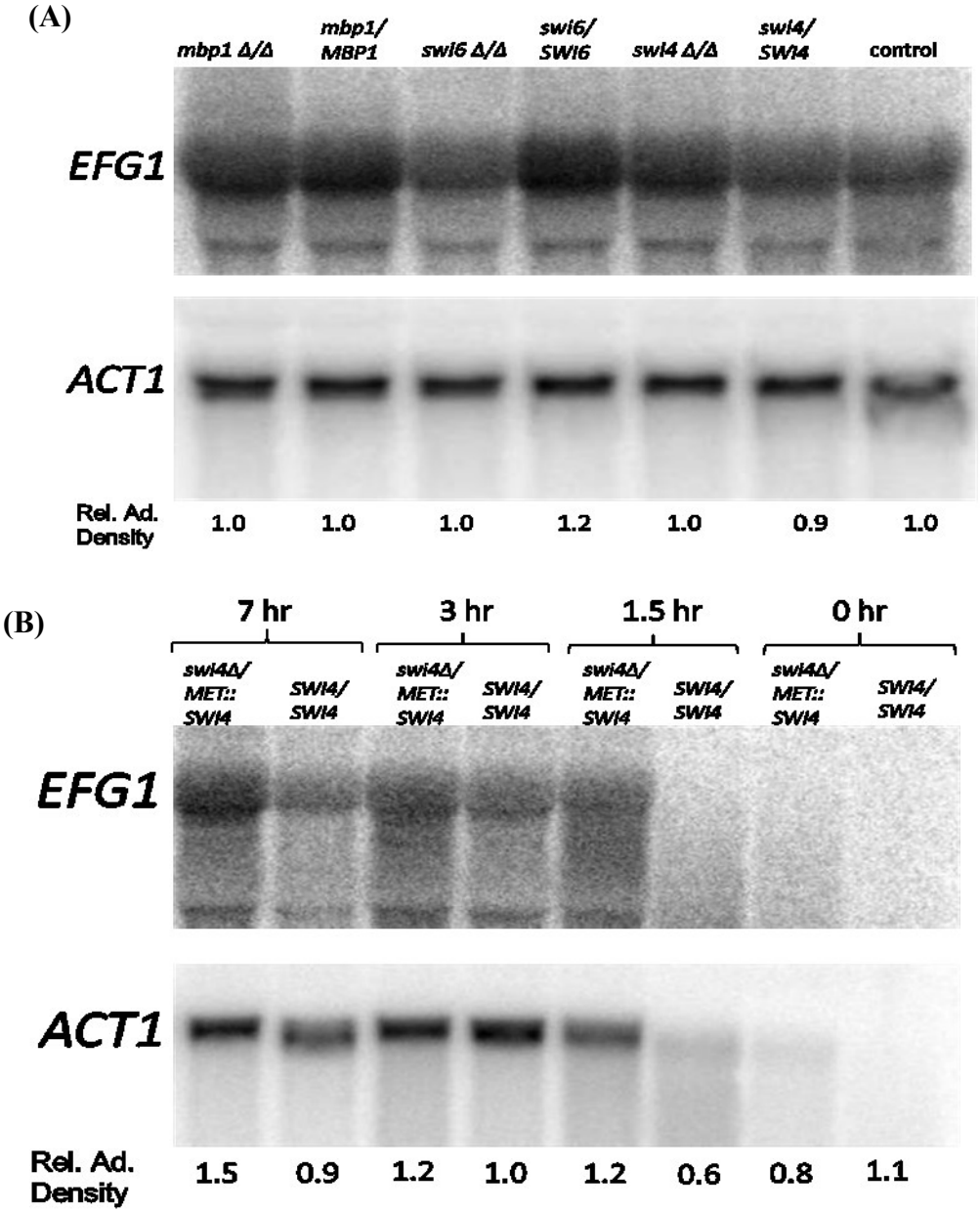

Figure 27. Northern blot showing *EFG1* expression in the presence or absence of *SWI4, SWI6, or MBP1.*

RNA was extracted from *swi4 Δ/Δ*, *swi6 Δ/Δ*, and *mbp1 Δ/Δ* mutant strains and their respective complement strains in addition to control strain, to analyze *EFG1* expression patterns. Expression of *EFG1* is slightly decreased in *swi6 Δ/Δ* mutant cells compared to *SWI6* containing cells. Expression of *EFG1* is slightly decreased in *swi4 Δ/Δ* mutant cells (part **A**). Next, RNA extracted from cells under *SWI4* repressing conditions was analyzed for *EFG1* expression patterns at different time points in the presence and absence of *SWI4*. *EFG1* is moderately induced as Swi4p is depleted over time (part **B**).

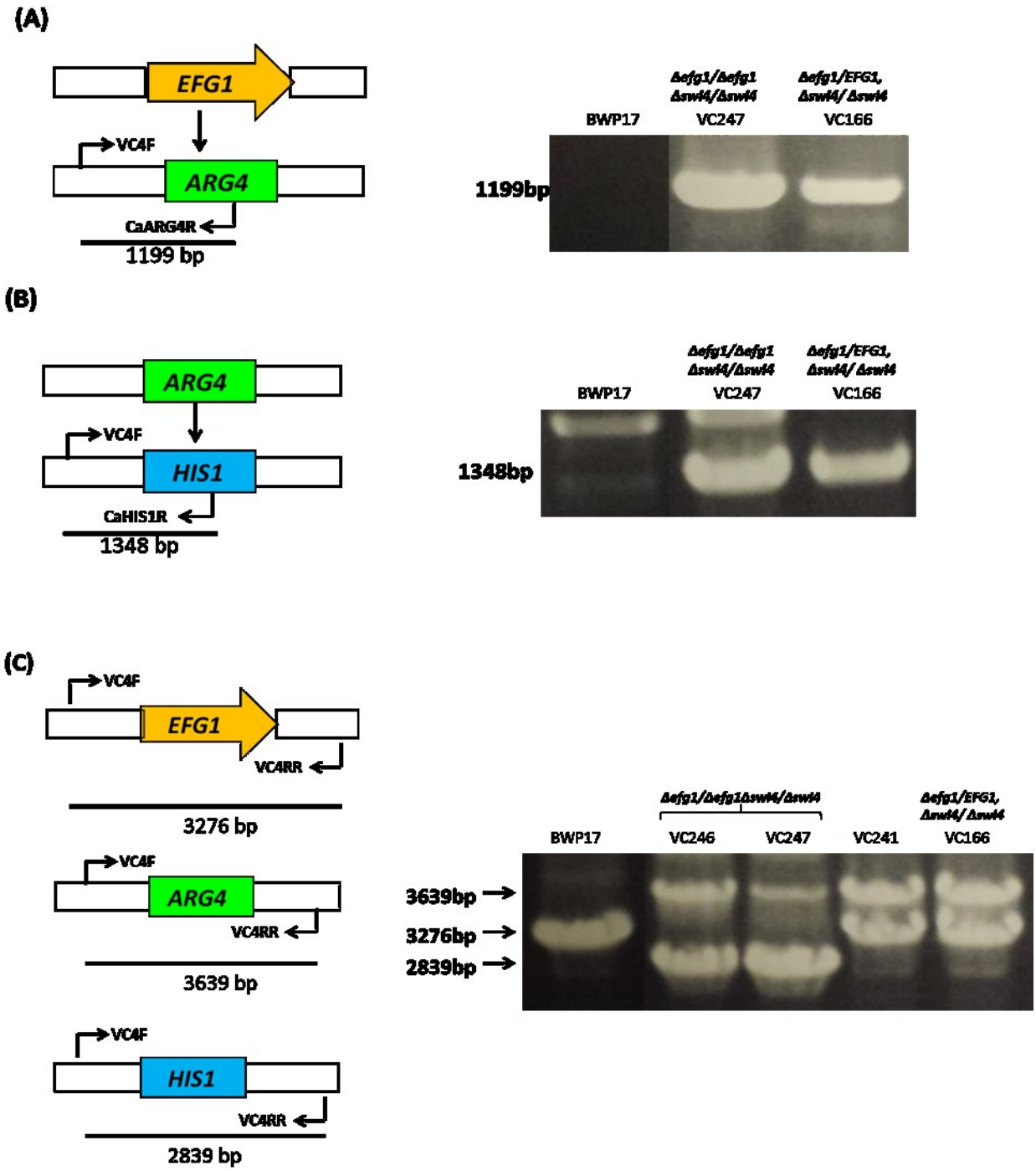

Figure 28. Construction of strain lacking *EFG1* in a *swi4 Δ/Δ* mutant background. PCR screens confirming *swi4/efg1* double mutant strains.
(A, B) Map and PCR screening gel of the deletion of first allele of *EFG1*, showing a 1199 bp band for *Δefgl::ARG4* (A) and second *EFG1* allele, showing a 1356 bp band for *Δefgl::HIS1* (B). **(C)** Map and PCR screening results for confirming the deletion of both *EFG1* alleles, showing 3276 bp band for *EFG1/EFG1*, 3639 bp band for *Δefgl::ARG4*, and 2839 bp band for *Δefgl::HIS1*.

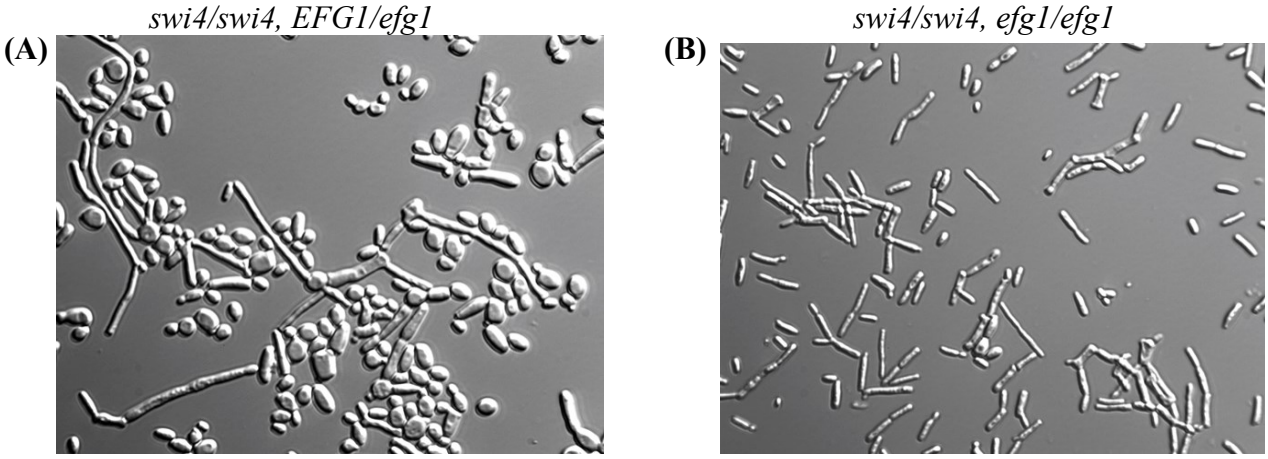

Figure 29. Influence of the absence of Efg1p on the *swi4/swi4* phenotype.
Strains VC166 (*Δefg1::ARG4/EFG1, Δswi4::hisG/Δswi4::URA3*) and VC247 (*Δefg1::ARG4/ Δefg1::HIS1, Δswi4::hisG/Δswi4::URA3*) were incubated in YPD media for 8 h, and fixed.

Table 4. Selected Swi6p-enriched targets[1]

Protein ID	Number of peptides	ORF Name	Present in control	Protein Description
CAL0005042	4	*CDC5/orf19.6010*	N	Verified ORF; Polo-like kinase; member of conserved Mcm1 regulon; depletion causes defects in spindle elongation and Cdc35-dependent filamentation; virulence-group-correlated expression; likely essential (UAU1 method); Spider biofilm repressed
CAL0001395	7	*orf19.5722*	N	Uncharacterized ORF; Has domain(s) with predicted DNA binding activity and role in regulation of transcription; DNA-dependent

[1]Complete list of Swi6p-enriched targets can be accessed from paper 'Characterization of putative G1/S transcription complex factors Swi6p, Swi4p and Mbp1p in the fungal pathogen *Candida albicans*' by Chen, Y (2013).

Table 5. Selected Swi4p-enriched targets[1]

Protein ID	Number of peptides	ORF Name	Present in control	Protein Description
CAL0006334	10	*RPN1/orf19.4956*	N	Uncharacterized ORF; Putative 19S regulatory particle of the 26S proteasome; regulated by Gcn2p and Gcn4p
CAL0001433	6	*RPN3/orf19.3054*	N	Uncharacterized ORF; Putative non-ATPase regulatory subunit of the 26S proteasome lid; amphotericin B repressed; oxidative stress-induced via Cap1p
CAL0006022	10	*RPT6/orf19.3593*	N	Uncharacterized ORF; Putative ATPase of the 19S regulatory particle of the 26S proteasome; transcript regulated by Mig1; regulated by Gcn2 and Gcn4
CAL0001552	9	*PR26/orf19.5793*	N	Uncharacterized ORF; Protein with similarity to proteasomal 26S regulatory subunit of S. cerevisiae, H. sapiens, Methanobacterium thermoautotrophicum (Archaebacterium)

[1]Complete list of Swi4p-enriched targets can be accessed from paper 'Characterization of putative G1/S transcription complex factors Swi6p, Swi4p and Mbp1p in the fungal pathogen *Candida albicans*' by Chen, Y (2013).

4. Discussion

A comprehensive understanding of the regulation of the G1/S transition in *C.albicans* has important implications for identifying factors that are important for cell proliferation and morphogenesis, both of which are important for virulence. Based on genetic and DNA expression data, previous reports suggested that *C. albicans* contained a single MBF-like G1/S transcription complex consisting of the major components Swi4p and Swi6p [42, 48, 49], although biochemical data supporting this interaction was lacking. However, additional factors were proposed to contribute to G1/S control in *C. albicans*, based on the fact that *C. albicans* cells lacking Swi6p and Swi4p or Swi4p and Mbp1p, were still viable [48]. Subsequent work from Y. Chen in the Bachewich lab demonstrated that Swi4p and Swi6p physically interact to form a complex, in support of the model based on affinity purification and co-immunoprecipitation experiments. However, the latter used a high amount of input protein. Mbp1p also interacted with Swi6p, and experiments to test for an interaction between Swi4p and Mbp1p were inconclusive, questioning the composition and number of complexes governing the G1/S transition. Further, systematic affinity purification of Swi6p, Swi4p and Mbp1p revealed additional putative interacting proteins. However, these interactions were not validated using other approaches. Finally, ChIP-chip analysis identified putative Swi4p targets involved in G1/S control, as predicted, but also in hyphal development, including the core hyphal regulator Efg1p. However, the functional significance of this occupation was not further explored.

In addressing these outstanding issues, we obtained results that confirm that Swi6p interacts with Swi4p but also Mbp1p. However, only a weak interaction between Swi4p and Mbp1p could be detected when Swi4p, but not Mbp1p, was pulled down, suggesting that *C. albicans* contains a Swi6p/Swi4p complex as well as a Swi6p/Mbp1p complex. Since the latter

does not appear to be important in G1/S control in yeast under standard growth conditions [65], its function thus remains unclear. The results also confirm an interaction between Swi6p and the mitotic polo kinase Cdc5p, which has not been reported in other systems. Finally, we also provide evidence that supports a functional link between Swi4p and the promoter of the core hyphal regulator Efg1p.

4.1 *C. albicans* Swi6p binds Swi4p and Mbp1p but in separate complexes

Although *C. albicans* contains homologues of Swi6p, Swi4p and Mbp1p, a single complex consisting of Swi6p and Swi4p was proposed to function in G1/S regulation, as absence of Mbp1p did not strongly affect yeast growth, unlike absence of Swi4p or Swi6p [48, 49], and promoters of G1/S-associated genes were enriched for an MBF motif [42]. However, our finding that Swi6p binds Swi4p and Mbp1p, even with reduced amounts of input protein in co-immunoprecipitation experiments, suggests that separate Swi4p/Swi6p and Swi6p/Mbp1p complexes exist in *C. albicans*. If all three proteins existed in a single complex, we predict that affinity purification of Swi4p or Mbp1p should reveal co-precipitation of the Mbp1p or Swi4p, respectively. However, affinity purification of these factors followed by mass spectrometry did not reveal binding. When tested further with co-immunoprecipitation, binding was detected only when Swi4p was pulled down with high amounts of input protein (40mg). This demonstrates that, if an interaction exists, it is not of the same strength as that observed between Swi6p and Swi4p or Swi6p and Mbp1p. We cannot rule out that this is due to an indirect interaction between Swi4p and Mbp1p through Swi6p, and that the three proteins may be present in a single complex. However, the fact that Mbp1p has little effect on yeast growth yet is a dominant interacting factor of Swi6p implies that a separate Swi6p/Mbp1p complex is present in *C. albicans.* The function of this, however, remains obscure. Possibilities include functions under

different growth conditions or in different cell types. Consistent with this, Res2p from the MBF complex in *S. pombe* has a more dominant function during meiosis compared to mitotic growth [18]. Intriguingly, the filamentous fungus *Aspergillus nidulans* has single sequence homologues of *SWI6* and *MBP1,* yet absence of both has little effect on vegetative growth [66]. Thus, there is precedence for divergence in G1/S regulation in fungi. Future experiments are aimed at determining the function of Mbp1p through ChIP-chip, gel-shift assays, and determining phenotype of the *mbp1/mbp1* strain, expression of *MBP1* and Mbp1p, and post-translational modifications of Mbp1p, under diverse growth conditions and in different cell types including the opaque cell form.

4.2 Swi6p interacts with polo-like kinase Cdc5p: a novel interaction

A putative interaction between Swi6p and the polo-like kinase Cdc5p was suggested by previous experiments involving affinity purification followed by mass spectrometry. We have now confirmed the interaction using co-immunoprecipitation. We were not able to detect a strong interaction in exponential phase vs. G1-blocked cells, agreeing with previous affinity purification/mass spectrometry data and raising the possibility that this interaction is specific or enhanced in G1 phase. This interaction has not been reported in other systems and is thus novel. However, the functional significance remains unclear. Cdc5p belongs to the polo-like kinase family of serine/threonine kinases that are conserved from yeast to man [67]. While the major conserved functions lie in mitosis and cytokinesis, multi-cellular organisms contain additional homologues that function during G1 and S phase. Cdc5p in *S. cerevisiae* functions in regulating mitotic progression through the APC/C [68], FEAR network [69] and MEN pathway [70], as well as in septation via RhoA [71]. Cdc5p is cell-cycle regulated and expression of protein levels peak at the G2/M transition [72]. However, the protein is present in low levels and can be

detected at the spindle pole body as early as G1 phase [73, 74]. Further, Cdc5p has a role in spindle pole body maturation [75]. In *C. albicans,* Cdc5p localizes to the spindle pole body and chromatin, even in unbudded, G1-phase cells [50], and Cdc5p is required for metaphase progression and spindle elongation [50]. However, it has not been extensively characterized at the biochemical level in a cell-cycle-dependent manner. Transcription profiles of Cdc5p-depleted cells indicated a global repression of histones, suggesting an S phase arrest, but FACS demonstrated that cells contained a 4n content of DNA [50]. However, *CDC5 is* upregulated at G2/M [42], prior to the time in the cell cycle when Swi6p is required. Thus, in one model to explain our results, Cdc5p may influence Swi6p function in early G1 phase through phoshorylation. In order to test this, we analyzed Swi6p mobility during a time course of Cdc5p repression. No significant difference was observed, but a decrease in Swi6p abundance was noted. This was not quantified, so we cannot rule out differences in loading. However, if real, the result suggests that Cdc5p may influence the stability of Swi6p. Little is currently known about the regulation of Swi6p in *C. albicans*, but more insights on the relevance of an interaction between Swi6p and Cdc5p may be gleaned by repeating the experiments with a more refined time course, synchronized cells, and under different growth conditions. In *S. cerevisiae*, Swi6p is shuttled between nucleus and cytoplasm as a means of regulation. To determine whether Cdc5p might influence Swi6p translocation in *C. albicans*, localization in living cells under conditions of Cdc5p depletion could be employed. Another model could involve indirect interactions through a common intermediate. Cdc5p and other Plks have been located at gene promoters through interactions with transcription factors [76], including Plo1p from *S. pombe*, which is required for regulating expression of genes at the M/G1 transition [77].

Another Swi6p interacting factor identified through previous affinity purification and mass spectrometry analysis included a hypothetical protein, orf19.5722p that has a DNA-binding domain. The orthologue in *S. cerevisiae* is *NSI1*, which is an RNA polymerase I termination factor and involved in ribosomal RNA transcription [78]. Since orf19.5722p has putative DNA-binding ability and may bind Swi6p, it is possible that it contributes to the G1/S transition. Oligonucleotides were designed to tag this protein for co-immunoprecipitation experiments to confirm an interaction with Swi6p, but this work was not yet completed.

4.3 Swi4p putative interactions with components of the proteasome: implications for regulation

In *S. cerevisiae*, *SWI4* expression is periodic and peaks during G1 phase, while Swi4p is present throughout the cell cycle and remains in the nucleus [79]. Its regulation has not been linked to cell-cycle-dependent, targeted degradation. In contrast, previous work from our lab demonstrated through affinity purification and mass spectrometry that Swi4p in *C. albicans* may bind several components of the 26S proteasome and the 19S regulatory subunit, including Pr26p, Rpn1p, Rpn3p, and Rpt6p. The 26S proteasome is comprised of many subunits that consist of a proteolytic core complex (the 20S proteasome) and 19S regulatory complexes. They remove ubiquitin chains and transfer the target proteins into the proteolytic core for degradation [62]. *SWI4* in *S. cerevisiae* shows genetic interactions with some *RPN* subunits [80-85] but no physical interactions have been reported. This has interesting implications for differential regulation of Swi4p and thus the G1/S transition in *C. albicans*. *SWI4* levels peak at the G1/S transition [42], but little is known about specific forms of regulation. Future work will involve determining Swi4p levels during normal cell cycle progression in synchronized cells to determine if the protein is modulated at the level of stability, and confirming putative

interactions between Swi4p and proteasome subunits using co-immunoprecipitation. With respect to the latter, I completed construction of strains and investigations will be carried out by a subsequent graduate student.

4.4 Swi4p targets *EFG1*: possible link between G1/S transition and filamentous development.

Another major finding from Y. Chen was the observation that Swi4p located at the promoter of *EFG1*, a core regulator of the hyphal development program [37, 63]. The notion that *EFG1* may be a target of Swi4p was significant since filamentous growth was associated with *swi4*Δ/Δ cells [48]. In an attempt to determine whether this location was functional, I determined the effect of deleting *EFG1* on the Swi4p-depleted phenotype, and measured *EFG1* levels in strains lacking Swi4p. First, I demonstrated that *swi4*Δ/Δ cells were reduced in size and showed less filamentation in the absence vs. presence of Efg1p, suggesting that Efg1p contributed in part to the phenotype. In comparison, Efg1p is required for hyphal growth under most hyphal-inducing conditions [21], and is a direct target of Protein Kinase A (PKA) [86, 87]. I then demonstrated that *EFG1* was moderately induced in response to absence of Swi4p, but this appeared to be a transient response since the change in expression was only noted during a period immediately following Swi4p depletion in the *SWI4* conditional strain, and not in the *swi4*Δ/Δ strain. This result suggests that Swi4p may have some repressive effect on *EFG1* expression under normal yeast growth conditions. Efg1p is a complex regulator as it is required for many processes in *C. albicans,* including the white phase yeast cell type [37, 38], biofilm formation [36], hyphal growth [21], adhesion and cell wall gene regulation [88], for example, and has both activating [39] and repressing activity [63]. *EFG1* is expressed in yeast cells, but repressed quickly after yeast are exposed to hyphal-inducing conditions such as serum or Lee's

medium, although expression levels eventually recover [63, 89]. This is due to the fact that Efg1p shows negative autoregulation [89]. Thus, with respect to hyphae development, Efg1p is required within a window immediately after hyphal induction to help down-regulate the repressor *NRG1,* negatively autoregulate itself, and control other genes [64]. Efg1p is suggested to have a negative effect on maintenance of hyphal growth, consistent with its down-regulation after hyphal induction [63, 64, 89]. Notably, overexpression of Efg1p can drive filamentous growth in the form of pseudohyphae [63].

With respect to our results, it is thus possible that under yeast growth conditions, Swi4p alone or in combination with other proteins has a repressive effect on *EFG1* that maintains expression at a specific level. Absence of Swi4p results in moderate induction of *EFG1*, and this may contribute to the phenotype, which includes filamentous growth. Given that cells depleted of Swi4p grew in a filamentous form and expressed some hyphal-specific genes [48], this result could provide a mechanism that links Swi4p function to development. However, it is important to note that the *swi4*Δ/Δ cells are pleiotropic and not all filaments are true hyphae. Further, cells in the yeast form were significantly enlarged, which we suggested was due to a delay in G1 phase [48]. Combined with the fact that Efg1p has multiple functions [21], we thus can't rule out the possibility that Swi4p occupation of the *EFG1* promoter is important for other processes. Intriguingly, the *swi4*Δ/Δ cells lacking Efg1p were also reduced in size, suggesting some suppression of the G1/S delay. Efg1p was previously shown to be capable of binding MCB sites in one hybrid and gel-retardation assays, but not in *in vivo* ChIP-chip studies [64, 90]. Thus, Efg1 is a target of Swi4p, but the functional significance of this occupation requires further investigation. Future experiments will include analysis of the *EFG1* promoter for the region binding Swi4p, cloning that region to a reporter to visualize *EFG1* expression in the presence

and absence of Swi4p *in vivo* under different growth conditions and in various cell types, and time-course-based ChIP experiments to investigate the dynamics of Swi4p occupation of the *EFG1* promoter.

In summary, this work has provided more insights on the G1/S transcription factor complex in *C. albicans,* including composition and function. Importantly, it has also identified a possible mechanism by which Swi4p is linked to Efg1p, a critical regulator of many processes important for virulence in *C. albicans*. The results also raise interesting questions on the function of the Swi6p/Mbp1p complex, the regulation of Swi4p, and the role of novel interactors of Swi6p, which will be the focus of future investigations aimed at understanding the regulation of cell proliferation and development in this important fungal pathogen of humans.

References

1. **Cooper G.** 2000. The Cell: A Molecular Approach, 2nd edition ed. ASM Press, Washington.
2. **Amon A.** 1997. Regualation of B-type cyclin proteolysis by Cdc28-associated kinases in budding yeast. EMBO J **16:**2693-2702.
3. **Yamamoto H, Monden T, Miyoshi H, et al.** 1998. Cdk2/cdc2 expression in colon carcinogenesis and effects of cdk2/cdc2 inhibitor in colon cancer cells. Int J Oncol **13:**233-242.
4. **Johnson D, Walker C.** 1999. Cyclins and cell cycle checkpoints. Annu Rev Pharmacool Toxicol **39:**295-312.
5. **White J, Dalton S.** 2005. Cell cycle control of embryonic stem cells. Stem Cell Rev **1:**131-138.
6. **Wittenberg C, La Valle R.** 2003. Cell-cycle-regulatory elements and the control of cell differentiation in the budding yeast. Bioessays **25:**856-867.
7. **Santos S, Ferrell J.** 2008. On the cell cycle and its switches. Nature **454:**288-289.
8. **Ren B, Cam H, Takahashi Y, et al.** 2001. E2F integrates cell cycle progression with DNA repair, replication, and G2/M checkpoints. Genes Dev **16:**245-256.
9. **Donjerkovic D, Scott D.** 2000. Regulation of the G1 phase fo the mammalian cell cycle. Cell Res **10:**1-16.
10. **Bracken AP CM, Cocito A, Helin K.** 2004. E2F target genes: unraveling the biology. Trends in Biochemical Sciences **29:**409-417.
11. **Xu M, Sheppard K, Peng C, et al.** 1994. Cyclin A/CDK2 binds directly to E2F-1 and inhibits the DNA-binding activity of E2F-1/DP-1 by phosphorylation. Mol Cell Biol **14:**8430-8431.
12. **Tyson C, Lord P, Wheals A.** 1979. Dependency of size of *Saccharomyces cerevisiae* cells on growth rate. J Bacteriol **138:**92-98.
13. **Costanzo M, Nishikawa J, Tang X, et al.** 2004. CDK activity antagonizes Whi5, an inhibitor of G1/S transcription in yeast. Cell **117:**899-913.
14. **de Bruin R, McDonald W, Kalashnikova T, et al.** 2004. Cln3 activates G1-specific transcription via phosphorylation of the SBF bound repressor Whi5. Cell **117:**887-898.
15. **Travesa A, Kalashnikova T, de Bruin R, et al.** 2013. Repression of G1/S transcription is mediated via interaction of the GTB motifs of Nrm1 and Whi5 with Swi6. Mol Cell Biol **33:**1476-1486.
16. **Harris M, Lee D, Farmer S, et al.** 2013. Binding specificity of the G1/S transcriptional regulators in budding yeast. PloS one **8:**e61059.
17. **Caetano C, Klier S, de Bruin R.** 2011. Phosphorylation of the MBF repressor Yox1p by the DNA replication checkpoint keeps the G1/S cell-cycle transcriptional program active. PloS one **6:**e17211.
18. **Ayte J, Leis J, DeCaprio J.** 1997. The fission yeast protein $p73^{res2}$ is an essential component of the mitotic MBF complex and a master regulator of meiosis. Mol Cell Biol **17:**6246-6254.
19. **Haase S, Wittenberg C.** 2014. Topology and control of the cell-cycle-regulated transcriptional circuitry. Genetics **196:**65-90.
20. **Whiteway M, Bachewich C.** 2007. Morphogenesis in *Candida albicans* Annu Rev Microbiol **61:**529-553.

21. **Sudbery P.** 2011. Growth of *Candida albicans* hyphae. Nat Rev Microbiol **9:**737-748.
22. **Sobel J.** 1997. Vaginitis. N Engl J Med **337:**1896-1903.
23. **Mayor A, Thewes S, Hube B.** 2005. Systemic fungal infections caused by *Candida albicans* species: epidemology, infection process and virulence attributes. Curr Drug Targets **6:**863-874.
24. **Hoehamer C, Cummings E, Hilliard G, et al.** 2010. Changes in the proteome of *Candida albicans* in response to azole, polyene, and echinocandin antifungal agents. Antimicrob Agents Chemother **54:**1655-1664.
25. **Hawser S, Islam K.** 1999. Comparisons of the effects if fungicidal and fungistatic antifungal agents on the morphogenetic transformation of *Candida albicans*. J Antimicrob Chemother **43:**411-413.
26. **Dalle F, Wachtler B, L'Ollivier C, et al.** 2010. Cellular interactions of *Candida albicans* with human oral epithelial cells and enterocytes. Cell Microbiol **12:**248-271.
27. **Braun B, Johnson A.** 2000. *TUP1, CPH1,* and *EFG1* make independent contributions to filamentation in *Candida albicans* Genetics **155:**57-67.
28. **Sundstrom P, Balish E, Allen C.** 2002. Essential role of the *Candida albicans* transglutaminase substrate, hyphal wall protein 1, in lethal oroesophageal candidasis in immunodeficient mice. J Infect Dis **185:**521-530.
29. **Zeidler U, Lettner T, Lassnig C, et al.** 2008. *UME6* is a crucial downstream target of other transcriptional regulators of true hyphal development in *Candida albicans*. Yeast Res **9:**126-142.
30. **Wang A, Lane S, Tian Z, et al.** 2007. Temporal and spatial control of *HGC1* expression results in Hgc1 localization to the apical cells of hyphae in *Candida albicans*. Eukaryot cell **6:**253-261.
31. **Zheng X, Wang Y, Wang Y.** 2004. Hgc1, a novel hypha-specific G1 cyclin-related protein regulates *Candida albicans* hyphal morphogenesis. EMBO J **23:**1845-1856.
32. **Carlisle P, Kadosh D.** 2010. *Candida albicans* Ume6, a filament-specific transcriptional regulator, directs hyphal growth via a pathway involving Hgc1 cyclin-related protein. Eukaryot cell **9:**1320-1328.
33. **Zheng X, Lee R, Wang Y, et al.** 2007. Phosphorylation of Rga2, a Cdc42 GAP, by CDK/Hgc1 is crucial for *Candida albicans* hyphal growth. EMBO J **26:**3760-3769.
34. **Park H, Bi E.** 2007. Central roles of small GTPases in the development of cell polarity in yeast and beyond. Microbiol Mol Biol Rev **71:**48-96.
35. **Wang A, Raniga P, Lane S, et al.** 2009. Hyphal chain formation in *Candida albicans:* Cdc28-Hgc1 phosphorylation of Efg1 represses cell separation genes. Mol cell Biol **29:**4406-4416.
36. **Nobile C, Fox E, Nett J, et al.** 2012. A recently evolved transcriptional network controls biofilm development in *Candida albicans* Cell **148:**126-138.
37. **Sonneborn A, Tebarth B, Ernst J.** 1999. Control of white-opaque phenotypic switching in *Candida albicans* by the Efg1 morphogenetic regulator. Infect Immun **67:**4655-4660.
38. **Srikantha T, Tsai L, Daniels K, et al.** 2000. *EFG1* null mutatnts of *Candida albicans* switch but cannot express the complete phenotype of white-phase budding cells. J Bacteriol **182:**1580-1591.
39. **Doedt T, Krishnamurthy S, Bochmuhl D, et al.** 2004. APSES proteins regulate morphogenesis and metabolism in *Candida albicans*. Mol Cell Biol **15:**3167-3180.

40. **Harcus D, Nantel A, Marcil A, et al.** 2004. Transcription profiling of cyclic AMP signaling in *Candida albicans*. Mol Cell Biol **15**.
41. **Molero G, Diez-Orejas R, Navarro-Garcia F, et al.** 1998. *Candida albicans*: genetics, dimorphism and pathogenicity. Int Microbiol **1:**95-106.
42. **Cote P, Hogues H, Whiteway M.** 2009. Transcriptional analysis of the *Candida albicans*. Mol Biol Cell **20:**3363-3373.
43. **Bruno V, Mitchell A.** 2004. Large-scale gene function analysis in *Candida albicans*. Trends Microbiol **12:**157-161.
44. **Umeyama T, Kaneko A, Niimi M, et al.** 2006. Repression of *CDC28* reduces the expression of the morphology-related transcription factors, Efg1p, Nrg1p, Rbf1p, Rim101p, Fkh2p and Tec1p and induces cell elongation in *Candida albicans*. Yeast **23:**537-552.
45. **Bachewich C, Whiteway M.** 2005. Cyclin Cln3p links G1 progression to hyphal and pseudohyphal development in *Candida albicans*. Eukaryot cell **4:**95-102.
46. **Chapa L, Bates S, Sudbery P.** 2005. The G1 cyclin Cln3 regulates morphogenesis in *Candida albicans*. Eukaryot Cell **4:**90-94.
47. **Di Como C, Chang H, Arndt K.** 1995. Activation of *CLN1* and *CLN2* G1 cyclin gene expression by *BCK2*. Mol Biol Cell **15:**1835-1846.
48. **Hussein B, Huang H, Glory A, et al.** 2011. G1/S transcriptional factor orthologues Swi4p and Swi6p are important but not essential for cell proliferation and influence hyphal development in the fungal pathogen *Candida albicans*. Eukaryot cell **10:**384-397.
49. **Ofir A, Hofmann K, Weindling E, et al.** 2012. Role of a *Candida albicans* Nrm1/Whi5 homolog in cell cycle gene expression and DNA replication stress response. Mol Microbiol **84:**778-794.
50. **Bachewich C, Thomas D, Whiteway M.** 2003. Depletion of a polo-like kinase in *Candida albicans* activates cyclase-dependent hyphal-like growth. Mol Biol Cell **14:**2163-2180.
51. **Gola S, Martin R, Walther A, et al.** 2003. New modules for PCR-based gene targeting in *Candida albicans*: rapid and efficient gene targeting using 100 bp of flanking homology region. Yeast **20:**1339-1347.
52. **Bensen E, Clemente-Blanco A, Finley K, et al.** 2005. The mitotic cyclins Clb2p and Clb4 affect morphogenesis in *Candida albicans*. Mol Cell Biol **16:**3387-3400.
53. **Bensen E, Filler S, Berman J.** 2002. A forkhead transcription factor is important for true hyphal as well as yeast morphogenesis in *Candida albicans*. Eukaryot cell **1:**787-798.
54. **Care R, Trevethick J, Binley K, et al.** 1999. The MET3 promoter: a new tool for *Candida albicans* molecular genetics. Mol Microbiol **34:**792-798.
55. **Kelly R, Miller S, Kurtz M.** 1998. One-step gene disruption by cotransformation to isolate double auxotrophs in *Candida albicans*. Mol Genet Genomics **214:**24-31.
56. **Lavoie H, Sellam A, Askew C, et al.** 2008. A toolbox for epitope-tagging and genome-wide location analysis in *Candida albicans*. BMC Genet **9:**578.
57. **Chen D, Yang B, Kuo T.** 1992. One-step transformation of yeast in stationary phase. Curr Genet **21:**83-84.
58. **Rose M, Winston F, Hieter P.** 1990. Methods in yeast genetics: A laboratory course manual. Cold Spring Harbor Laboratory Press, Cold Spring Harbor, NY.
59. **Liu H, Osmani A, Ukil L, et al.** 2010. Single-step affinity purification for fungal proteomics. Eukaryot cell **9:**831-833.

60. **Mogilevsky K, Glory A, Bachewich C.** 2012. The Polo-like kinase *PLKA* in *Aspergillus nidulans* is not essential but plays important rules during vegetative growth and development. Eukaryot cell **11:**194-205.
61. **Chou H, Glory A, Bachewich C.** 2011. Orthologues of the anaphase-promoting complex/cyclosome coactivators Cdc20p and Cdh1p are important for mitotic progression and morphogenesis in *Candida albicans*. Eukaryot cell **10:**696-709.
62. **Kohler A, Cascio P, Leggett D, et al.** 2001. The axial channel of the proteasome core particle is gated by the Rpt2 ATPase and controls both substrate entry and product release. Mol Cell **7:**1143-1152.
63. **Stoldt V, Sonneborn A, Leuker C, et al.** 1997. Efg1p, an essential regulator of morphogenesis of the human pathogen *Candida albicans*. EMBO J **16:**1982-1991.
64. **Lassak T, Schneider E, Bussmann M, et al.** 2011. Target specificity of the *Candida albicans* Efg1 regulator. Mol Microbiol **82:**602-618.
65. **Bahler J.** 2005. Cell-cycle control of gene expression in budding and fission yeast. Annu Rev Genet **39:**69-94.
66. **Fujioka T, Mizutani O, Furukawa K, et al.** 2007. MpkA-Dependent and -independent cell wall integrity signaling in *Aspergillus nidulans*. Eukaryot cell **6:**1497-1510.
67. **Archambault V, Glover D.** 2009. Polo-like kinases: conservation and divergence in their functions and regulation. Nat Rev Mol Cell Biol **10:**265-275.
68. **Visintin C, Tomson B, Rahal R, et al.** 2007. APC/C-Cdh1-mediated degradation of the polo kinase Cdc5 promotes the return of Cdc14 into the nucleolus. Genes Dev **22:**79-90.
69. **Rahal R, Amon A.** 2008. The polo-like kinase Cdc5 interacts with FEAR network components and Cdc14. Cell Cycle **7:**3262-3272.
70. **Wang Y, Ng T.** 2006. Phosphatase 2A negatively regulates mitotic exit in *Saccharomyces cerevisiae*. Mol Biol Cell **17:**80-89.
71. **Yoshida S, Kono K, Lowery D, et al.** 2006. Polo-like kinase Cdc5 controls the local activation of Rho1 to promote cytokinesis. Science **313:**108-111.
72. **Hardy C, Pautz A.** 1996. A novel role for Cdc5p in DNA replication. Mol Cell Biol **16:**6775-6782.
73. **Shirayama M, Zachariae W, Ciosk R, et al.** 1998. The polo-like kinase Cdc5p and the WD-repeat protein Cdc20p/fizzy are regulators and substrates of the anaphase promoting complex in *Saccharomyces cerevisiae*. EMBO J **17:**1336-1349.
74. **Song S, Grenfell T, Garfield S, et al.** 2000. Essential function of the polo box of Cdc5 in subcellular localization and induction of cytokinetic structures. Mol Cell Biol **20:**286-298.
75. **Ratsima H, Ladouceur A, Pascariu M, et al.** 2011. Independent modulation of the kinase and polo-box activities of Cdc5 protein unravels unique roles in the maintenance of genome stability. PNAS **108:**E914-E923.
76. **Darieva Z, Bulmer R, Pic-Taylor A, et al.** 2006. Polo kinase controls cell cycle-dependent transcription by direct targeting of a coactivator protein. Nature **444:**494-498.
77. **Papadopoulou K, Ng S, Ohkura H, et al.** 2008. Regulation of gene expression during M-G1-phase in fission yeast through Plo1p and forkhead transcription factors. J Cell Sci **121:**38-47.
78. **Reiter A, Hamperl S, Seitz H, et al.** 2012. The Reb1-homologue Ydr026c/Nsi1 is required for efficient RNA polymerase I termination in yeast The EMBO J **31:**3480-3493.

79. **Baetz K, Andrews B.** 1999. Regulation of cell cycle transcription factor Swi4 through auto-inhibition of DNA binding. Mol Cell Biol **19:**6279-6741.
80. **Fiedler D, Braberg H, Mehta M, et al.** 2009. Functional organization of the S.cerevisiae phosphorylation network. Cell **136:**952-963.
81. **Collins S, Miller K, Maas N, et al.** 2007. Functional dissection of protein complexes involved in yeast chromosome biology using a genetic interaction map. Nature **446:**806-810.
82. **Costanzo M, Baryshnikova A, Bellay J, et al.** 2010. The genetic landscape of a cell. Science **327:**425-431.
83. **Pan X, Ye P, Yuan D, et al.** 2006. A DNA integrity network in the yeast *Saccharomyces cerevisiae*. Cell **124:**1069-1081.
84. **Bandyopadhyay S, Mehta M, Kuo D, et al.** 2010. Rewiring of genetic networks in response to DNA damage. Science **330:**1385-1389.
85. **Batenchuk C, Tepliakova L, Kaern M.** 2010. Identification of response-modulated genetic interactions by sensitivity-based epistatic analysis. BMC Genomics **11:**493.
86. **Sonneborn A, Bochmuhl D, Gerads M, et al.** 2000. Protein kinase A encoded by *TPK2* regulates dimorphism of *Candida albicans*. Mol Microbiol **35:**386-396.
87. **Bochmuhl D, Ernst J.** 2001. A potential phosphorylation site for an A-type kinase in the Efg1 regulator protein contributes to hyphal morphogenesis of *Candida albicans*. Genetics **157:**1523-1530.
88. **Sohn K, Schwenk J, Urban C, et al.** 2006. Getting in touch with *Candida albicans:* The cell wall of a fungal pathogen. Curr Drug Targets **7:**1-8.
89. **Tebarth B, Doedt T, Krishnamurthy S, et al.** 2003. Adaptation of the Efg1p morphogenetic pathway in *Candida albicans* by negative autoregulation and PKA-dependent repression of the *EFG1* gene. J Mol Biol **329:**949-962.
90. **Noffz C, Leidschulte V, Lengeler K, et al.** 2008. Functional mapping of the *Candida albicans* Efg1 regulator. Eukaryot cell **7:**881-893.